Journal of Vertebrate Paleontology

ISSN: (Print) (Online) Journal homepage: https://www.tandfonline.com/loi/ujvp20

A new titanosaurian (Dinosauria: Sauropoda) from the Upper Cretaceous (Campanian) Quseir Formation of the Kharga Oasis, Egypt

Eric Gorscak, Matthew C. Lamanna, Daniela Schwarz, Verónica díez Díaz, Belal S. Salem, Hesham M. Sallam & Marc Filip Wiechmann

To cite this article: Eric Gorscak, Matthew C. Lamanna, Daniela Schwarz, Verónica díez Díaz, Belal S. Salem, Hesham M. Sallam & Marc Filip Wiechmann (2023): A new titanosaurian (Dinosauria: Sauropoda) from the Upper Cretaceous (Campanian) Quseir Formation of the Kharga Oasis, Egypt, Journal of Vertebrate Paleontology, DOI: 10.1080/02724634.2023.2199810

To link to this article: https://doi.org/10.1080/02724634.2023.2199810

Journal of Vertebrate Paleontology e2199810 (30 pages)
Published with license by the Society of Vertebrate Paleontology
DOI: 10.1080/02724634.2023.2199810

ARTICLE

A NEW TITANOSAURIAN (DINOSAURIA: SAUROPODA) FROM THE UPPER CRETACEOUS (CAMPANIAN) QUSEIR FORMATION OF THE KHARGA OASIS, EGYPT

ERIC GORSCAK, [1*] MATTHEW C. LAMANNA, [2*] DANIELA SCHWARZ,[3] VERÓNICA DÍEZ DÍAZ,[3] BELAL S. SALEM,[4,5,6,7] HESHAM M. SALLAM,[5,8] and MARC FILIP WIECHMANN[9]

[1]Department of Anatomy, Midwestern University, 555 31st Street, Downers Grove, Illinois 60515, U.S.A., egorsc@midwestern.edu;
[2]Section of Vertebrate Paleontology, Carnegie Museum of Natural History, 4400 Forbes Avenue, Pittsburgh, Pennsylvania 15213, U.S.A., lamannam@carnegiemnh.org;
[3]Museum für Naturkunde, Leibniz-Institut für Evolutions-und Biodiversitätsforschung, Invalidenstraße 43, 10115 Berlin, Germany;
[4]Department of Geology, Faculty of Science, Benha University, Benha, Egypt;
[5]Mansoura University Vertebrate Paleontology Center, Department of Geology, Faculty of Science, Mansoura University, Mansoura, Egypt;
[6]Department of Biological Sciences, Ohio University, 228 Irvine Hall, Athens, Ohio 45701, U.S.A.;
[7]Ohio Center for Ecological and Evolutionary Studies, Ohio University, Athens, Ohio 45701, U.S.A.;
[8]Institute of Global Health and Human Ecology, School of Sciences and Engineering, American University in Cairo, New Cairo, Egypt;
[9]Bundesanstalt für Geowissenschaften und Rohstoffe, Geozentrum Hannover, Stilleweg 2, 30655 Hannover, Germany

ABSTRACT—Dinosaur fossils from the latest Cretaceous (Campanian–Maastrichtian) of Africa and the Arabian Peninsula are rare. Most discoveries to date have consisted of limited fossils that have precluded detailed phylogenetic and paleobiogeographic interpretations. Fortunately, recent discoveries such as the informative Egyptian titanosaurian sauropod dinosaur *Mansourasaurus shahinae* are beginning to address these long-standing issues. Here we describe an associated partial postcranial skeleton of a new titanosaurian taxon from the Upper Cretaceous (Campanian) Quseir Formation of the Kharga Oasis, Western Desert of Egypt. Consisting of five dorsal vertebrae and 12 appendicular elements, *Igai semkhu* gen. et sp. nov. constitutes one of the most informative dinosaurs yet recovered from the latest Cretaceous of Afro-Arabia. The relatively gracile limb bones and differences in the coracoid and metatarsal I preclude referral of the new specimen to *Mansourasaurus*. Both model-based Bayesian tip-dating and parsimony-based phylogenetic analyses support the affinities of *Igai semkhu* with other Late Cretaceous Afro-Eurasian titanosaurs (e.g., *Mansourasaurus*, *Lirainosaurus astibiae*, *Opisthocoelicaudia skarzynskii*), a conclusion supported by posterior dorsal vertebrae that lack a postzygodiapophyseal lamina, for example. *Igai semkhu* strengthens the hypothesis that northern Africa and Eurasia shared closely related terrestrial tetrapod faunas at the end of the Cretaceous and further differentiates this fauna from penecontemporaneous assemblages elsewhere in Africa, such as the Galula Formation in Tanzania, that exhibit more traditional Gondwanan assemblages. At present, the specific paleobiogeographic signal appears to vary between different dinosaur groups, suggesting that Afro-Arabian Cretaceous biotas may have experienced evolutionary and paleobiogeographic histories that were more complex than previously appreciated.

http://zoobank.org/urn:lsid:zoobank.org:pub:1B44C579-EFBE-4889-A157-5DD6786CACC4

SUPPLEMENTARY FILES—Supplementary files are available for this article for free at www.tandfonline.com/UJVP.

Citation for this article: Gorscak, E., Lamanna, M. C., Schwarz, D., Díez Díaz, V., Salem, B. S., Sallam, H. M., & Wiechmann, M. F. (2023) A new titanosaurian (Dinosauria: Sauropoda) from the Upper Cretaceous (Campanian) Quseir Formation of the Kharga Oasis, Egypt. *Journal of Vertebrate Paleontology*. https://doi.org/10.1080/02724634.2023.2199810

Submitted: July 6, 2022
Revisions received: February 20, 2023
Accepted: April 1, 2023

INTRODUCTION

Paleontological discoveries over the past three decades have substantially improved the fossil record of latest Cretaceous (Campanian–Maastrichtian) non-avian dinosaurs and other terrestrial vertebrates from landmasses that formerly comprised the Gondwanan supercontinent. Phylogenetically and paleobiogeographically informative Campanian and/or Maastrichtian dinosaur finds have come from South America (Bonaparte, 1986, 1996; Leanza et al., 2004; Novas, 2009; Novas et al., 2013; de Jesus Faria et al., 2015; Ezcurra and Novas, 2016; Rozadilla et al., 2021), Madagascar (Krause et al., 1999, 2006, 2019), Indo-Pakistan (e.g., Jain and Bandyopadhyay, 1997; Wilson et al., 2003, 2005; Novas et al., 2010; Khosla and Bajpai, 2021),

*Corresponding authors.

Color versions of one or more of the figures in the article can be found online at www.tandfonline.com/ujvp.

Published online 20 Jul 2023

and even Antarctica (Reguero et al., 2013, 2022; Lamanna et al., 2019). Nevertheless, the latest Cretaceous dinosaur records of two major Gondwanan land areas—Australasia and mainland Africa (i.e., Africa to the exclusion of Madagascar)—remain woefully incomplete, hindering meaningful insights into the evolutionary and paleobiogeographic relationships of their respective dinosaur faunas during this time (Krause et al., 1999, 2006, 2019; Wilson et al., 2001; Ali and Krause, 2011; Lamanna, 2013; Sallam et al., 2018). In particular, and although this situation is beginning to change (e.g., Sertich et al., 2005, 2006, 2013; El-Dawoudi et al., 2017; Sallam et al., 2018; Abu El-Kheir et al., 2019; Salem et al., 2020), the Campanian–Maastrichtian dinosaur record of mainland Africa is exceptionally poor, with most discoveries consisting of isolated skeletal elements of often limited morphological and phylogenetic utility (e.g., Gemmellaro, 1921; Stromer and Weiler, 1930; Rauhut and Werner, 1995, 1997; Martill et al., 1996; Rauhut, 1999; Schulp et al., 2000, 2008; Buffetaut et al., 2005, 2015; Smith and Lamanna, 2006; Mateus et al., 2012; Kear et al., 2013; Sallam et al., 2016; Owusu Agyemang et al., 2019; Abu El-Kheir et al., 2019; Salem et al., 2021).

At present, the most complete—and critically, diagnostic—dinosaur fossil that is unquestionably from the latest Cretaceous of mainland Africa is the holotypic partial skeleton of the titanosaurian sauropod *Mansourasaurus shahinae* from the Campanian Quseir Formation of the Dakhla Oasis, Western Desert of Egypt (Sallam et al., 2018). Although the specimen includes craniomandibular, postcranial axial, appendicular, and possible dermal elements, and therefore preserves a broad representation of the skeleton, many bones are incomplete and/or significantly deformed, hindering their full anatomical interpretation and potential. A partial hind limb of a titanosauriform sauropod has also been reported from Maastrichtian phosphatic deposits in the Ouled Abdoun Basin of Morocco (Pereda Suberbiola et al., 2004; Lamanna and Hasegawa, 2014), and additional associated titanosauriform material from these beds was briefly mentioned by Longrich et al. (2017, 2021), who also described the abelisaurid theropod *Chenanisaurus barbaricus* (Longrich et al., 2017) and the hadrosaurid ornithopod *Ajnabia odysseus* (Longrich et al., 2021) based on isolated dentigerous elements. Other informative latest Cretaceous dinosaur fossils have been recovered from Kenya and Jordan, but most of these specimens await formal description and analysis (Sertich et al., 2005, 2006, 2013; Wilson et al., 2006; D'Emic and Wilson, 2012; O'Connell et al., 2012; Gorscak, 2016; Gorscak et al., 2019). Moreover, two partial titanosaurian skeletons (*Rukwatitan bisepultus* and *Shingopana songwensis*) and multiple isolated dinosaur bones have been described from the Upper Cretaceous Namba Member of the Galula Formation of southwestern Tanzania (O'Connor et al., 2006; Roberts et al., 2010; Gorscak et al., 2014, 2017). Although the Namba Member may potentially date to the Campanian, the possibility remains that this unit is somewhat older, perhaps Cenomanian–Santonian in age based on an alternative interpretation of the paleomagnetic data derived from this unit (Widlansky et al., 2018; Gorscak and O'Connor, 2019; Orr et al., 2021).

Although most of the abovementioned fossils were discovered during the past two decades, in 1977, a field team from the Technische Universität Berlin (TUB) recovered a variety of fossil vertebrate remains from the Western Desert of Egypt (Barthel and Böttcher, 1978; Barthel and Herrmann-Degen, 1981). Among the most significant of these was a closely associated partial postcranial skeleton of a medium-sized titanosaurian sauropod collected from the Campanian Quseir Formation of the Kharga Oasis (Fig. 1). The specimen was briefly reported in abstracts by Brinkmann and Buffetaut (1990) and Wiechmann (1999a) and was the focus of a degree thesis by one of the current authors (M.F.W.; Wiechmann, 1999b), but it has never been formally described or analyzed within a broader phylogenetic and paleobiogeographic context. Although the skeleton is fragmentary, and many elements are incomplete and/or taphonomically distorted, it is currently the second-most complete and informative (after the *Mansourasaurus* holotype) Campanian–Maastrichtian dinosaur specimen from mainland Africa. Owing to the rarity of latest Cretaceous terrestrial tetrapod fossils from the continent, plus exhibiting several uncommon morphologies, we provide a detailed description and phylogenetic assessment of the skeleton herein, following from the brief reports presented by Lamanna et al. (2017), Díez Díaz et al. (2017), and Gorscak et al. (2020). Another titanosaurian partial skeleton that was recently discovered from the Quseir Formation of the Kharga Oasis (El-Dawoudi et al., 2017; Salem et al., 2020) will be described elsewhere.

Institutional Abbreviations—**FMNH**, Field Museum of Natural History, Chicago, U.S.A.; **FUB**, Freie Universität Berlin, Berlin, Germany; **MAL**, Malawi Department of Antiquities, Lilongwe and Blantyre, Malawi; **MCNA**, Museo de Ciencias Naturales de Álava/Arabako Natur Zientzien Museoa, Vitoria-Gasteiz, Spain; **MDE**, Musée des Dinosaures, Esperaza, France; **MfN**, Museum für Naturkunde, Berlin, Germany; **MPCA**, Museo Provincial Carlos Ameghino, Cipolletti, Argentina; **MRS**, Museo Argentino Urquiza, Rincón de los Sauces, Argentina; **MUVP**, Mansoura University Vertebrate Paleontology Center, Mansoura, Egypt; **SFB**, Sonderforschungsbereiches (= Collaborative Research Center) of the Technische Universität Berlin; **TMM**, Texas Memorial Museum, Austin, Texas, U.S.A.; **TUB**, Technische Universität Berlin, Berlin, Germany; **USNM**, United States National Museum (now National Museum of Natural History), Washington, U.S.A.; **Vb**; vertebrate fossil collections of the Sonderforschungsbereiches 69 of the Technische Universität Berlin, Germany.

HISTORICAL CONTEXT

The titanosaurian specimen described herein has a complicated history. It was discovered and collected in early November 1977 by K. Werner Barthel and Ronald Böttcher of the TUB, who recovered it over the course of three days (Wiechmann, 1999b). Barthel and Böttcher were conducting research under the auspices of the TUB Sonderforschungsbereiches (SFB, = Collaborative Research Center) 69, "Geoscientific Problems in Arid and Semiarid Regions." The skeleton was sent to the TUB in 27 plaster jackets, where it was kept in the SFB 69 collection for nearly two decades. According to Wiechmann (1999b), translated from German by one of the present authors (D.S.), "Barthel's field records prove that the titanosaur partial skeleton was in a much better state of preservation before salvage in 1977. The first damage occurred during the salvage campaign due to the use of insufficient preservatives. Further damage was caused before and during preparation in the SFB … and due to insufficient storage facilities."

The Kharga Oasis titanosaur skeleton was first mentioned in the scientific literature as the subject of an abstract by Brinkmann and Buffetaut (1990), and again in another abstract by one of the present authors (M.F.W.; Wiechmann, 1999a). At approximately the time of the latter publication, the specimen, then including the currently missing left tibia, was transferred to the former Institut für Paläontologie (today the Institut für Geowissenschaften, Sektion Paläontologie) of the Freie Universität Berlin, and was studied by M.F.W. as the focus of his Diplomarbeit (= Diploma thesis) (Wiechmann, 1999b). Other fossils collected by the SFB 69 from the Egyptian Western Desert were also part of this transfer including TUB Vb-646, the titanosauriform sauropod femur from the Maastrichtian of the Dakhla

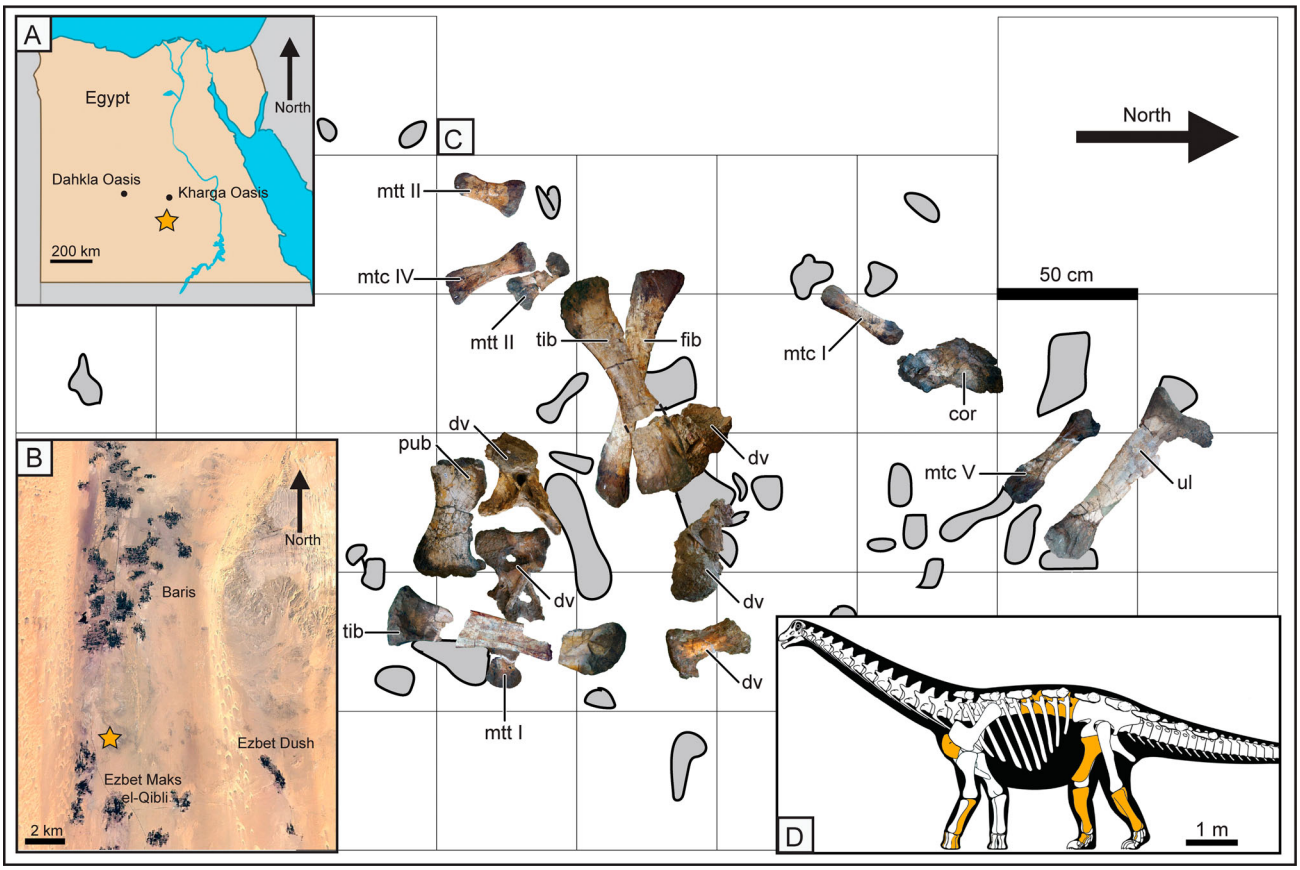

FIGURE 1. Location of discovery and quarry map of *Igai semkhu* (Vb-621–640). **A**, map of Egypt showing the location of the town of Baris in the Kharga Oasis region, denoted by orange star (modified from Sallam et al., 2018:fig. 1a); **B**, satellite image from Google Earth Pro of the research area south of Baris with approximate quarry location indicated by orange star; **C**, quarry map showing disposition of skeletal elements in situ with currently missing and/or obliterated elements in gray, modified from Wiechmann (1999b:17); and **D**, skeletal silhouette (reversed and modified from Sallam et al., 2018:fig. 1c) with elements described in the current study shown in orange. **Abbreviations**: **cor**, coracoid; **dv**, dorsal vertebra; **fib**, fibula; **mtc I**, metacarpal I; **mtc IV**, metacarpal IV; **mtc V**, metacarpal V; **mtt I**, metatarsal I; **mtt II**, metatarsal II; **pub**, pubis; **tib**, tibia; **ul**, ulna.

Oasis described by Rauhut and Werner (1997). The Kharga skeleton was examined by one of us (M.C.L.) at the FUB in 2000 at the invitation of M.F.W. but was not made the subject of a formal publication at that time.

Roughly eight years later, the Institut für Geowissenschaften, Sektion Paläontologie of the FUB elected to abandon its vertebrate paleontological research program and to transfer its vertebrate fossil collection to the MfN. On September 11, 2008, the Kharga Oasis titanosaur skeleton and many other Cretaceous fossils from Egypt and Sudan were relocated to the MfN. In 2017, the present authors formed a collaborative project to study the skeleton, publishing two associated abstracts during that year (Díez Díaz et al., 2017; Lamanna et al., 2017). Finally, in September 2019, several of us (E.G., M.C.L., and D.S.) convened at the MfN to complete work on the specimen. Nearly all bones described by Wiechmann (1999b) were accounted for, and most were unchanged from their condition as depicted in his Diplomarbeit, although a few suffered damage that has since been largely restored and/or ameliorated by the existence of three-dimensional photogrammetric models made by one of us (V.D.D.) prior to damage. Unfortunately, however, the left tibia (Vb-634) is currently missing, and it appears to have never been transferred to the MfN; this is also the case for the isolated Dakhla Oasis femur TUB Vb-646. The current whereabouts of these two bones are unknown. However, documentation (i.e., images, description, measurements) of the left tibia based on Wiechmann's (1999b) thesis and M.C.L.'s previous examination of this bone is presented in the current study.

SYSTEMATIC PALEONTOLOGY

DINOSAURIA Owen, 1842
SAUROPODA Marsh, 1878
TITANOSAURIA Bonaparte and Coria, 1993
LITHOSTROTIA Upchurch et al., 2004
IGAI SEMKHU gen. et sp. nov.
(Figs. 2–16; Tables 1–2)

Holotype—Vb-621–640, a closely associated partial postcranial skeleton consisting of five fragmentary dorsal vertebrae, partial left coracoid, partial left ulna, three left metacarpals (I, IV, and V), the proximal part of the left pubis, both tibiae (a partial right and the complete and well-documented but currently missing left, Vb-634), the left fibula, and three metatarsals (left I, left and right II). Numerous additional fragments of the specimen were apparently discovered (Fig. 1C) but were not described by previous authors (Brinkmann and Buffetaut, 1990; Wiechmann, 1999a, 1999b) and cannot be accounted for at present.

Locality and Horizon—East of Maks El-Bahari, southeast of the town of Baris, roughly 500 m east of the Darb Al

Arbaein, Kharga Oasis, Western Desert of Egypt (approximately 24°35′36′′N, 30°35′57′′E based on Wiechmann 1999b; Fig. 1A, B). Upper Cretaceous (Campanian) Quseir Formation. See Churcher (1995), Mahmoud (1998, 2003), El Atfy et al. (2016), Sallam et al. (2016), Fathy et al. (2021), and Zaghloul (2021) for discussions of the geology and age of the Quseir Formation. For additional locality and stratigraphic context, see Figures S1–3 in the Supplementary Files.

Etymology—"Igai" is the name of the enigmatic "lord of the oasis" deity that was venerated by inhabitants of the Dakhla and Kharga oases (and surrounding regions) in Egypt from roughly the Old Kingdom to the Late Period. The species epithet "semkhu" is the perfect passive singular participle, "the forgotten," of "semekh," the ancient Egyptian verb "to forget." Collectively, "the forgotten lord of the oasis" alludes to both the relatively recent emergence of latest Cretaceous nonmarine vertebrate fossils from continental Africa (particularly Egypt) and the lengthy and complicated history of the holotypic specimen (see above).

Diagnosis—Characters supporting *Igai semkhu* as a titanosaurian sauropod dinosaur: dorsal vertebrae lacking hyposphene-hypantrum articulations; and ulna with prominent olecranon process. Autapomorphic characters of *Igai semkhu*: metacarpal V with proximomedial and distomedial tubercles; reduced cnemial crest of the tibia (does not exceed anterior margin of distal end of the tibia); and distal groove along dorsal margins of metatarsals I and II.

DESCRIPTION AND COMPARISONS

Terminology—We employ the terminology for saurischian dinosaur vertebral laminae presented by Wilson (1999, 2012), and the terminology for vertebral fossae developed by Wilson et al. (2011a). Furthermore, we describe the coracoid of *Igai* (Vb-627) with its anteroposterior axis aligned with the long axis of the (missing) scapula such that the coracoid foramen and scapular articulation are posteriorly located.

Computed Tomography and Digital Models—The computed tomographic (CT) scans were acquired at the Leibniz Institute for Zoo- and Wildlife Research Berlin (IZW) in 2021, using a high-resolution 64 row multislice CT scanner (Aquilion CX; Toshiba, Otawara, Japan). For each specimen, a separate 134 spiral scan with a 0.5 mm interval was made and saved as a DICOM stack. CT images were taken with a setting of 135 kV and 250 mA. Data reconstruction (bone algorithm) was done with a Vitrea Workstation (Vitrea 2, Version 4.1.2.0, Vital Images, Inc., Minnetonka, Minnesota, U.S.A.) and an OsiriX Workstation (OsiriX Version 3.9.4, 64 Bit). Additionally, fossils were digitized via structure-from-motion photogrammetry, following the protocols of Mallison and Wings (2014). A digital SLR camera (Canon EOS 70D with Canon 10–18 mm f4.5–5.6 lens) was used with an LED ring light. Images were processed in Agisoft PhotoScan Professional Version 1.4.3 in order to obtain three-dimensional models of each bone. High-quality polygon mesh files were created for curatorial and museological purposes, but also lower resolution color-free STL files (50,000 polygons) were created to facilitate visualization. All created files were saved following the best practice guidelines proposed by Davies et al. (2017), which are also accessible under request. Scanning data, digital models, and supporting phylogenetic files are available on the Morphobank Project page for *Igai* (http://morphobank.org/permalink/?P4387).

Preservation—Although *Igai* includes a variety of axial and appendicular bones, and therefore preserves a wide representation of the postcranial skeleton, most of these elements are incomplete and/or taphonomically distorted. This is especially true for the five dorsal vertebrae, all of which are at least slightly deformed and only four of which preserve parts of both the centrum and neural arch. For example, Vb-622 and Vb-623 are severely anteroposteriorly compressed and sheared toward the left dorsolateral direction, whereas Vb-624 is missing nearly its entire left side. Several of the more proximal appendicular elements (the coracoid, ulna, pubis, and right tibia) are also lacking significant portions, and most of the metapodials have been compressed primarily along their respective dorsopalmar or dorsoplantar axes. The ends of several limb bones are preserved essentially as loosely compacted sediment and are thus extremely prone to damage (especially crumbling) in the absence of delicate care. Regions of several bones (e.g., the ventrolateral area of the coracoid, the anterior surface of the distal end of the ulna, and roughly the medial half of the proximal right tibia) have been completely cleaved away and as such these surfaces consist of flat, featureless areas of exposed internal bone.

The quarry map of the *Igai* excavation that is based on a field sketch by K. Werner Barthel of the TUB, redrawn by Brinkmann and Buffetaut (1990) and Wiechmann (1999b), indicates that, upon discovery, many skeletal elements remained in approximate life position (Fig. 1C). The five dorsal vertebrae, all of which appear to represent the posterior half of the series, were found clustered adjacent to the pelvic and hind limb bones; of the latter, the left tibia was found above the left fibula. The pectoral and most forelimb elements (i.e., coracoid, ulna, metacarpals I and V) were found approximately 1 meter north of the pelvic and hind limb bones apart from the metacarpal IV located closer to posterior elements such as the metatarsals (Fig. 1C). Most of the skeleton pertains the left side of the individual, although there are a few elements from the right side as well. According to Wiechmann (1999b), Barthel's field notes indicate that the skeleton was substantially more complete and better preserved prior to its attempted recovery, and indeed, this is borne out by his field sketch, which suggests the presence of more than 30 other elements that cannot currently be accounted for (see the gray shapes in Fig. 1C). Presumably, the delicate nature of these elements (judging from the fragility of currently preserved material of *Igai*) led to their destruction at some point between their initial discovery and the completion of Wiechmann's (1999b) thesis (i.e., they may have been unintentionally destroyed or lost in the field, in transit to Berlin, during scientific preparation, during transport between institutions, and/or even during study).

Ontogenetic Stage and Body Size—The neural arches of all preserved dorsal vertebrae are fused to their respective centra; as such, the holotypic specimen of *Igai* was probably somatically mature, or nearly so, at the time of death. This, however, is not totally certain, as the presence of a possible articular surface for the scapula on the left coracoid suggests that these two bones may not have been fully co-ossified at time of death. Absent other vertebrae from different regions of the axial skeleton and a complete scapulocoracoid to compare, the assessment of the ontogenetic stage remains incomplete, as sauropodomorphs tend to exhibit differing orders of skeletal element fusion through ontogeny (Griffin et al., 2021). Comparisons of the dimensions of known limb elements of *Igai* (i.e., the ulna, tibiae, and fibula; Table 2) to more complete titanosaurs suggest that the individual was relatively medium-sized for the clade, perhaps 10–15 m in estimated total body length (e.g., approximately in the range of *Diamantinasaurus matildae*, *Epachthosaurus sciuttoi*, and *Opisthocoelicaudia skarzynskii*). Therefore, the specimen of *Igai* was probably at least slightly larger than the holotype specimen of *Mansourasaurus shahinae*, the other named titanosaur species from the Quseir Formation and nearby the Dakhla Oasis, the total body length of which is estimated at 8–10 m (Sallam et al., 2018).

Interestingly, and perhaps not coincidentally, all known titanosaurians from Campanian–Maastrichtian deposits in northern

Africa (i.e., *Igai*, *Mansourasaurus*, and an unidentified form from Morocco) and the then-conjoined Arabian Peninsula (an unnamed taxon from Jordan; D'Emic and Wilson, 2012; O'Connell et al., 2012) were small to medium-sized for sauropod dinosaurs. The same is true for most Campanian–Maastrichtian titanosaurs from southern Europe, such as *Ampelosaurus atacis* (Le Loeuff, 2005), *Atsinganosaurus velauciensis* (Díez Díaz et al., 2018), *Garrigatitan meridionalis* (Díez Díaz et al., 2021), *Lirainosaurus astibiae* (Sanz et al., 1999), *Lohuecotitan pandafilandi* (Díez Díaz et al., 2016), *Magyarosaurus dacus* (Jianu and Weishampel, 1999), and *Paludititan nalatzensis* (Csiki et al., 2010), except for the recently described, large-bodied Iberian titanosaur *Abditosaurus kuehnei* (Vila et al., 2022). By contrast, some Campanian–Maastrichtian titanosaurians from the Americas (e.g., *Alamosaurus sanjuanensis*, *Dreadnoughtus schrani*, *Puertasaurus reuili*) reached much greater body dimensions, and similarly large-bodied taxa occurred at more southerly latitudes in Africa during a roughly equivalent geologic period such as reported yet-undescribed giant titanosaur bones from the ?Maastrichtian Lapur Sandstone of northwestern Kenya (Gorscak et al., 2019).

Postcranial Axial Skeleton

Dorsal Vertebrae—The *Igai* holotype includes five partial dorsal vertebrae (Vb-621–625; Figs. 2–7). Of these, Vb-623 is a largely complete posterior dorsal vertebra, Vb-624 and Vb-622 are partial posterior dorsal vertebrae, Vb-621 is a portion of a middle–posterior dorsal centrum, and Vb-625 is a middle–posterior dorsal vertebral fragment that includes parts of the centrum and neural arch. Vertebrae Vb-623, Vb-624, and to a lesser extent Vb-622 are substantially more complete and anatomically informative than the others, and as such, much of our description of the dorsal vertebrae of *Igai* focuses on these three elements. All preserved centra are opisthocoelous, have large, deep, elliptical pleurocoels (i.e., lateral pneumatic fossae), and, as demonstrated by CT images acquired during study and exposed breaks, are internally comprised of camellate (i.e., spongy, somphospondylous) bone tissue (see below for detailed description of pneumaticity). There is no evidence for a hypantrum-hyposphene articulation complex in any of the dorsal vertebrae with neural arches as preserved, a feature that is absent in most titanosaurian sauropods (Wilson, 2002; Powell, 2003; D'Emic, 2012). As noted above, all five vertebrae have been taphonomically deformed to varying degrees, so we opted to describe the elements based on preservation, from least to most complete and informative, rather than a traditional order of anatomical position due to the degree of ambiguity due to preservation.

Dorsal vertebrae Vb-621 (Fig. 2) and Vb-625 (Fig. 3) consist of incomplete centra, with the latter also preserving a small part of the neural arch. The spool-shaped centrum of Vb-621 preserves only the left lateral surface and is relatively elongate compared with those of the other dorsal vertebrae (Table 1), suggesting that this vertebra was placed nearer the middle section of the dorsal vertebral column. The ventral surface appears only slightly transversely constricted, but this may be an artifact of taphonomic compression. What remains of the pleurocoel suggests that it was relatively large, extending almost the entire length of the centrum (Fig. 2A). Dorsal vertebra Vb-625 is significantly distorted, being compressed at an oblique angle between the anteroposterior and mediolateral axes (Fig. 3A). The posterior cotyle and a small portion of the anterior condyle are preserved. Both pleurocoels are present; the left is significantly smaller and penetrates deeper into the centrum (Fig. 3A), whereas the right pleurocoel is larger and shallower, hinting at potential asymmetry in the expression of pneumatic features as previously noted in other sauropod fossils (e.g., Wedel et al., 2000; Wedel, 2003). The remnants of the neural canal floor are present near the preserved fragment of the neural arch (Fig. 3A). This part of the neural arch may include lamina(e) that connect with the prezygapophysis, but it is too distorted to enable confident interpretation.

Dorsal vertebra Vb-622 is incomplete and deformed, preserving only the centrum and the ventral region of the neural arch, the latter of which is more complete anteriorly and on the left side (Fig. 4). The deformation is asymmetric, exhibiting oblique shearing and compression relative to the anteroposterior axis. Both the anterior condyle and the posterior cotyle of the centrum are worn but appear to have been wider than tall (Fig. 4A, D). The ventral surface of the centrum is smooth, with no indication of ridges or foramina, whereas the other surfaces are abraded, exposing camellate (somphospondylous) internal tissue. The pleurocoels (i.e., lateral fossae) are deep and elliptical. The dorsal surface of the left pleurocoel exhibits ridges, although these are less pronounced than those in vertebra Vb-624 (see below). The neural canal is indistinguishable from the rest of the element, and only a handful of laminae are evident on the neural arch. A notably developed X-lamina complex (see further description below) is present anteriorly, bordered ventrally by the neural canal and laterally by the right and left centroprezygapophyseal fossae; the latter is in turn bordered by the left centroprezygapophyseal lamina, but the right counterpart of this lamina is not preserved (Fig. 4A). The left transverse process is incomplete, but the preserved part suggests that it may have been dorsolaterally angled.

Of the three relatively complete *Igai* dorsal vertebrae (Vb-622–624), Vb-623 is tentatively interpreted as the most anterior, situated roughly towards the middle–posterior region of the series (Fig. 5). Previous work (Wiechmann, 1999b) interpreted the presence of the partial left parapophysis near the junction of the centrum and neural arch, but our observations suggest that this structure is in fact an artifact of deformation and erosion of bone in this area. Instead, we interpret that the parapophysis is positioned further dorsally on the neural arch, closer to the diapophysis, as would be expected in a middle-posterior dorsal vertebra. Immediately anteroventral to the right diapophysis is an erosional surface that exposes internal camellate structures (Fig. 5B). Furthermore, the structure previously interpreted as the left diapophysis (Wiechmann, 1999b) is now recognized as the left parapophysis since it is at the same height on the neural arch as the inferred right parapophysis (Fig. 5A, B). This is further supported by the fact that the area posterodorsal to the left parapophysis is an eroded structure, implying the existence of the diapophysis on this side of the vertebra, as well as the remaining part of the left transverse process.

The vertebra is mostly complete but severely compressed, primarily in the anteroposterior direction and especially within the neural arch. The centrum is strongly convex anteriorly and concave posteriorly, and appears anteroposteriorly short, although this latter condition has probably been exaggerated by compression. The centrum is slightly wider than tall whereas the posterior cotyle is more subcircular but with eroded margins and the overall state of preservation obscures the true dimensions (Fig. 5A, C). However, the centrum does not reach the markedly wide extent seen in taxa such as *Pellegrinisaurus powelli* (Salgado, 1996; Cerda et al., 2021) and *Opisthocoelicaudia* (Borsuk-Bialynicka, 1977). The pleurocoels are ovate along their margins and unusually large, spanning almost the entire length of the centrum. Unlike in the other dorsal vertebrae, the dorsal surface of the right pleurocoel is nearly smooth whereas that of the left is lightly rugose. The pleurocoels extend deep into the centrum and, as evidenced by CT images, are separated only by a thin midline bony wall (Fig. 5B, 7B). The preserved portion of the neural arch is approximately as tall as the

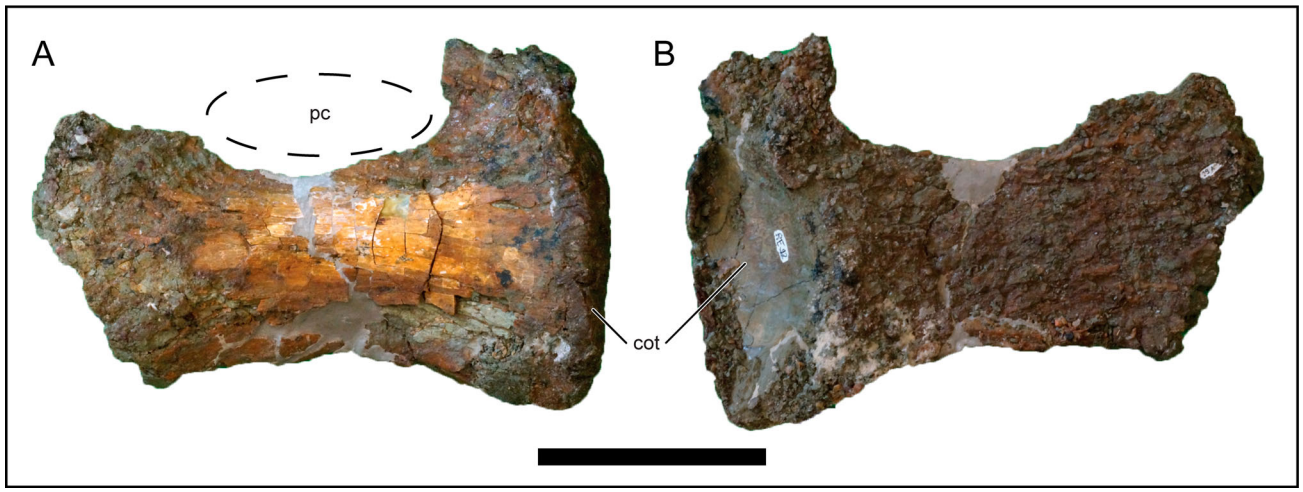

FIGURE 2. Middle–posterior dorsal vertebral centrum of *Igai semkhu* (Vb-621). **A**, left lateral; and **B**, internal views. **Abbreviations**: **cot**, cotyle; **pc**, pleurocoel. Scale bar equals 10 cm.

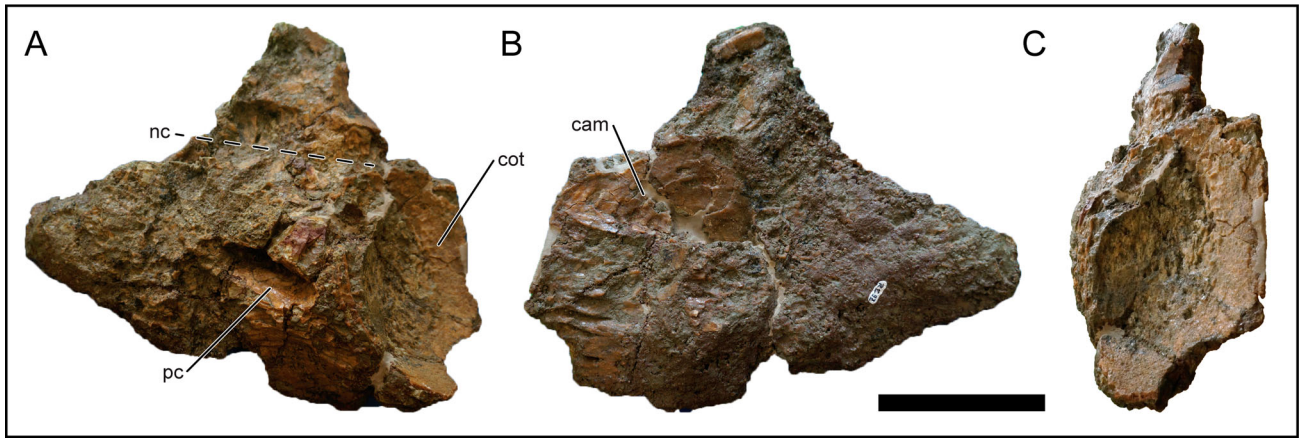

FIGURE 3. Partial middle–posterior dorsal vertebra of *Igai semkhu* (Vb-625). **A**, left lateral; **B**, right lateral; and **C**, posterior views. **Abbreviations**: **cam**, camellate internal texture; **cot**, cotyle; **nc**, neural canal; **pc**, pleurocoel. Scale bar equals 10 cm.

TABLE 1. Measurements (mm) of posterior dorsal vertebrae of *Igai semkhu* (Vb-621–640; from Wiechmann, 1999b). Specimen Vb-623 is regarded as the most anteriorly positioned of the three relatively well-preserved posterior dorsal vertebrae, whereas Vb-622 and Vb-624 were situated further posteriorly. The specific positions of Vb-621 and Vb-625 within the posterior dorsal series are uncertain. **Abbreviations**: +, element incomplete, dimension would have been greater in life; **?**, uncertain; **NR**, not reported by Wiechmann (1999b).

Measurement/element	Vb-621	Vb-625	Vb-622	Vb-623	Vb-624
Anteroposterior length, centrum	240+	263+	125?	115+	275
Dorsoventral height, centrum, anterior articular surface	122+	133+	133?	100+	130+
Transverse width, centrum, anterior articular surface	NR	NR	155?	115+	NR
Dorsoventral height, centrum, posterior articular surface	158+	NR	112?	115+	153+
Transverse width, centrum, posterior articular surface	NR	NR	146?	115+	NR
Anteroposterior length, neural arch	NR	NR	NR	NR	224+
Transverse width, neural arch	NR	NR	165+	257+	NR
Dorsoventral height, vertebra, total	NR	212+	325+	321+	325+

centrum. The neural canal is small, and teardrop shaped (with the acute end directed dorsally) along the margins of its anterior and posterior openings. Interestingly, the anterior floor of the neural canal exhibits a shallow fossa that does not appear to be a product of erosion because it is surrounded by a nearly smooth bony surface (Fig. 5G), whereas a similar condition is present in the caudal vertebrae of the geologically older and phylogenetically distant eusauropods *Wamweracaudia* and '*Bothriospondylus*' (Mannion et al., 2019).

Among the most distinctive features of the neural arch is the prominent, well-developed X-shaped lamina complex comprised by what Wiechmann (1999b) termed "supra-neural canal laminae" ("supraneuralkanalleiste") ventrally and likely a modified interprezygapophyseal lamina with the potential

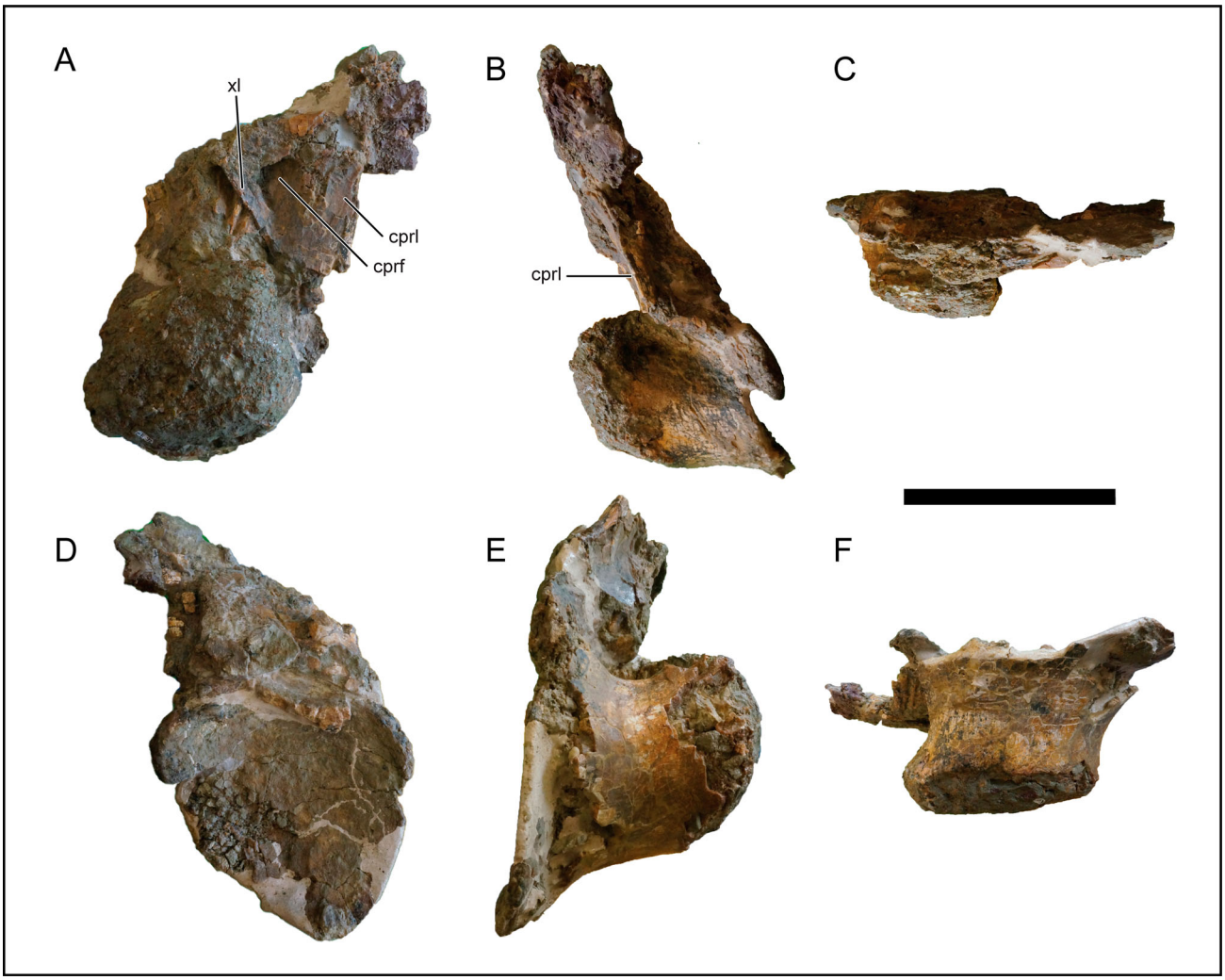

FIGURE 4. Middle-posterior dorsal vertebra of *Igai semkhu* (Vb-622). **A**, anterior; **B**, left lateral; **C**, dorsal; **D**, posterior; **E**, right lateral; and **F**, ventral views. **Abbreviations**: **cprf**, centroprezygapophyseal fossa; **cprl**, centroprezygapophyseal lamina; **xl**, X-lamina complex (see Description for details). Scale bar equals 10 cm.

development of accessory laminae to form the X-shape configuration. The ventral laminae of the X-lamina complex may potentially correspond to an accessory medial ramus of the centroprezygapophyseal lamina, given that a bilaterally paired centroprezygapophyseal lamina occurs in the dorsal vertebrae of *Saltasaurus loricatus* from the Upper Cretaceous of northern Argentina, although only in the anterior part of the series (e.g., Zurriaguz and Powell, 2015:fig. 7a). For consistency, we refer to this structure as the X-lamina complex (Fig. 5A) given its distinct morphology. The X-lamina complex is rare within Titanosauria, seen elsewhere only in posterior dorsal vertebrae of *Saltasaurus* (Zurriaguz and Powell, 2015), *Lirainosaurus* from the Upper Cretaceous of Spain but exhibits thicker laminae and smaller surrounding fossae (Díez Díaz et al., 2013a), and *Tapuiasaurus macedoi* from the Early Cretaceous of Brazil (Zaher et al., 2011:fig. 4a), albeit not as well-developed and defined as in *Igai*. The titanosauriform *Yongjinglong datangi* from the Lower Cretaceous of China also exhibits a similar condition in its dorsal vertebrae (Li et al., 2014). Immediately lateral to the X-lamina complex is a well-defined cavity that we interpret as the centroprezygapophyseal fossa following Wilson et al. (2011a) and Voegele et al. (2017). The X-lamina complex is bordered dorsally by a shallow midline fossa that is subequal to the neural canal in dorsoventral diameter. The anterior and posterior centroparapophyseal laminae are present on both sides, with the latter lamina less developed; however, these laminae on the left side are not as well-preserved (Fig. 5B, F). The postzygapophyses and centropostzygapophyseal laminae are not preserved. Interestingly, the right side of this dorsal vertebra preserves a well-defined 'unnamed diapophyseal lamina' that connects the diapophysis on the dorsal surface of the transverse process to the base of the confluent spinoprezygapophyseal + prezygapophyseal spinodiapophyseal fossa (i.e., anterior portion of the neural arch and dorsal to the neural canal). This enigmatic lamina is present in the dorsal vertebrae of *Saltasaurus* and *Neuquensaurus australis* (Zurriaguz and Powell, 2015) and does not appear to be present in any other titanosaurian (Fig. 5A, C). The parapophyses likely would have been placed ventral or slightly anteroventral to the diapophyses, a feature present in some European titanosaurians such as *Ampelosaurus* (Le Loeuff, 2005), *Lirainosaurus* (Díez Díaz et al., 2013a), *Lohuecotitan* (Díez Díaz et al., 2016), and *Paludititan* (Csiki et al., 2010), as well as the South American taxa *Saltasaurus* (Zurriaguz and Powell, 2015) and *Neuquensaurus* (Salgado et al., 2005).

Although middle–posterior dorsal vertebra Vb-624 consists of only the right half of the element, it includes several identifiable,

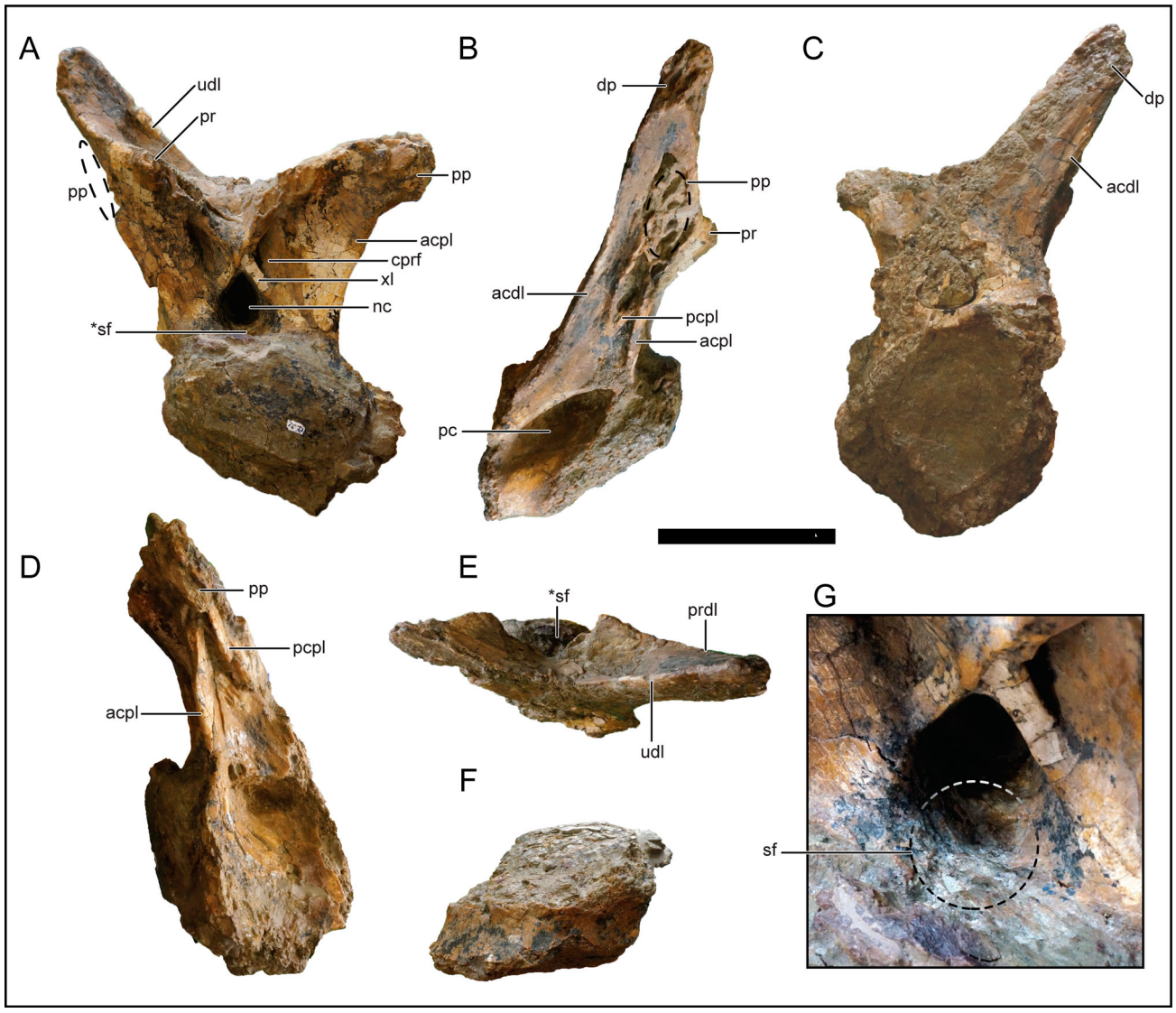

FIGURE 5. Posterior dorsal vertebra of *Igai semkhu* (Vb-623). **A**, anterior; **B**, right lateral; **C**, posterior; **D**, left lateral; **E**, dorsal; **F**, ventral; and **G**, close-up of neural canal in anterodorsal views. **Abbreviations**: **acdl**, anterior centrodiapophyseal lamina; **acpl**, anterior centroparapophyseal lamina; **cprf**, centroprezygapophyseal fossa; **dp**, diapophysis; **nc**, neural canal; **pc**, pleurocoel; **pcpl**, posterior centroparapophyseal lamina; **pp**, parapophysis; **pr**, prezygapophysis; **prdl**, prezygodiapophyseal lamina; **sf**, shallow fossa (asterisk denotes **G** inset view); **udl**, unnamed diapophyseal lamina; **xl**, X-lamina complex (see Description for details). **A**-**F** scale bar equals 10 cm.

informative laminae and portions of the neural arch that are not preserved in the other vertebrae (Fig. 6). Notably, the element lacks a postzygodiapophyseal lamina, a structure that is similarly absent in posterior dorsal vertebrae of many Laurasian titanosaurs (e.g., *Ampelosaurus*, *Opisthocoelicaudia*) and variably developed and oriented throughout the middle and posterior dorsal vertebral region in some South American taxa such as *Bonitasaura* (Gallina and Apesteguía, 2015), *Neuquensaurus* (Salgado et al., 2005), and *Trigonosaurus* (Campos et al., 2005; Wilson, 2012). There is no sign of this lamina, reduced or fully developed, spanning the area between the approximate locations of the diapophysis and postzygapophysis in Vb-624 (Fig. 6A). Eroded surfaces expose the camellate internal texture that is present in all other *Igai* vertebrae. The spool-shaped centrum is relatively elongate compared with those of the other dorsal vertebrae (Table 1), with the neural arch pedicel encompassing approximately half its length and being situated symmetrically over roughly the anteroposterior midline of the centrum. The anterior condyle is heavily eroded and the posterior cotyle appears to have been deep despite its incomplete preservation. The ventral surface may have a midline ridge, but this could also be an artifact of taphonomic distortion. The teardrop-shaped pleurocoel is deep, artificially appearing to completely pierce the centrum since the entire left half of the vertebra is missing. The pleurocoel itself appears set within a larger fossa. As in other dorsal vertebrae (Table 1), the posterior region of the dorsal margin of the pleurocoel exhibits several ridges. The partially preserved right wall of the neural canal is exposed on the left side of the element (Fig. 6B).

Several identifiable laminae are evident, exhibiting interesting configurations alongside associated accessory laminae; unfortunately, however, the transverse compression of the vertebra precludes assessment of any lateral or dorsolateral projection of these and other neural arch landmarks. Part of the right

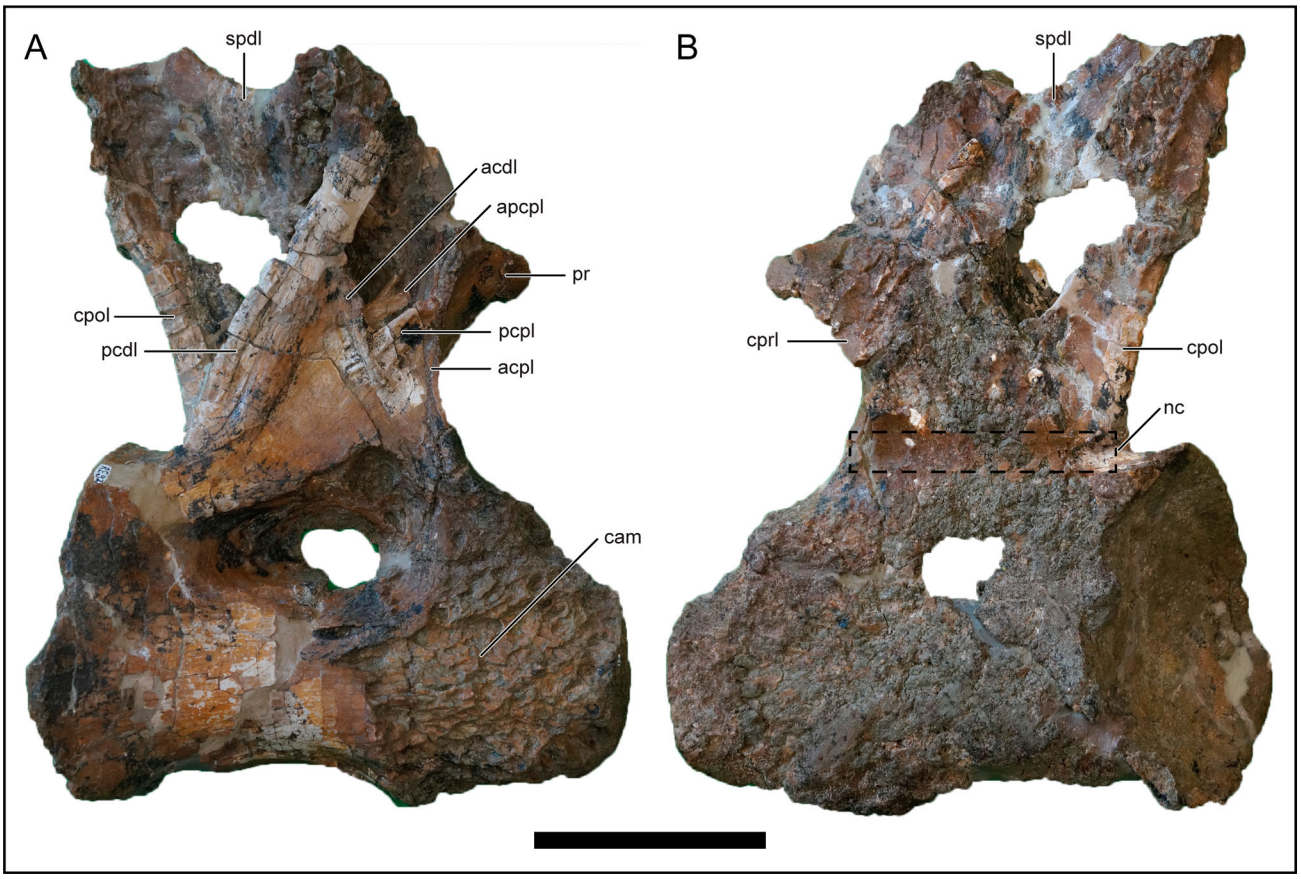

FIGURE 6. Posterior dorsal vertebra of *Igai semkhu* (Vb-624). **A**, right lateral; and **B**, left lateral views. **Abbreviations**: **acdl**, anterior centrodiapophyseal lamina; **acpl**, anterior centroparapophyseal lamina; **apcpl**, accessory posterior centroparapophyseal lamina; **cam**, camellate internal texture; **cpol**, centropostzygapophyseal lamina; **cprl**, centroprezygapophyseal lamina; **nc**, neural canal; **pcdl**, posterior centrodiapophyseal lamina; **pcpl**, posterior centroparapophyseal lamina; **pr**, prezygapophysis; **spdl**, spinodiapophyseal lamina. Scale bar equals 10 cm.

prezygapophysis is preserved, but its degree of inclination and the development of its articular facet have been obscured by erosion. The remnants of the postzygapophysis, parapophysis, and diapophysis are almost entirely eroded, but the laminae that connected these structures provide some indication of their respective locations. The centroprezygapophyseal lamina is singular and curves anterodorsally to the base of the prezygapophysis. Both the anterior and posterior centroparapophyseal laminae have wide ventral bases and merge at roughly half their lengths toward the eroded parapophysis. A less prominent ridge extends parallel and immediately ventral to the posterior centroparapophyseal lamina. Interestingly, an accessory lamina, which bifurcates anterodorsally, within the parapophyseal centrodiapophyseal fossa extends parallel and dorsal to the posterior centroparapophyseal lamina (see Fig. 6A, "apcpl"). This resembles the 'unnamed parapophyseal lamina' present in the saltasaurines *Neuquensaurus* and *Rocasaurus muniozi* (Salgado et al., 2005); however, this lamina is better developed in these taxa. This accessory lamina is also more notably developed in *Diamantinasaurus* from Australia, in which it has been described as a dorsal posterior parapophyseal lamina (Poropat et al., 2021). A lamina in this fossa that is similar in development to that seen in *Igai* appears present in *Lirainosaurus* (Díez Díaz et al., 2013a: fig. 4c), where it does not intersect the centroparapophyseal or centrodiapophyseal laminae. These parallel parapophyseal laminae tend to be common within titanosauriforms (D'Emic, 2012; Mannion et al., 2013). The anterior centrodiapophyseal lamina is present and intersects the posterior centrodiapophyseal lamina near the midpoint of the latter (Fig. 6A). This latter lamina is anteroposteriorly thick and its ventral portion is incipiently divided by a shallow groove. The centropostzygapophyseal lamina is singular and nearly vertical. As mentioned above, the postzygodiapophyseal lamina is absent in this dorsal vertebra of *Igai* but the other dorsal vertebrae do not preserve this region to assess the variation of this lamina along the vertebral column. The preserved remnant of the spinodiapophyseal lamina is short and curved dorsally upon the neural spine remnant (Fig. 6A).

Computed tomographic (CT) scans of the dorsal vertebrae were taken to investigate their internal morphology and pneumatic qualities (Fig. 7). All are fully camellate, corresponding to the somphospondylous pattern of pneumaticity (e.g., Wedel et al., 2000; Wedel, 2003). The centrum typically contains only small camellae and deep, elliptical pleurocoels, whereas the neural arch houses a few larger, rounded camellae that are mostly related with the pneumatization of the diapophysis. The typical somphospondylous pattern of honeycomb-shaped camellae is most evident in anterior and lateral cross-sectional views (Fig. 7). Pneumatic camellae within the centrum are mostly torpedo-shaped, with an average length of 10–20 mm, a width of 3–9 mm, and a height of 5–10 mm (Fig. 7C). The camellae are evenly distributed between the anterior condyle and the pleurocoel, but less ordered and ovoid in shape more posteriorly, with some variation toward the dorsal part of the centrum.

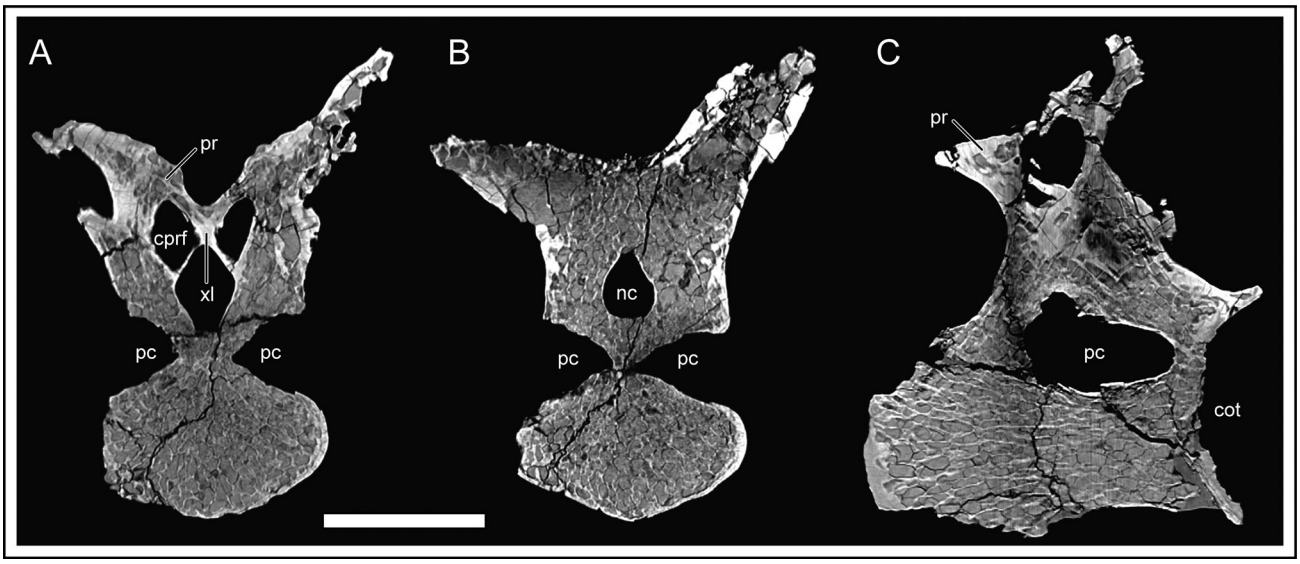

FIGURE 7. Computed tomographic (CT) scans of posterior dorsal vertebrae of *Igai semkhu* Vb-623 in **A**, coronal cross section view taken near anterior end of vertebra and **B**, coronal cross section view taken near mid-length of vertebra; and Vb-624 in **C**, right parasagittal cross section view. **Abbreviations**: **cot**, cotyle; **cprf**, centroprezygapophyseal fossa; **nc**, neural canal; **pc**, pleurocoel; **pr**, prezygapophysis; **xl**, X-lamina complex (see Description for details). Scale bar equals 10 cm.

Locally, clusters of smaller camellae are interwoven within the general pattern. The posterior cotyle is hollowed out, with more rectangular and evenly distributed camellae up to the rim of this structure (Fig. 7C). The dorsal vertebral pleurocoels are elliptical at their outermost margins and penetrate relatively deeply into the centra. The pleurocoels are funnel-shaped, narrowing in diameter toward their deepest extent (Fig. 7B). Openings along the anterodorsal and posterior margins of the pleurocoel often communicate with the camellae within the neural arch and posterior cotyle. Other communicating pneumatic foramina are present within the prezygapophyseal centrodiapophyseal fossa (e.g., Vb-623) and are typically elliptical in shape. The ventral surface of the pleurocoel is generally smooth as it transitions to the remainder of the centrum. The dorsal surface of the pleurocoel varies with the presence of a few, subtle laminae, and is sharp-lipped at its margin with the rest of the centrum and neural arch.

The pneumatic architecture of the anteroventral region of the prezygapophysis (see, e.g., vertebra Vb-623) is similar to that of the centrum (Fig. 7A); however, the dorsal half is only pneumatized medially to the anteriormost tip and along the margin of the articular surface. Here, the camellae are rounder and larger than in the centrum (length 13–18 mm, width 9–13 mm) and oriented with their long axis in the vertical plane with the prezygapophysis. Between the neural arch and the prezygapophyseal articular surface is a complex of smaller cavities (Fig. 7B). In vertebra Vb-624, the interior of the prezygapophysis consists only of isolated, slightly larger camellae (Fig. 7C). The postzygapophyseal region is comprised by small, rounded camellae like those in the base of the neural arch. The remainder of the neural arch (including the diapophysis) is fully pneumatized by small cavities and a few larger, rounded camellae. These are generally evenly distributed, slightly larger, and more rectangular than those in the centrum. Even the laminae, such as the X-lamina complex, are pneumatized by diminutive camellae (Fig. 7A). The centroprezygapophyseal fossae diminish in cross section and adopt a more rounded triangular shape the deeper they penetrate the vertebra; moreover, they have some connections to the adjacent pneumatic camellae. The neural canal is not connected to the surrounding pneumatic structures in the neural arch (Fig. 7B). Dorsal to the prezygodiapophyseal lamina and prezygapophysis, the camellae are more rectangular (roughly 6–12 mm in both length and width) and have crosshatched walls; some of these are oriented obliquely anteroventrally–posterodorsally whereas others are posteroventrally–anterodorsally oriented. The neural arch is filled with many small, thin-walled, irregular, slightly vertically oriented cavities with sigmoidal vertical walls that can themselves contain sub-chambers (Fig. 7B, C). Toward the posterior part of the neural arch, the pneumatic cavities appear smaller and less ordered in the center but larger on the lateral side. In Vb-624, the dorsal, laminar part of the remnant neural spine is preserved and filled with larger, isolated camellae (Fig. 7C). The diapophysis is fully pneumatized by two large, rounded camellae in its anterior half and some smaller, rounded camellae parallel to its dorsal margin. The posterior diapophyseal process exhibits a deep pneumatic cavity that is developed into a canal. In this part, the dorsal half of the diapophysis is filled with small, subrectangular camellae and houses another large chamber in its ventral half.

All *Igai* dorsal vertebrae show a fully camellate pattern of internal bony structure that is comparable to that seen in vertebrae of other somphospondylous titanosauriforms (Wedel et al., 2000; Wedel, 2003; Aureliano et al., 2021). The architecture and distribution of the camellae appears similar to the patterns observed in cervical vertebrae of *Uberabatitan ribeiroi* (Silva Junior et al., 2019:figs. 3, 4; Aureliano et al., 2020), *Bonitasaura salgadoi* (Gallina and Apesteguía, 2015:fig. 4), and possibly *Sarmientosaurus musacchioi* (Martínez et al., 2016), the dorsal vertebrae of indeterminate titanosaurs from Brazil (Castro et al., 2007), a dorsal neural spine of *Alamosaurus* (see Wedel, 2003: fig. 11a, b), the dorsal centra of *Austrosaurus mckillopi* (Longman, 1933:fig. 3; Poropat et al., 2017) and *Savannasaurus elliottorum* (Poropat et al., 2020:figs. 6c, 7d), and the caudal vertebrae of *Yamanasaurus lojaensis* (Apesteguía et al., 2020). *Saltasaurus* is also extensively pneumatized, but has a more spongy pattern of pneumatic cavities in the dorsal centra, with larger

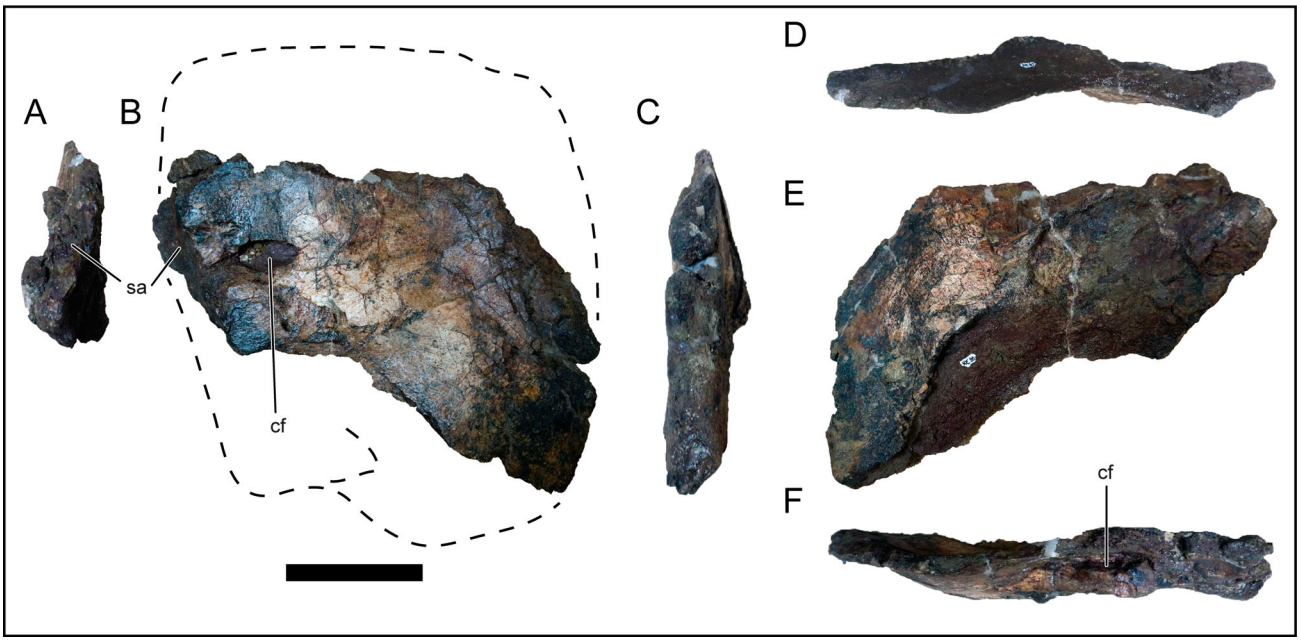

FIGURE 8. Left coracoid of *Igai semkhu* (Vb-627). **A**, posterior; **B**, medial; **C**, anterior; **D**, dorsal; **E**, lateral; and **F**, ventral views. **Abbreviation**: **cf**, coracoid foramen; **sa**, scapula articulation. Scale bar equals 10 cm.

and less clearly separated camellae (Powell, 1986:pl. 30; Wedel, 2003:fig. 11e, f). However, a figured CT section of a caudal vertebra of this Argentinean titanosaur (Cerda et al., 2012; Zurriaguz and Cerda, 2017:fig. 4m) shows a pattern of pneumatic camellae similar to that in dorsal vertebrae of *Igai*, so this variation might be local or regional within the postcranial axial skeleton. Furthermore, middle caudal vertebrae of *Rocasaurus* (Cerda et al., 2012; Zurriaguz and Cerda, 2017:fig. 4a–l) exhibit a somphospondylous pattern of camellae comparable to that observed in dorsal vertebrae of *Igai*. Camellate texturing in the presacral vertebrae has been confirmed in *Malawisaurus dixeyi* (Gomani, 2005); however, as illustrated by Wedel and Taylor (2013:fig. 1), one caudal neural arch of this African taxon has an internal pattern of pneumaticity resembling that in dorsal vertebrae of *Igai*. Due to the taphonomic flattening of all *Igai* vertebrae, the presence of the circumferential camellae in the cotylar area and the internal bony plate that supports these structures described in a small-bodied saltasaurid from the Upper Cretaceous of Brazil (Aureliano et al., 2021) cannot be confirmed in the new Egyptian taxon.

Appendicular Skeleton

Coracoid—The left coracoid (Vb-627) is missing substantial portions dorsally and ventrally (Fig. 8). Judging from fortuitous breaks, the bone appears apneumatic, unlike the rare condition in saltasaurines that exhibit a partially pneumatized coracoid as in *Saltasaurus* (Cerda et al., 2012). The medial (i.e., internal) and lateral (external) surfaces are slightly concave and convex, respectively. There appears to be a modest mediolateral thickening in the anterior half of the coracoid, best visible in dorsal and ventral views (Fig. 8D, F). The coracoid foramen is evident on both the lateral and medial surfaces of the element. It is ovoid with its long axis oriented anteroposteriorly and is fully enclosed by bone. A small part of the scapular articulation is preserved, demonstrating that the coracoid was not—at least at this location—fully co-ossified to the scapula at the time of death of this individual of *Igai* (Fig. 8A, B). The preserved portion of Vb-627 generally resembles the corresponding area of the coracoid of *Mansourasaurus*, which is also from the Campanian Quseir Formation of Egypt (Sallam et al., 2018). This, however, is not necessarily indicative of a close relationship between these titanosaurs, as the *Mansourasaurus* coracoid differs from that of *Igai* in having a more circular coracoid foramen that is located at the scapular articulation and thus not fully enclosed by bone (see below). Nevertheless, the ontogenetic stage of the *Mansourasaurus* holotype is unclear, given that it has yet to be subjected to osteohistological analysis; moreover, whereas the centra of the three preserved cervical vertebrae are fully fused to their respective neural arches, the scapula and coracoid appear only partially co-ossified (Sallam et al., 2018). Small nutrient foramina are evident across the medial surface of the *Igai* coracoid.

Ulna—The left ulna Vb-631 is generally poorly preserved and missing most of its posterolateral portion; nevertheless, the anteromedial process and the base of the moderately developed olecranon process are largely intact but compressed, forming a concave articular surface for the humerus on the proximal end (Fig. 9). As is typical of sauropods, this surface is slightly rugose in a manner that suggests the attachment of cartilage. The anteromedial process is subtriangular at its proximal corner, the medial margin of the ulnar shaft is slightly concave, and the distal end is rounded and moderately expanded mediolaterally. The distal end also appears to either bow or slightly expand posteromedially as preserved, and the anterior surface of this end appears to preserve part of an interosseous ridge along its medial margin (Fig. 9B, D). Overall, and like the other limb bones (see also below), the preserved part of the *Igai* ulna gives the impression of a long, gracile element, comparable in slenderness to that of *Atsinganosaurus* (Díez Díaz et al., 2018:fig. 10k–p), *Mendozasaurus neguyelap* (González Riga et al., 2018:fig. 16e–h), and the juvenile *Rapetosaurus krausei* FMNH PR 2209 (Curry Rogers, 2009:fig. 37). It is considerably less robust than the ulnae of stout-limbed titanosaurians such as *Aeolosaurus rionegrinus* (Powell, 2003:pl. 12, fig. 3), *Dreadnoughtus* (Lacovara et al., 2014; Ullmann and Lacovara, 2016), *Elaltitan lilloi* (Mannion and Otero, 2012:fig. 7e–h), *Isisaurus colberti* (Jain

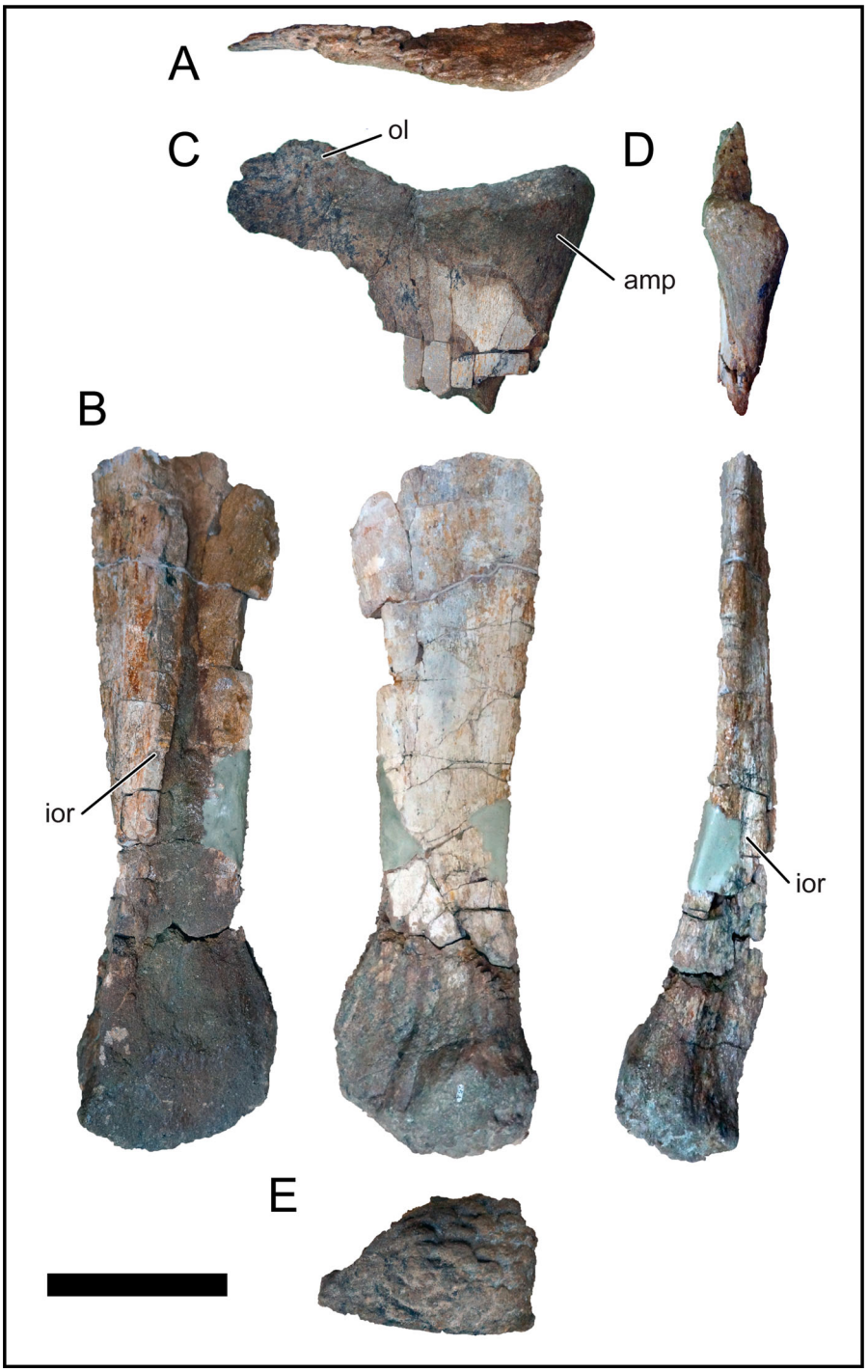

FIGURE 9. Left ulna of *Igai semkhu* (Vb-631). **A**, proximal; **B**, lateral; **C**, medial; **D**, anterior; and **E**, distal views. **Abbreviations**: **amp**, anteromedial process; **ior**; interosseus ridge; **ol**, olecranon process. Scale bar equals 10 cm.

and Bandyopadhyay, 1997:figs. 21c, d, 22), *Opisthocoelicaudia* (Borsuk-Bialynicka, 1977), and saltasaurines such as *Neuquensaurus* and *Saltasaurus* (e.g., Powell, 1992, 2003; Otero, 2010). The ulna also seems slightly more gracile than those of taxa such as *Aegyptosaurus baharijensis* (Stromer, 1932:pl. I, fig. 2), *Ampelosaurus* (Le Loeuff, 2005:fig. 4.15), *Bonitasaura* (Gallina and Apesteguía, 2015:fig. 12d–h), *Lirainosaurus* (Díez Díaz et al., 2013b:fig. 3.5–8), *Pitekunsaurus macayai* (Filippi and Garrido, 2008:fig. 8.2), and perhaps *Argyrosaurus superbus* (Mannion and Otero, 2012:fig. 2f, g). Apart from the lateral surface of the anteromedial process, the anterolateral side of the proximal end has been almost completely 'sheared off,' exposing the interior of the bone.

Metacarpus—Three left metacarpals (I, IV, and V; Vb-639, Vb-638, and Vb-633, respectively) were recovered from the *Igai* quarry. As is the case for most other elements, metacarpals I and IV are strongly compressed; metacarpal V, however, remains largely or perhaps even entirely undeformed. The compression of metacarpals I and IV has complicated their interpretation, as most osteological features have been reduced in prominence and/or obscured as a result; nevertheless, we are confident in our identifications of these bones based on comparisons

FIGURE 10. Left metacarpal I of *Igai semkhu* (Vb-639). **A**, medial; **B**, palmar; **C**, lateral; **D**, dorsal; **E**, proximal; and **F**, distal views. **Abbreviations**: **II**, articulation with metacarpal II; **rid**, ridge. Scale bar equals 10 cm.

to the metacarpus of other titanosaurians (e.g., *Alamosaurus*, *Argyrosaurus*, *Choconsaurus baileywillisi*, *Lirainosaurus*). Generally, metacarpals I and IV are mediolaterally compressed. As is the case for other *Igai* appendicular elements, all appear to have been slender, consistent with a relatively gracile-limbed animal.

Wiechmann (1999b) identified Vb-639 as a metacarpal but did not assign it to a more specific position. One surface is convex, whereas the opposite surface is nearly flat but with a slight concavity for articulation with the adjacent metacarpal (Fig. 10), demonstrating that it represents either a medialmost or a lateralmost metacarpal. Given that the lateralmost left metacarpal (V) was also recovered (see description of Vb-633 below), and differs significantly in morphology from Vb-639, this leaves the medialmost metacarpal (I) as its only likely identity. Accordingly, we identify Vb-639 as a metacarpal I; the convex surface is therefore the medial side and the opposing surface is the lateral side. The proximal and distal ends of the metacarpal are partially eroded (the latter more so than the former), but the element is otherwise well preserved, exhibiting only minor cracks and crushing artifacts. However, determining whether it pertains to the left or the right side of the animal is not straightforward due to the compression and the relative incompleteness of the articular ends. Considering that the remaining two metacarpals are from the left side, we tentatively suggest that Vb-639 is the left metacarpal I. The proximal and distal ends are slightly expanded along the dorsopalmar axis, lending the element an hourglass shape, although this is less marked than in the first metacarpals referred to *Atsinganosaurus* (Díez Díaz et al., 2018) and *Garrigatitan* (Díez Díaz et al., 2021). The proximal end is teardrop-shaped in proximal view, with the converging edges pointing toward the palmar region (Fig. 10E). The medial surface is gently concave along its long axis, whereas the lateral surface is nearly flat, consistent with bordering metacarpal II. A low, proximodistally aligned ridge or thickening is present within the proximal area of the medial surface, extending toward midshaft (Fig. 10A). The surface of the distal end is fragile, being internally composed of a loosely consolidated amalgamation of bone and sandy matrix. The distal end appears slightly bowed like in *Atsinganosaurus* (Díez Díaz et al., 2021:fig.10a–f), but is more markedly present in titanosaurs such as *Andesaurus delgadoi* (Mannion and Calvo, 2011), and *Argyrosaurus* (Mannion and Otero, 2012). The generally poor state of preservation precludes any further definitive statements regarding the morphology of the distal articular surface. There appear to be two subtle ridges on the medial surface of the distal end, suggesting the original presence of weakly developed condyles. Overall, metacarpal I of *Igai* closely resembles that of *Mnyamawamtuka moyowamkia* from Tanzania (Gorscak and O'Connor, 2019).

Although Wiechmann (1999b) identified Vb-638 as the left metacarpal III, we suggest this element is most likely the left metacarpal IV based on the morphology of its proximal end, comparisons to the articulated metacarpus of other titanosaurians, and the

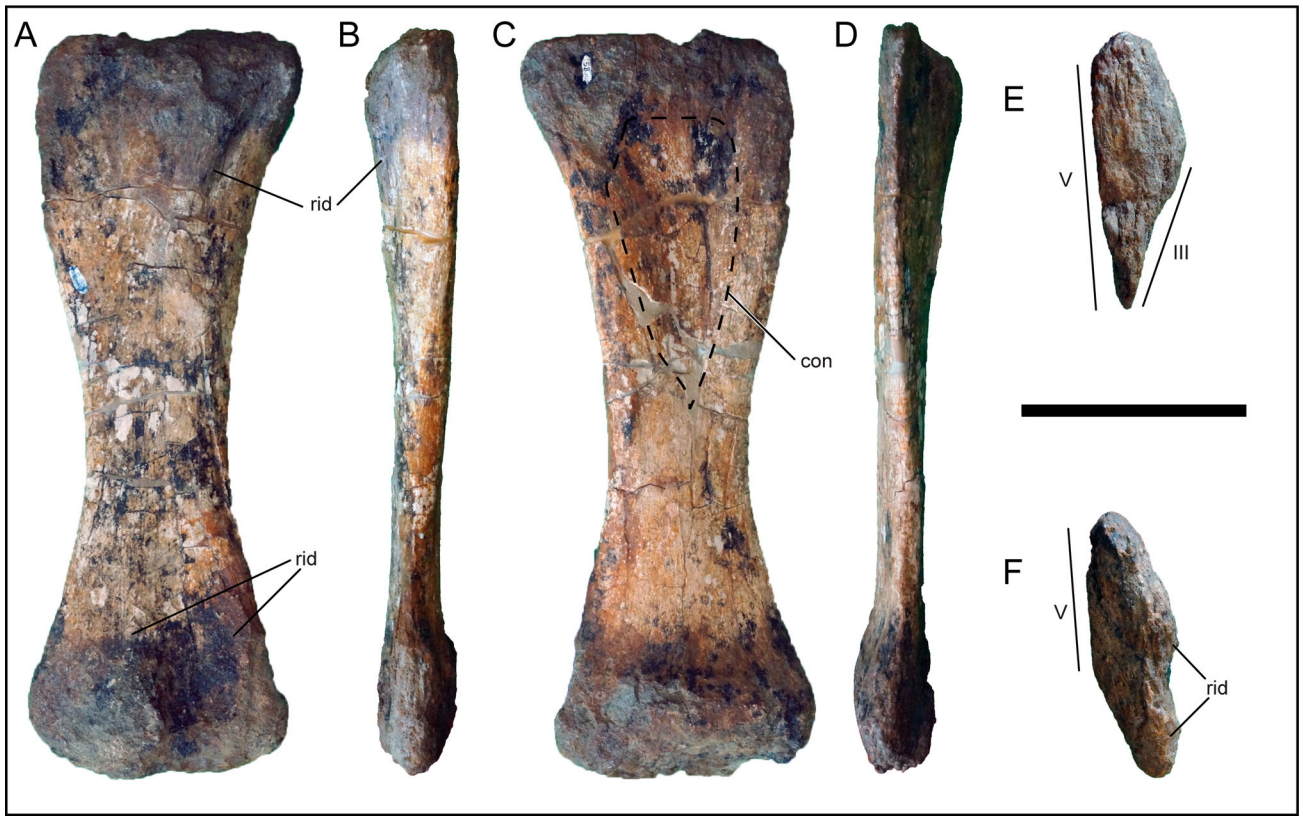

FIGURE 11. Left metacarpal IV of *Igai semkhu* (Vb-638). **A**, medial; **B**, palmar; **C**, lateral; **D**, dorsal; **E**, proximal; and **F**, distal views. **Abbreviations**: **III**, articulation with metacarpal III; **V**, articulation with metacarpal V; **con**, concavity; **rid**, ridge. Scale bar equals 10 cm.

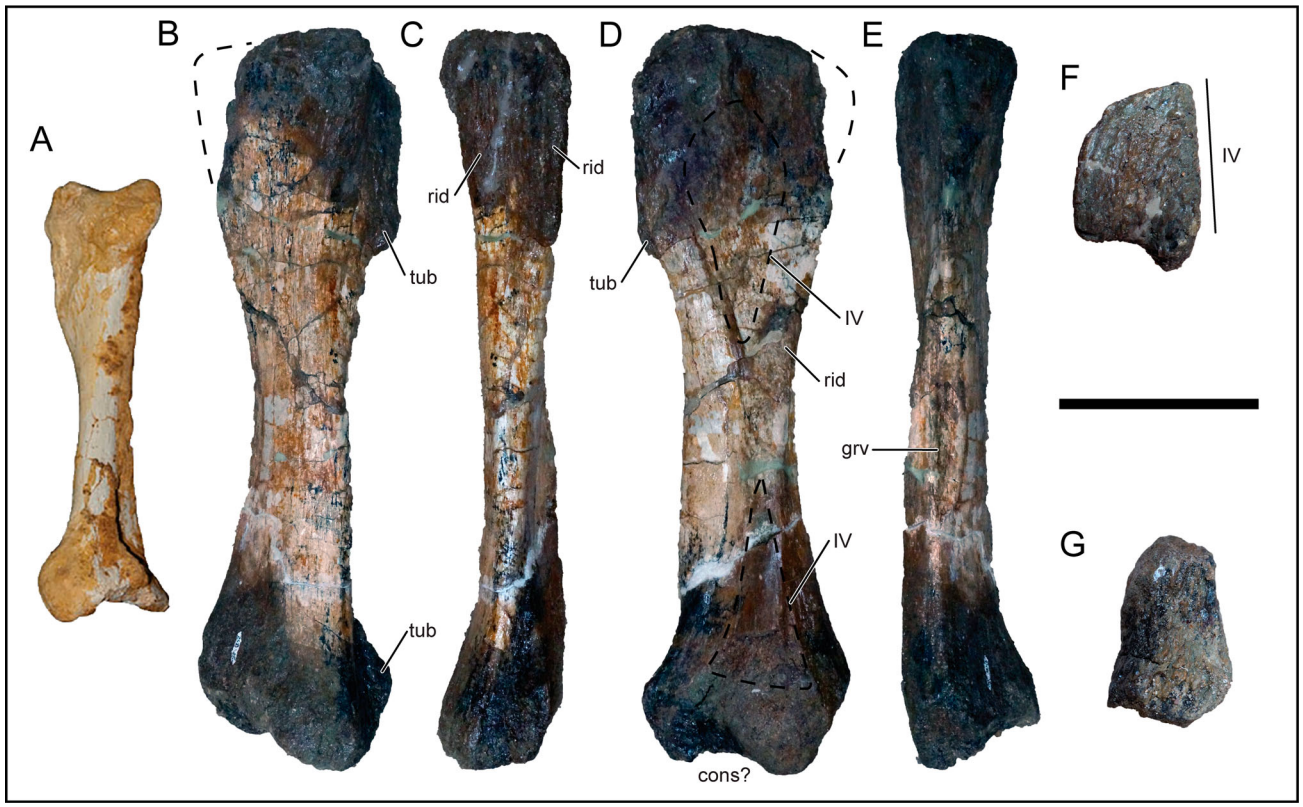

FIGURE 12. Left metacarpal V of *Igai semkhu* (Vb-633) (**B**–**G**) and *Lirainosaurus astibiae* (MCNA 14474) (**A**). **A** and **B**, lateral; **C**, palmar; **D**, medial; **E**, dorsal; **F**, proximal; and **G**, distal views. **Abbreviations**: **IV**, articulation with metacarpal IV; **cons?**, possible distal condyles; **grv**, groove; **rid**, ridge; **tub**, tubercle. Scale bar equals 10 cm.

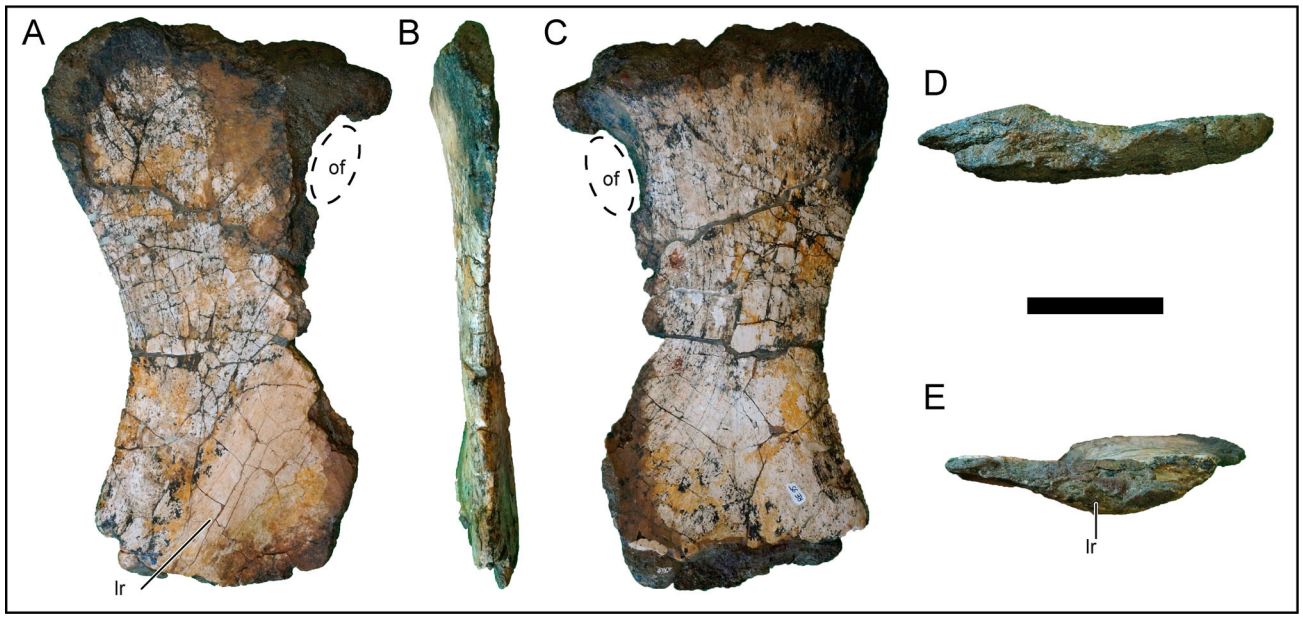

FIGURE 13. Left pubis of *Igai semkhu* (Vb-628). **A**, lateral; **B**, anterior; **C**, medial; **D**, proximal; and **E**, distal views. **Abbreviations**: **lr**, lateral ridge; **of**, obturator foramen. Scale bar equals 10 cm.

near-perfect fit between this bone and Vb-633 (identified as the left metacarpal V) when directly articulated. The proximal end of Vb-638 is subtriangular (Fig. 11E), with the medial margin slightly concave to articulate with metacarpal III and the lateral margin nearly flat to accommodate metacarpal V, a condition seen in many titanosaurians (e.g., *Argyrosaurus*, *Rapetosaurus*). The element is compressed mainly along the mediolateral axis, with a slight degree of oblique compression along the dorsopalmar axis as suggested by the alignment of the slightly rounded distal condyles. Metacarpal IV resembles metacarpal I in being generally hourglass-shaped with expanded proximal and distal ends. The proximal part of the medial surface exhibits a shallow ovoid fossa between two low, rounded ridges that would have articulated with metacarpal III (Fig. 11A). The proximopalmar margin is more expanded than its proximodorsal counterpart, which is more rounded. The palmolateral margin aligns nearly perfectly with the palmomedial margin of metacarpal V; however, the dorsomedial margin of the latter element is not fully preserved (see below). The lateral surface of Vb-638 is slightly convex proximally, but its distal half is nearly flat (Fig. 11C). The subrectangular distal end has two subtle medial ridges that may be partially preserved condyles; however, the distal and lateral margins of this end are slightly eroded and too taphonomically compressed for positive identification (Fig. 11A).

Specimen Vb-633 is the least deformed and most informative of the *Igai* metacarpals (Fig. 12B–G). Originally identified as the left metacarpal II by Wiechmann (1999b), the bone is currently recognized as the left metacarpal V as it articulates well with Vb-638. Moreover, its generally convex lateral surface lacks morphologies that would indicate articulation with another metacarpal. Furthermore, the element bears a general resemblance to MCNA 14474, a left metapodial of *Lirainosaurus* that was previously identified as metatarsal III but is now reinterpreted as metacarpal V (contra Díez Díaz et al., 2013b). Overall, metacarpal V also resembles that of *Argyrosaurus* from the Upper Cretaceous of Argentina (Mannion and Otero, 2012), and also bears some resemblance to that of *Alamosaurus* from North America, although the best-preserved metacarpus of the latter is also somewhat deformed and fragile (USNM 15560; E.G. pers. obs. 2014). Metacarpal V is narrowly hourglass shaped with slightly expanded proximal and distal ends. The proximal end is missing part of the dorsal margin, and the distal end is partially eroded. Interestingly, metacarpal V appears to bear incipient distal condyles (Fig. 12D), which may suggest the presence of a phalanx that is uncommonly seen in other titanosaurians such as the metacarpal IV of *Epachthosaurus* and *Opisthocoelicaudia* (Borsuk-Bialynicka, 1977; Martínez et al., 2004). The medial edge of the proximal articular surface is flat, whereas the lateral margin is convex. The palmar portion is concave, such that metacarpal V is somewhat heart-shaped in proximal view (Fig. 12F). This concavity persists along the proximal one-quarter of the palmar surface, defined by a small ridge laterally and a larger ridge medially (Fig. 12C). This medial ridge terminates in a pronounced proximomedial tubercle (Fig. 12B, D). The proximal region of the medial surface is largely flat. The dorsal margin of the metacarpal persists distally as a sharp angle between the medial and lateral regions. The lateral face is largely smooth and convex but is otherwise featureless. On the medial face at mid-length, close to the dorsal margin, is a low, rounded ridge that persists to the eroded distal end that is like the dorsomedial flange in the metacarpal V of *Mendozasaurus*, *Muyelensaurus pecheni*, and *Petrobrasaurus puestohernandezi* (González Riga et al., 2018). On the distal end, opposite the abovementioned proximomedial tubercle, there is another pronounced tubercle that appears unique to *Igai* (Fig. 12B). These tubercles appear not as well-defined or absent in *Alamosaurus*, *Argyrosaurus*, *Epachthosaurus*, *Lirainosaurus* (Fig. 12A), *Mendozasaurus*, and *Rapetosaurus*, and are therefore considered autapomorphic of *Igai*. A similar feature appears present on the distal end of metacarpal V of the Australian titanosaur *Diamantinasaurus* (termed the palmomedial bulge by Poropat et al., 2015), but it is not as well-defined as in *Igai*.

Pubis—The left pubis Vb-628 is a generally flat, plate-like bone that is lacking almost all the shaft; however, the element

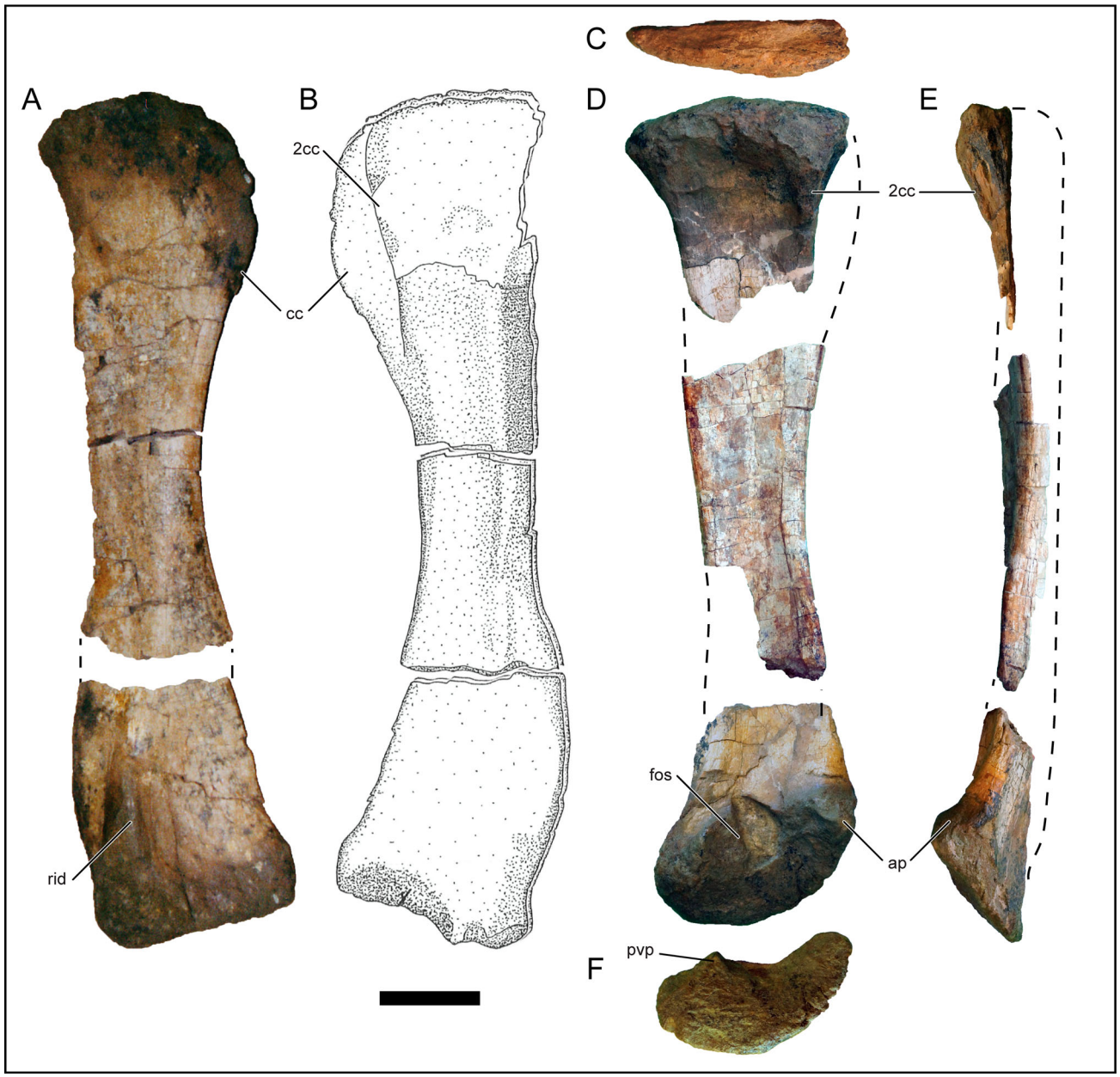

FIGURE 14. Left tibia (Vb-634) (**A**, **B**) and right tibia (Vb-630) (**C**–**F**) of *Igai semkhu* (**B** modified from Wiechmann, 1999b:fig. 24b). **A**, medial; **B** and **D**, lateral; **C**, proximal; **E**, anterior; and **F**, distal views. **Abbreviations**: **2cc**, 'second' cnemial crest; **ap**, articular surface for ascending process of astragalus; **cc**, cnemial crest; **fos**, fossa; **pvp**, posteroventral process; **rid**, ridge. Scale bar equals 10 cm.

has been taphonomically compressed and has therefore lost most of its original mediolateral depth and curvature (Fig. 13). Most of the posterior (i.e., the posteromedial, in life) edge is missing, including the posterior margin of the obturator foramen (Fig. 13A, C). The iliac peduncle and the acetabular margin are reasonably well-preserved on the proximal end of the bone, and, despite the compression, their proximal faces appear to have been nearly aligned with one another. The anterior edge of the obturator foramen is intact, indicating that this opening was ovoid in contour with its long axis oriented proximodistally, seemingly subparallel to the preserved anterior and posterior margins of the shaft. In life, the foramen was probably fully enclosed by bone, with rare exceptions such as *Bonitasaura* MPCA 460 that may be related to ontogeny (Gallina and Apesteguía, 2015).

As in other sauropods, the anterior margin of the proximal end of the pubic shaft is concave. There is a proximodistally oriented ridge on the lateral surface (Fig. 13A), as in many other titanosaurs such as *Dreadnoughtus* (Ullmann and Lacovara, 2016), *Futalognkosaurus dukei* (Calvo et al., 2007), *Isisaurus* (Jain and Bandyopadhyay, 1997), and *Uberabatitan* (Salgado and de Souza Carvalho, 2008), but its original prominence, whether due to general shaft convexity or a truly developed ridge as in the mentioned taxa, is unclear due to taphonomic compression. The anterior margin of this ridge is clearly defined, but its posterior portion grades smoothly into

FIGURE 15. Left fibula of *Igai semkhu* (Vb-635). **A**, lateral; **B**, posterior; **C**, medial; **D**, anterior; **E**, proximal; and **F**, distal views. **Abbreviations**: **con**, concavity; **grv**, groove; **lt**, lateral tuberosity; **pit**, pits; **se**, secondary eminence. Scale bar equals 10 cm.

the remainder of the bone. Following Borsuk-Bialynicka's (1977) study of *Opisthocoelicaudia*, Wiechmann (1999b) regarded this ridge as an attachment site for the M. puboischiofemoralis externus; more specifically, it may correspond to the origin of the M. puboischiofemoralis externus I, with the second head of this muscle originating nearer to the distal end of the pubis (Voegele et al., 2021). The ridge is angled more steeply anterodistally–posteroproximally than is the anterior edge of the pubic shaft, such that the anterior margin and the ridge converge distally. The symphysis with the contralateral pubis (i.e., the posterior margin of the proximal end of the pubic shaft) is mostly incomplete; however, approximately 25 mm of this symphysis is intact, and demonstrates that the proximal shaft of Vb-628 is 186 mm in anteroposterior (i.e., anterolateral–posteromedial, in life) breadth. As such, the proximal portion of the pubic shaft was likely proportionally narrow compared with those of many other titanosaurs; however the extent of the narrowness or if the shaft expanded distally is unknown at this time.

Tibia—Both tibiae were originally preserved, the left (Vb-634) nearly complete and the right (Vb-630) substantially less so, especially proximally and on its medial side (Fig. 14). Regrettably, the better-preserved left tibia cannot currently be located; as such, our description of the tibia of *Igai* is based primarily on firsthand observations of the right element, supplemented by the images and description of the left tibia provided by Wiechmann (1999b) and photos of this bone taken by J. Smith and one of us (M.C.L.) during a visit to the FUB in the first half of 2000. Overall, and as is the case for the other limb elements of *Igai*, both tibiae are slender for a titanosaurian; this is especially evident in the left element. In this sense, the tibia of *Igai* is generally comparable to those of taxa such as *Abditosaurus* (Vila et al., 2022:suppl. fig. 26), *Aegyptosaurus* (Stromer, 1932:pl. I, fig. 6), *Ampelosaurus* (MDE C3-1303; Le Loeuff, 2005:fig. 4.19a–c),

TABLE 2. Measurements (mm) of appendicular elements of *Igai semkhu* (Vb-621–640; from Wiechmann, 1999b). **Abbreviations**: **+**, element incomplete, dimension would have been greater in life; **L**, left; **R**, right.

Element/measurement	
Coracoid^{L} (Vb-627)	
Anteroposterior length	357+
Dorsoventral height	185+
Anteroposterior length, coracoid foramen, medial surface	48+
Dorsoventral height, coracoid foramen, medial surface	24+
Ulna^{L} (Vb-631)	
Proximodistal length	658
Mediolateral width, proximal	185+
Mediolateral width, distal	173+
Minimum circumference, shaft	300+
Metacarpal I^{L} (Vb-639)	
Proximodistal length	343
Mediolateral width, proximal	88
Mediolateral width, distal	85
Minimum circumference, shaft	133
Metacarpal IV^{L} (Vb-638)	
Proximodistal length	332
Mediolateral width, proximal	119
Mediolateral width, distal	116
Minimum circumference, shaft	148
Metacarpal V^{L} (Vb-633)	
Proximodistal length	341
Mediolateral width, proximal	95+
Mediolateral width, distal	93+
Minimum circumference, shaft	138
Pubis^{L} (Vb-628)	
Proximodistal length	400+
Anteroposterior breadth, proximal	237+
Anteroposterior breadth, distal	180+
Tibia^{L} (Vb-634)	
Proximodistal length	812
Mediolateral width, proximal	223+
Mediolateral width, distal	197
Minimum circumference, shaft	264
Tibia^{R} (Vb-630)	
Proximodistal length	810
Mediolateral width, proximal	207+
Mediolateral width, distal	165
Minimum circumference, shaft	247
Fibula^{L} (Vb-635)	
Proximodistal length	845
Anteroposterior breadth, proximal	183
Anteroposterior breadth, distal	130+
Minimum circumference, shaft	194
Metatarsal I^{R} (Vb-636)	
Proximodistal length	177
Mediolateral width, proximal	133
Mediolateral width, distal	113
Minimum circumference, shaft	184
Metatarsal II^{L} (Vb-640)	
Proximodistal length	240
Mediolateral width, proximal	135
Mediolateral width, distal	78
Minimum circumference, shaft	158
Metatarsal II^{R} (Vb-637)	
Proximodistal length	242
Mediolateral width, proximal	142
Mediolateral width, distal	114
Minimum circumference, shaft	169

Atsinganosaurus (Díez Díaz et al., 2018:fig. 13c–h, k–p), *Lohuecotitan* (Díez Díaz et al., 2016:fig. 5k), *Malawisaurus* (Gomani, 2005: fig. 25a–d), and *Mnyamawamtuka* (Gorscak and O'Connor, 2019: fig. 25a–f). Some other titanosaurs, especially stout-limbed taxa such as *Aeolosaurus rionegrinus*, *Antarctosaurus wichmannianus*, *Diamantinasaurus*, *Dreadnoughtus*, *Opisthocoelicaudia*, *Uberabatitan*, and saltasaurines, have substantially more robust tibiae (see, e.g., González Riga et al., 2019:fig. 8a–e).

The preserved parts of the proximal and distal ends of the right tibia exhibit rugosities for cartilage attachment. The proximal end of the left tibia is nearly complete, at least at times of study, whereas that of the right is mediolaterally compressed and missing the entire medial side and almost all the cnemial crest. Due to taphonomy and compression, the degree of anterior/anteromedial deflection of the cnemial crest of the left tibia is ambiguous, although, as preserved, it appears to have been more anteriorly directed. The cnemial crest of the left tibia is proportionally smaller and less anteriorly projected (reaches near the anterior extent of the distal end, not beyond it) than in many titanosaurs (e.g., *Aeolosaurus rionegrinus*, *Atsinganosaurus*, *Bonitasaura*, *Dreadnoughtus*, *Epachthosaurus*, *Kaijutitan maui*, *Laplatasaurus araukanicus*, *Lirainosaurus*, *Lohuecotitan*, *Malawisaurus*, *Mnyamawamtuka*, *Petrobrasaurus puestohernandezi*, saltasaurines), more closely resembling the juvenile *Rapetosaurus* FMNH PR 2209, and at least some specimens of *Mendozasaurus* in this regard (González Riga et al., 2018, 2019). The underdeveloped cnemial crest and proximal end could be due, in part, to taphonomic distortion and/or erosion, so this autapomorphy is considered tentative. However, an articulated proximal tibia and fibula, MUVP 182, that was also collected from the Quseir Formation, is similar to the proximal tibia of *Igai* in that it exhibits a comparably developed cnemial crest morphology (Salem et al., 2021:fig. 3c–e). The lateral surface of the proximal end of the right tibia exhibits a well-defined, proximodistally oriented ridge that is present in many titanosauriforms, such as in *Dreadnoughtus* (Ullmann and Lacovara, 2016:fig. 13a), and has been coined as the "second cnemial crest" (Bonaparte et al., 2000; Mannion et al., 2013). Wiechmann (1999b) also illustrated this crest in the left tibia (Fig. 14B). The *Igai* tibia is narrowest in anteroposterior dimension near midshaft. Unfortunately, the right tibial shaft is currently less complete than was depicted by Wiechmann (1999b); presumably, some portions of this bone were lost between the completion of that study and the transfer of the specimen to the MfN nearly a decade later.

Judging from the condition evident in the right tibia, the lateral surface of the shaft is anteroposteriorly concave, such that it exhibits a broad, shallow longitudinal furrow. This may be an artifact of taphonomic compression or crushing; however, a similar furrow may be present in the left tibia, as illustrated and described as concave by Wiechmann (1999b:fig. 24) (Fig. 14B). The entire medial surface of the right tibia has been broken away, revealing that the cortex of the bone is roughly 25 mm thick. The distal end of the tibia is anteroposteriorly expanded and gently bowed anteriorly, a condition that is more apparent in the left element than the right. The distal articular face is laterally oriented. It is possible that this appearance is due to taphonomic deformation, but its presence, at least in some form, in both tibiae—plus the fact that the distal end of the fibula Vb-635 has a similar anterior projection (see below)—suggests that it may be an authentic feature. If so, the distal tibia of *Igai* differs from those of many titanosaurs (e.g., *Aegyptosaurus*, *Atsinganosaurus*, *Bonitasaura*, *Lirainosaurus*, *Malawisaurus*) in this respect, although *Abditosaurus* (Vila et al., 2022:suppl. fig. 26c), *Lohuecotitan* (Díez Díaz et al., 2016:fig. 5k), and perhaps some tibiae of *Mendozasaurus* (e.g., González Riga et al., 2018: fig. h–j) exhibit a somewhat comparable condition. The distal end of the right tibia is mediolaterally expanded; however, the extent of this expansion is impossible to determine since part of the medial side of the element has been eroded away. The articular surface for the ascending process of the missing astragalus, i.e., the lateral condyle (Gallina and Apesteguía, 2015:fig. 15b), is evident on the anterolateral surface of the distal end of the right tibia, and projects further laterally than the remaining part of the bone. It is separated from the posteroventral process (i.e., the posterior condyle of Gallina and Apesteguía,

2015:fig. 15b) by a fossa, the depth and diameter of which have probably been exaggerated by crushing. Wiechmann (1999b) regarded this fossa as a site of tendon attachment. Finally, the missing left tibia is described with a convex curvature on the medial surface of the distal end (Wiechmann, 1999b; Fig. 13A), which could be interpreted as the anteromedial ridge that is present in *Atsinganosaurus* (Díez Díaz et al., 2018) and *Lirainosaurus* (Díez Díaz et al., 2013b).

Fibula—The complete left fibula Vb-635 is among the best-preserved bones of *Igai* (Fig. 15). Compared with the fibulae of many other titanosaurians (e.g., *Aeolosaurus rionegrinus*, *Alamosaurus*, *Ampelosaurus* (MDE C3-48 and especially MDE C3-137; see Le Loeuff, 2005:fig. 4.20), *Antarctosaurus wichmannianus*, *Bonitasaura*, *Diamantinasaurus*, *Dreadnoughtus*, *Elaltitan*, *Epachthosaurus*, *Laplatasaurus*, *Mendozasaurus*, *Opisthocoelicaudia*, *Uberabatitan*, saltasaurines; see, for example, González Riga et al., 2019:fig. 8f–l), it is unusually elongate and gracile, resembling those of taxa such as *Abditosaurus* (Vila et al., 2022:fig. 2n), *Argentinosaurus huinculensis* (Bonaparte and Coria, 1993:fig. 8), *Bonatitan reigi* (Salgado et al., 2015:fig. 12a), *Jainosaurus septentrionalis* (Wilson et al., 2011b:fig. 8), *Lirainosaurus* (Díez Díaz et al., 2013b:fig. 5.10–13), *Lohuecotitan* (Díez Díaz et al., 2016:fig. 5j), *Malawisaurus* (Gomani, 2005:fig. 25e–h), *Mnyamawamtuka* (Gorscak and O'Connor, 2019:fig. 25g–l), and the juvenile *Rapetosaurus* FMNH PR 2209 (Curry Rogers, 2009) in this aspect. The proximal end is only slightly anteroposteriorly expanded relative to the shaft, a morphology that is again comparable to those seen in *Bonatitan*, *Jainosaurus*, *Lirainosaurus*, *Lohuecotitan*, *Malawisaurus*, *Rapetosaurus,* and MUVP 182 (Salem et al., 2021), but differs markedly from that of many other titanosaurs, especially forms such as *Alamosaurus*, *Diamantinasaurus*, *Dreadnoughtus*, *Epachthosaurus*, *Uberabatitan*, and saltasaurines. Consequently, the insertion site for the M. flexor digitorum longus (Voegele et al., 2021; identified as that of the M. iliofibularis by Wiechmann, 1999b) was probably proportionally smaller in *Igai* than in many other titanosaurians. The proximal and posterior margins of the fibula meet at an acute angle, forming a subtriangular process, a condition that is also seen in titanosaurs such as *Mnyamawamtuka* (Gorscak and O'Connor, 2019), *Uberabatitan* (Salgado and de Souza Carvalho, 2008), and saltasaurines (e.g., Powell, 1992; Otero, 2010). The proximal end of the fibula is slightly expanded mediolaterally, although much less so than in titanosaurs such as *Antarctosaurus wichmannianus* (Huene, 1929:pl. 33, fig. 3b), *Bonatitan* (Salgado et al., 2015:fig. 12a), *Bonitasaura* (Gallina and Apesteguía, 2015: fig. 16e), *Diamantinasaurus* (Poropat et al., 2015:fig. 21e), *Laplatasaurus* (Gallina and Otero, 2015:fig. 3.6, 3.13), *Neuquensaurus* (Otero, 2010:fig. 13c), and *Rapetosaurus* (Curry Rogers, 2009: fig. 45e). The proximal mediolateral expansion more closely resembles, but is still less pronounced than, those of *Alamosaurus* (Lehman and Coulson, 2002:fig. 10.3), *Dreadnoughtus* (Ullmann and Lacovara, 2016:fig. 14e), *Jainosaurus* (Wilson et al., 2011b:fig. 8e), *Malawisaurus* (Gomani, 2005:fig. 25e), *Mendozasaurus* (González Riga et al., 2018:fig. 20q), and *Mnyamawamtuka* (Gorscak and O'Connor, 2019:fig. 25k). The proximomedial surface of the fibula is marked by multiple (~10) pits aligned parallel to the proximal edge of the bone that likely constitute osteological correlates for ligamentous attachment to the tibia, as is also seen in, for example, *Opisthocoelicaudia* (Borsuk-Bialynicka, 1977:fig. 16a).

The distal two-thirds of the lateral surface of the fibula is convex. The lateral trochanter (i.e., the proximodistally elongate eminence for insertion of the M. iliofibularis) is more subtly developed than in many titanosaurs (e.g., *Dreadnoughtus*, *Elaltitan*, *Laplatasaurus*, *Neuquensaurus*, *Uberabatitan*), and its anteroposteriorly widest portion is positioned proximal to midshaft, as in most titanosaurians with a few exceptions (e.g., *Opisthocoelicaudia*, *Rapetosaurus*). The lateral trochanter on the lateral surface of the fibula is decently pronounced near midshaft as a shallow anterior groove separates it from an anteroproximally located secondary eminence (Fig. 15A). Thus, the lateral trochanter appears to consist of a pair of subtle prominences, albeit proximodistally offset from one another, as is the case in *Antarctosaurus wichmannianus* (Huene, 1929:pl. 33, fig. 3a), *Elaltitan* (Mannion and Otero, 2012), *Epachthosaurus* (Martínez et al., 2004), *Lohuecotitan* (Díez Díaz et al., 2016), and *Mendozasaurus* (González Riga et al., 2018). However, the lateral trochanter does not appear as robust and singular as in the fibula of *Dreadnoughtus* (Lacovara et al., 2014). The medial surface of the fibular midshaft exhibits a longitudinal concavity that shallows and flattens distally from subtle ridges antero- and posteromedially. In contrast to the condition in some titanosaurs (e.g., *Elaltitan*, *Laplatasaurus*, *Malawisaurus*, *Rapetosaurus*), the distal end of the fibula is substantially anteriorly expanded into a mediolaterally thin, blade-like process, rendering the anterior margin of the distal shaft noticeably concave. This blade-like anterior process is slightly incomplete near its anterior extreme. A comparable morphology occurs in *Alamosaurus*, *Bonitasaura*, *Dreadnoughtus*, *Lirainosaurus*, *Mnyamawamtuka*, and *Opisthocoelicaudia*, among other titanosaurs. The distalmost end of the fibula is slightly mediolaterally expanded, though not as much as in taxa such as *Alamosaurus* (Lehman and Coulson, 2002:fig. 10.3), *Antarctosaurus wichmannianus* (Huene, 1929:pl. 33, fig. 3c), *Bonatitan* (Salgado et al., 2015:fig. 12a), *Bonitasaura* (Gallina and Apesteguía, 2015:fig. 16d), *Diamantinasaurus* (Poropat et al., 2015:fig. 21c), *Dreadnoughtus* (Ullmann and Lacovara, 2016:fig. 14f), *Laplatasaurus* (Gallina and Otero, 2015:fig. 3.7, 3.14), *Lirainosaurus* (Díez Díaz et al., 2013b:fig. 5.13), *Malawisaurus* (Gomani, 2005:fig. 25g), *Mendozasaurus* (González Riga et al., 2018:fig. 20p), *Mnyamawamtuka* (Gorscak and O'Connor, 2019:fig. 25l), *Neuquensaurus* (Otero, 2010:fig. 13d), and *Rapetosaurus* (Curry Rogers, 2009:fig. 45f).

Metatarsus—Three metatarsals were collected and represent the right metatarsal I and both left and right metatarsal II. Like the other elements of *Igai*, the metatarsals are taphonomically compressed but retain most of their anatomical information otherwise. The right metatarsal I Vb-636 exhibits significant dorsoplantar taphonomic compression; however, much of its anatomy is still interpretable as the element is otherwise largely intact (Fig. 16A–F). The bone is generally stout but, due to the abovementioned compression, it is unclear to what degree it was twisted about its long axis. Both the proximal and distal ends are expanded, with the former being slightly wider than the latter. Unlike metatarsal I of some other titanosaurians (e.g., *Epachthosaurus*, *Mansourasaurus*, *Mendozasaurus*, *Mnyamawamtuka*, *Neuquensaurus*), the sides are subequal in length; thus, neither the proximal nor the distal end are significantly beveled, as is also seen in a few other titanosaurians such as *Atsinganosaurus* (Díez Díaz et al., 2018), *Dreadnoughtus* (Lacovara et al., 2014; Ullmann and Lacovara, 2016), and *Notocolossus gonzalezparejasi* (González Riga et al., 2016). The proximal articular surface is comma-shaped in proximal view, with the concavity facing plantarly (i.e., posteriorly, if the bone is oriented vertically). Both the lateral and the medial margins are concave. A subtle ridge is present on the medial surface near the apex of the dorsal curvature of the proximal margin. There is also a small foramen or 'divot' near the lateral margin of the medial surface. The lateral surface exhibits a strong ridge for articulation with metatarsal II, though this structure has been reduced in prominence by taphonomic compression. Near the distolateral end of this ridge, there is a narrow, sharply delineated groove (see Fig. 16B, C, F) that is not present in, for example, *Mansourasaurus* (although the distal end of metatarsal I is damaged and probably incomplete in the only known specimen of that titanosaur), *Mendozasaurus*, and *Rapetosaurus*; however, a shallower, wider canal appears present in metatarsal

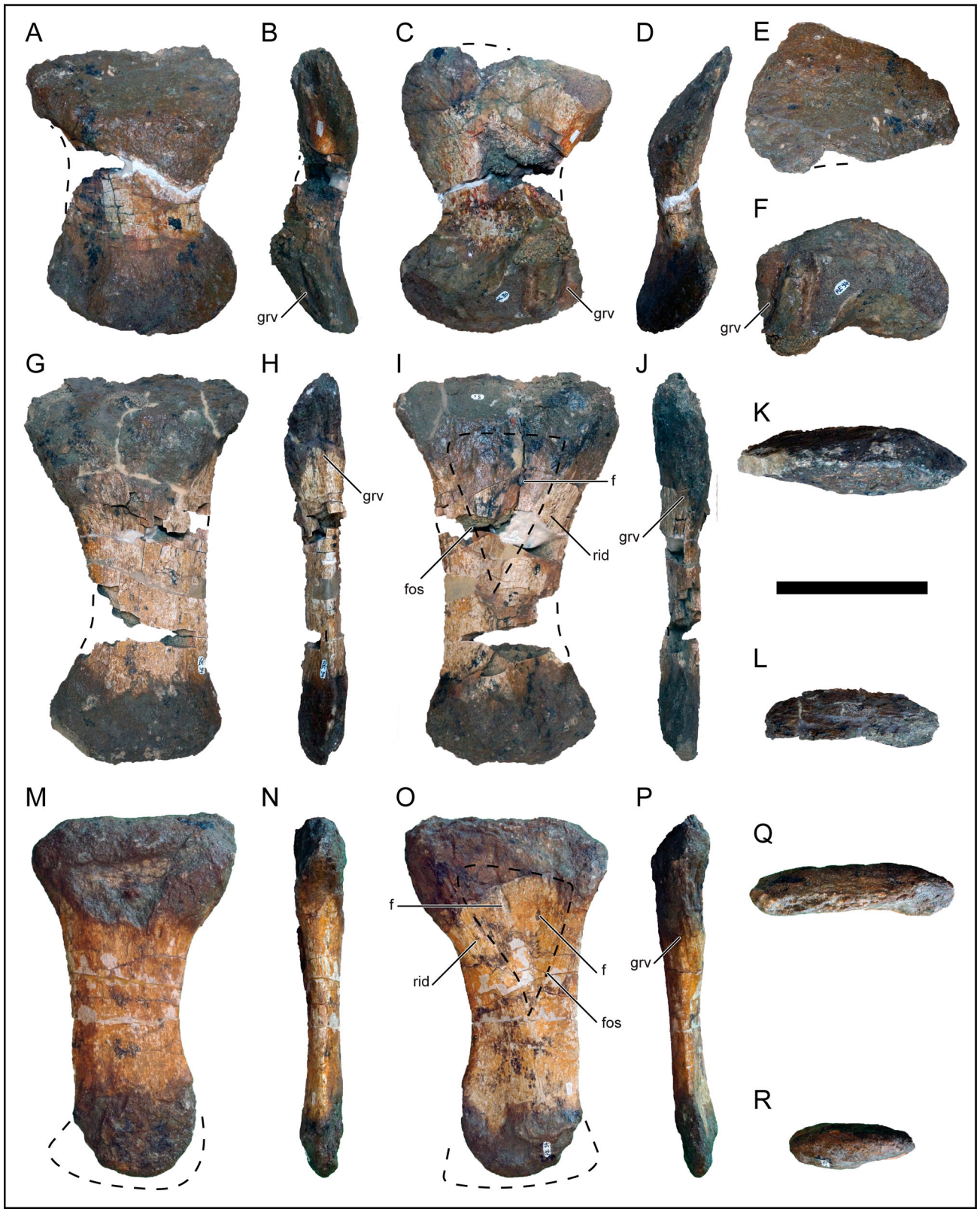

FIGURE 16. Metatarsals of *Igai semkhu*. Right metatarsal I (Vb-636) (**A**–**F**), right metatarsal II (Vb-637) (**G**–**L**), and left metatarsal II (Vb-640) (**M**–**R**). **A**, **G**, **M**, medial; **B**, **H**, **N**, dorsal; **C**, **I**, **O**, lateral; **D**, **J**, **P**, plantar; **E**, **K**, **Q**, proximal; and **F**, **L**, **R**, distal views. **Abbreviations**: **f**, foramen; **fos**, fossa; **grv**, groove; **rid**, ridge. Scale bar equals 10 cm.

I of *Dreadnoughtus*. The well-defined groove is tentatively considered unique to *Igai*. The distal end of metatarsal I resembles the proximal end in that it too is comma-shaped, but with a thicker lateral area. Both the proximal and distal ends are slightly rugose, suggesting cartilage attachment.

Like the right metatarsal I Vb-636, the metatarsal II Vb-637 is compressed along the dorsoplantar axis (Fig. 16G–L). Wiechmann (1999b) identified this latter element as being from the left side of the animal, but its overall similarity to Vb-636 instead suggests it was ipsilateral to this bone; Vb-637 is therefore herein identified as the right metatarsal II. Similarly, Wiechmann (1999b) identified Vb-640 (Fig. 16M–R) as the right metatarsal V and it looks similar to one without taking the compression and taphonomy into account. However, taking the compression into account, Vb-640 is closely comparable in morphology (e.g., topology of grooves and fossae) and dimensions (Table 2) to Vb-637, so it instead appears to be the contralateral complement to this element. Specimen Vb-640 is therefore interpreted as the left metatarsal II. However, the preservational state of both Vb-637 and Vb-640 had rendered these bones difficult to interpret, and as such, we acknowledge the slight possibility that they may instead correspond to metatarsal III rather than metatarsal II while adopting the latter identification herein.

Of the two second metatarsals, Vb-637 is the more complete and less deformed (given that, for instance, Vb-640 has a poorly preserved distal end), so our description of this element in *Igai* is derived largely from the former specimen. Overall, metatarsals I and II of *Igai* are similar except that the latter are longer proximodistally. However, metatarsal II is slenderer than its counterparts in the giant titanosaurs *Dreadnoughtus* (Lacovara et al., 2014) and *Notocolossus* (González Riga et al., 2016). Both the proximal and distal ends of metatarsal II are expanded, with the former more so than the latter. The dorsomedial margin is concave whereas the plantar margin is straighter. A small groove originates near the proximomedial corner of the bone and extends along the plantar margin distally to approximately one-third its length. A similar groove is present but more pronounced in *Bonitasaura* (Gallina and Apesteguía, 2015); its seemingly greater development in this Patagonian titanosaur may be a consequence of the exquisite preservation of the holotype. In *Igai*, the proximomedial corner of metatarsal II has a subtle boss with a plantarly aligned ridge that extends distolaterally along the plantar surface toward another boss near the distolateral corner that is assumed to articulate with the ipsilateral metatarsal III. A shallow, subtriangular fossa is present lateral to this plantar ridge near the proximal end (Fig. 16I, O). There are two small foramina within this fossa (Fig. 16O). At the proximolateral corner, there is a shallow plantar fossa delineated by a sharp ridge. Little can be confidently discerned about the proximal and distal articular surfaces of metatarsal II, except that they were rugose.

COMPARISONS WITH *MANSOURASAURUS SHAHINAE*

Comparisons of *Igai semkhu* to *Mansourasaurus shahinae*—the other named titanosaurian taxon from the Upper Cretaceous Quseir Formation of the Egyptian Western Desert—are unfortunately limited due to a paucity of overlapping bones. The holotypic and only unquestionable specimen of *Mansourasaurus* (MUVP 200) consists mainly of elements from the anterior part of the individual; specifically, craniomandibular, cervical, anterior dorsal, and pectoral girdle and forelimb bones comprise most of the specimen, with only a few, fragmentary elements known from elsewhere in the skeleton (Sallam et al., 2018). On the other hand, *Igai* preserves bones from the middle portion of the individual, including posterior dorsal vertebrae and elements from both sets of appendicular girdles and limbs. Indeed, only two bones, the coracoid and metatarsal I, are directly comparable between the *Igai* and *Mansourasaurus* holotypes. Otherwise, general limb proportions suggest that *Mansourasaurus* was a stockier animal than *Igai* (e.g., the proportionally short, robust humerus and radius of the former taxon versus the relatively gracile ulna, tibia, and fibula of the latter). However, this putative distinction is rendered tentative by the lack of directly comparable long bones and the taphonomic biases seen in both specimens: fragmented and damaged in MUVP 200 versus compressed in *Igai*. In this context, it is worth noting that the ulna (MUVP 201) found ~20 m from the *Mansourasaurus* holotype—and that, given the rarity of dinosaur fossils in the Quseir Formation, could conceivably pertain to the same individual—appears substantially more robust than that of *Igai* (see Sallam et al., 2018:fig. s18).

Comparisons of the coracoids of these two Quseir Formation titanosaurians are limited by the fact that *Igai* preserves only the middle portion of the element whereas in *Mansourasaurus* the coracoid is nearly complete but broken into fragments. One apparent difference concerns the position and morphology of the coracoid foramen. In *Mansourasaurus*, this opening is more circular in shape, and its posterior margin is confluent with the scapulocoracoid suture, such that the foramen is not fully enclosed by bone (i.e., it is patent with the suture). In *Igai*, by contrast, this opening is more elliptical with the long axis oriented anteroposteriorly (i.e., aligned with the long axis of the coracoid as this bone is preserved). Furthermore, the foramen is fully enclosed by bone and located anterior to the scapulocoracoid suture. Rather than being indicative of taxonomic distinction, these differences may potentially be due to ontogenetic variation within and among different titanosaurian species, with less mature individuals possibly tending to exhibit a patent coracoid foramen (see Martin, 1994 and Sallam et al., 2018). However, both the referred coracoid of *Malawisaurus* (MAL-235) and *Rukwatitan* exhibit a patent coracoid foramen and appear to have been mature, or nearly so, individuals based on vertebral centrum and neural arch fusion (Gomani, 2005; Gorscak et al., 2014), yet *Tapuiasaurus* exhibits a patent coracoid foramen but exhibits unfused cranial elements, such as the braincase, suggesting this specimen was subadult (Zaher et al., 2011; Wilson et al., 2016). Furthermore, the juvenile specimen of *Rapetosaurus* (FMNH PR 2209) exhibits both unfused vertebrae and scapulocoracoid, with the latter exhibiting a patent coracoid foramen, but on the other hand the juvenile specimen of *Alamosaurus* (TMM 43621-1) is similar in its extent of skeletal fusion as FMNH PR 2209 but exhibits a fully enclosed coracoid foramen (Lehman and Coulson, 2002). These patterns suggest that the extent of skeletal fusion through ontogeny for titanosaurians may be variable and/or the coracoid foramen location is independent from the timing of skeletal fusions. Taken at face value, the shape and location of the coracoid foramen differs between the two Egyptian titanosaurian specimens.

Lastly, although they are hindered by the taphonomic compression of this bone in *Igai*, general morphological comparisons may be made between the first metatarsals of the two Quseir Formation taxa. One of their main differences involves the alignment of the proximal and distal articular surfaces relative to the proximodistal (i.e., long) axis of the element. In *Mansourasaurus*, these surfaces are beveled to a greater degree than is seen in metatarsal I of *Igai* (Vb-636). Although the latter bone is compressed, there is no evidence to suggest that it originally exhibited the same extent of beveling. Instead, the articular surfaces appear to have been oriented roughly perpendicular to the proximodistal axis. Stated another way, the proximodistal lengths of the lateral and medial margins of metatarsal I are roughly the same in *Igai* but significantly different in *Mansourasaurus*. Unfortunately, further morphological comparisons between these two titanosaurians are presently curtailed by their respective states

of preservation. Nevertheless, the differences between the coracoid and metatarsal I and apparent distinctions in limb bone robustness suggest that, despite having been preserved in the same geologic unit, *Igai* and *Mansourasaurus* are separate titanosaurian taxa.

PHYLOGENETIC METHODS AND RESULTS

Although there is general agreement on the monophyly of certain titanosaurian subclades across recent phylogenetic studies (e.g., Aeolosaurini, Lognkosauria, Rinconsauria, Saltasaurini, etc.), deeper nodes and relationships within Titanosauria remain unclear (Carballido et al., 2022). Although this is outside the scope of the current study, this lack of consensus regarding the titanosaurian 'phylogenetic backbone' may be due to a combination of factors, including disparate character and taxon sampling across the various 'dataset families' that are currently active. These include the following: the (1) Gallina and Apesteguía (2011) dataset family (which includes the datasets employed by, for example, Salgado et al., 2015 and Díez Díaz et al., 2021); (2) the Mannion et al. (2013) dataset family (e.g., González Riga et al., 2018; Poropat et al., 2021); (3) the Carballido and Sander (2014) dataset family (e.g., Cerda et al., 2021; Gallina et al., 2021); and (4) the Gorscak and O'Connor (2016) dataset family (e.g., Sallam et al., 2018; Gorscak and O'Connor, 2019; Vila et al., 2022; current study). For example, European and/or African representatives of Titanosauria tend to be underrepresented or even nearly absent in many phylogenetic analyses despite the fact that these continents have produced numerous new titanosaurian taxa in recent decades (e.g., Smith et al., 2001; Gomani, 2005; Csiki et al., 2010; Garcia et al., 2010; Curry Rogers and Wilson, 2014; Gorscak et al., 2014, 2017; Díez Díaz et al., 2016, 2021; Sallam et al., 2018; Gorscak and O'Connor, 2019; Vila et al., 2022). A similar phenomenon has occurred with the surge in Australian titanosauriform discoveries within the past ~15 years (e.g., *Australotitan cooperensis*, *Diamantinasaurus*, *Savannasaurus*, and *Wintonotitan wattsi*), which have typically been analyzed using datasets within the Mannion et al. (2013) family (e.g., Hocknull et al., 2021; Poropat et al., 2021). Thus, vast geographic regions and substantial evolutionary branches remain absent from or underrepresented in most analyses, which may in turn skew, bias, and/or limit resulting interpretations, especially given that the majority of titanosaurians have historically been known from South America. This is not to say that one dataset family is more appropriate than any of the others—especially given the logistical challenges associated with studying this globally distributed sauropod clade and the fact that titanosaurian discoveries have outpaced the construction of any comprehensive phylogenetic data matrix—but rather to recognize where deficiencies may exist within the currently utilized datasets and in the interpretations of analyses thereof.

Following the general protocols of previous analyses (e.g., Sallam et al., 2018; Gorscak and O'Connor, 2019), *Igai semkhu* was scored (based on the holotype Vb-621–640) into the working phylogenetic dataset of the first author (E.G.). This dataset was revised to include several new characters and updated taxonomic scorings based on recent publications and observations (see Appendix S2–5 for taxon stratigraphic data, morphological characters, dataset modifications, and citations used for the phylogenetic analyses). Tip-dating Bayesian analyses were utilized to include both morphological characters and temporal data to inform the phylogenetic model in calculating branch lengths, nodal age estimates, and to account for phylogenetic uncertainty. The updated dataset consists of 587 characters that include 285 variable characters and 302 autapomorphies, with the latter character type incorporated to inform branch lengths and overall model likelihoods (Lewis, 2001; Matzke and Irmis, 2018). The dataset includes 57 taxa with a specific focus on representatives of Titanosauria as opposed to non-titanosaurian members of more inclusive clades such as Titanosauriformes or Sauropoda. All characters were regarded as independent and unordered. The MkV likelihood model of evolution was assumed to account for ascertainment bias (Lewis, 2001). Asymmetric rates of state changes (i.e., different rates are estimated among the different state changes) with gamma distribution governing rate variation were also implemented into the model in addition to an alternative model using equal rates of rate variation ran for model comparison. The BDSKY tree model (birth-death-skyline serial sampling) was assumed, allowing birth and death (= speciation and extinction) rates to vary through time (Stadler et al., 2013), coupled with a relaxclock using a lognormal distribution of sampled rates. The stratigraphic range of each terminal taxon was sampled from an assumed uniform distribution. The XML files were constructed using the R package BEASTmasteR (Matzke, 2015) to run in BEAST v2.1.3 along with the installation of the packages BEASTlabs, BDSKY, SA, phylodynamics, and CA in BEAUTI v2.1.3 (Bouckaert et al., 2014). The MCMC ran for a total of 20 million generations, a sufficient duration for the sampling process which reached convergence relatively early, with sampling occurring every 1,000 generations. The first 20% of sampled trees were discarded to eliminate the initial burn-in phase of the analysis prior to reaching convergence. A similarly constructed uncalibrated (i.e., no temporal information such as taxon stratigraphic ranges and a clock-like model) Bayesian analysis was utilized using MrBayes v3.2.7a, testing two models of equal and variable rates of character change (Ronquist et al., 2012), with the same MCMC sampling protocols as the tip-dating analyses. Additionally, a parsimony analysis was conducted in TNT 1.5 (Goloboff et al., 2008; Goloboff and Catalano, 2016) to complement the Bayesian analyses with a more 'traditional' analytical perspective. The New Technology search algorithm was employed with 10 replications using constraint, exclusive, and random sectorial searches. Ten rounds of fusion, ratchet, and drifting at their default settings were implemented in the New Technology search.

The results of the tip-dating analysis are largely consistent with studies that have employed previous analytical iterations of the current dataset (Fig. 17; Sallam et al., 2018; Gorscak and O'Connor, 2019). However, caution is warranted by the substantial range of nodal statistics (e.g., posterior probabilities), which indicate a degree of uncertainty in the hypothesized phylogenetic relationships, also seen in the results of the standard Bayesian analysis (Fig. 18B). This should not be surprising given the heterogeneity of the data among the sampled taxa (e.g., variable skeletal completeness, trait homoplasy, degree of overlapping elements among taxa), which in some ways reflects the patchy nature of the titanosaurian fossil record and the associated challenges inherent in reconstructing the phylogeny of these sauropods. In the tip-dating analysis, the model likelihood of the variable rates model was −4711.13 compared with −4839.63 for the equal-rates model, and −5128.18 compared with −5231.44, respectively, for the uncalibrated Bayesian analyses. For both the tip-dating and the uncalibrated Bayesian analyses, the variable-rates model greatly outperformed its equal-rates counterpart by significant margins, with particularly strong Bayes factors of 257.00 and 206.52, respectively (Kass and Raftery, 1995). The results of the parsimony analysis recovered 2,271 most parsimonious trees, with each tree totaling a length of 985 steps with a Retention Index of 0.53 and Consistency Index of 0.46 (Fig. 18A). The resulting consensus trees (Fig. 18A) resemble those generated by prior parsimony analyses of this dataset and exhibit selected concordances with the trees yielded by both Bayesian analyses; however, significant differences between the two topologies are noted below.

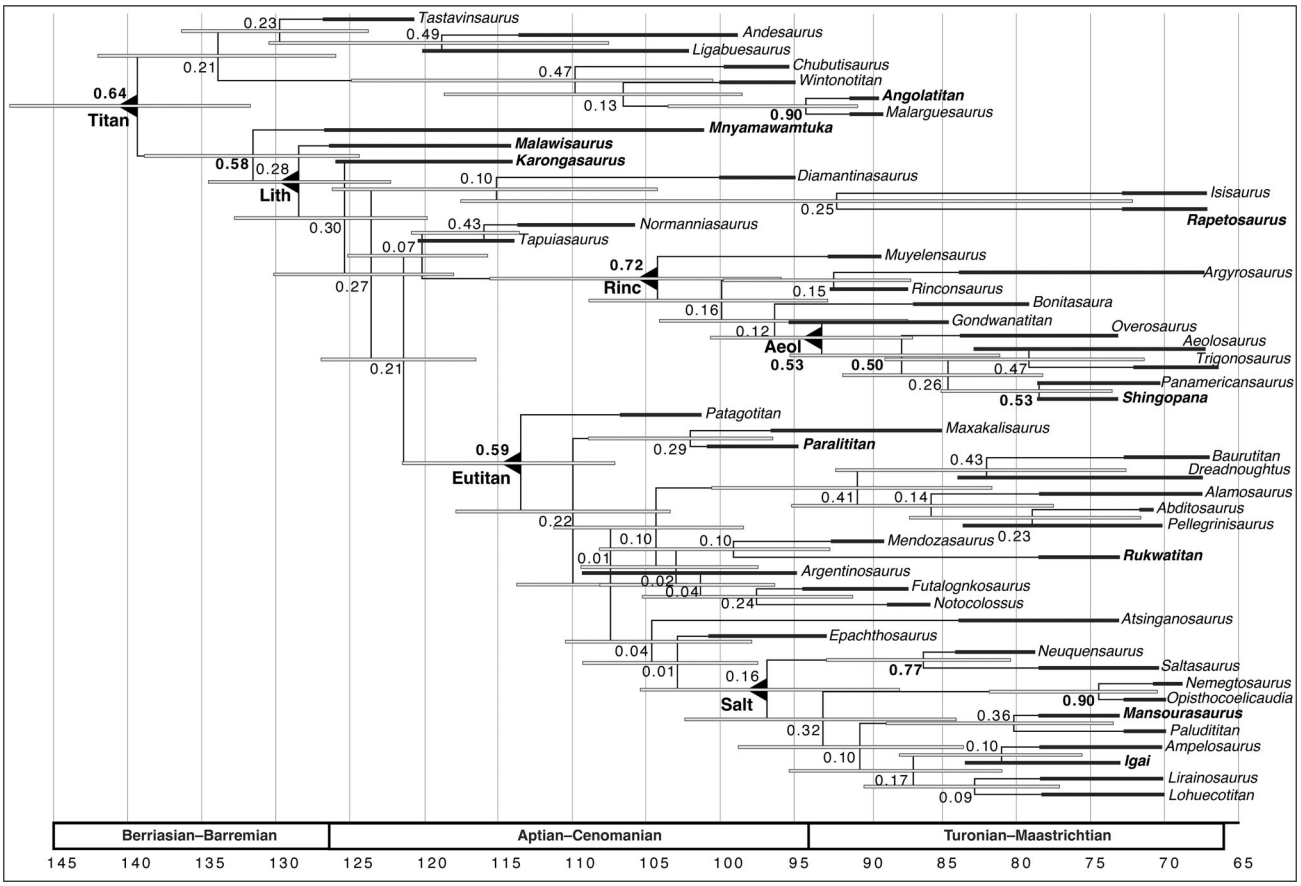

FIGURE 17. Maximum clade credibility tree for variable-rates tip-dated Bayesian phylogenetic analysis of *Igai semkhu* within Titanosauria. Numbers at nodes represent posterior probabilities (posterior probabilities at or above 50% are in bold), light gray bars at each node represent 95% highest posterior density of each node age. African terminal taxa are denoted in bold. Time scale is in units of millions of years. **Abbreviations**: **Aeol**, Aeolosaurini; **Eutitan**, Eutitanosauria; **Lith**, Lithostrotia; **Rinc**, Rinconsauria; **Salt**, Saltasauridae; **Titan**, Titanosauria.

Concerning the results of the tip-dating analysis, *Igai* is hypothesized as positioned within the Afro-Eurasian titanosaurian clade previously recognized by Sallam et al. (2018), which includes *Ampelosaurus*, *Lirainosaurus*, *Mansourasaurus*, *Opisthocoelicaudia*, among others (32% posterior probability, moderately supported given the nature of the data). This clade is equivalent to the definition of Opisthocoelicaudiinae (most inclusive clade with *Opisthocoelicaudia* but not *Saltasaurus*; McIntosh, 1990; Carballido et al., 2022). Both Egyptian titanosaurians *Igai* and *Mansourasaurus* are unlikely to be sister taxa within this clade, as this result was also obtained via the parsimony and standard Bayesian analyses. These results are further supported by the morphological differences between the coracoid and metatarsal I of these taxa discussed above. Support for the inclusion of *Igai* in this Afro-Eurasian clade includes the absence of the postzygodiapophyseal lamina from the posterior dorsal vertebrae (which is also absent in, for example, *Ampelosaurus*, *Lirainosaurus*, and *Opisthocoelicaudia*). The relationship with the outgroup of this clade is relatively weak in support (16% posterior probability), consisting of the saltasaurines *Neuquensaurus* and *Saltasaurus*, a clade equivalent to Saltasaurinae and relatively well-supported with 77% posterior probability (Carballido et al., 2022). The posterior dorsal vertebrae of the saltasaurine taxa exhibit a weakly developed postzygodiapophyseal lamina which suggests support for this close placement with the Afro-Eurasian clade (= Opisthocoelicaudiinae). Furthermore, the presence of the X-lamina complex in posterior dorsal vertebrae of *Lirainosaurus*, *Igai*, and *Saltasaurus* and the unnamed diapophyseal lamina in the same bones of the latter two genera plus *Neuquensaurus* appears to draw the saltasaurine and Afro-Eurasian (= Opisthocoelicaudiinae) clades closer together in the analysis. Together, these two groups compose Saltasauridae according to the definition of this clade (*Saltasaurus*, *Opisthocoelicaudia*, their most recent common ancestor and all descendants; Bonaparte and Powell, 1980; Wilson and Upchurch, 2003; Carballido et al., 2022). A similar result was obtained via the uncalibrated Bayesian analysis; however, with slightly different clade compositions within Saltasauridae (Fig. 18B). On the other hand, the parsimony result differs in this region of the tree in two ways: Saltasauridae includes the eastern Gondwanan titanosaurians *Isisaurus* and *Diamantinasaurus*, and these eastern Gondwanan taxa are the sister group to the *Igai* and saltasaurine group. Otherwise, this group (= Saltasaurinae) is sister to the Afro-Eurasian (= Opisthocoelicaudiinae) group consisting of *Ampelosaurus*, *Lirainosaurus*, *Mansourasaurus*, and *Opisthocoelicaudia* in a majority (69%) of the recovered most parsimonious trees (Fig. 18A). Overall, there are similarities among the results of the phylogenetic analyses, recovering the following clades and consistent members: (1) a titanosaurian clade united by the presence of a

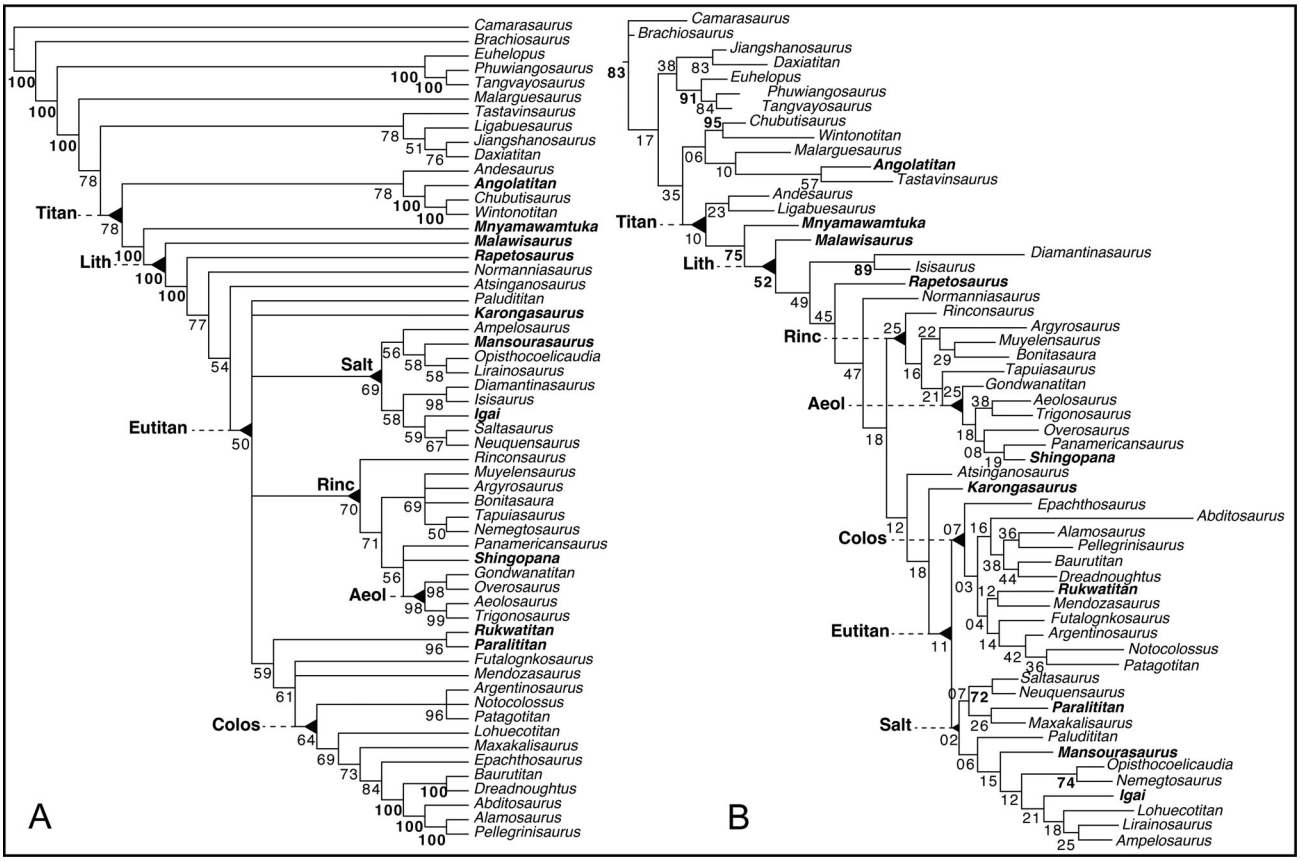

FIGURE 18. Results of parsimony (**A**) and Bayesian (non-tip dated, variable-rates model) (**B**) phylogenetic analyses of *Igai semkhu*. **A**, 2,271 most parsimonious trees (MPTs) summarized into a 50% majority-rule consensus tree with node percentages representing clade frequency within recovered MPTs (frequencies of 100% are in bold to indicate the nearest node where branches collapse for the strict consensus tree). **B**, maximum clade credibility summary tree from atemporal Bayesian analysis with posterior probabilities of recovered clades at each node (posterior probabilities at or above 50% are in bold). African terminal taxa are denoted in bold. **Abbreviations**: **Aeol**, Aeolosaurini; **Colos**, Colossosauria; **Eutitan**, Eutitanosauria; **Lith**, Lithostrotia; **Rinc**, Rinconsauria; **Salt**, Saltasauridae; **Titan**, Titanosauria.

biconvex first caudal vertebra (e.g., *Alamosaurus*, *Baurutitan britoi*, *Dreadnoughtus*, *Pellegrinisaurus*); (2) Aeolosaurini within a larger Rinconsauria (e.g., *Aeolosaurus*, *Bonitasaura*, *Gondwanatitan faustoi*, *Overosaurus paradasorum*, *Rinconsaurus*, *Shingopana*, *Trigonosaurus*); (3) Colossosauria (e.g., *Futalognkosaurus*, *Patagotitan*, and the titanosaurian clade with a biconvex first caudal vertebra); (4) an early branching titanosaurian clade Andesauroidea (e.g., *Andesaurus*, *Ligabuesaurus leanzai*); and (5) Euhelopodidae (e.g., *Daxiatitan binglingi*, *Euhelopus zdanskyi*, *Phuwiangosaurus sirindhornae*), which is positioned as an outgroup to Titanosauria. Otherwise, membership of Colossosauria, which can only be properly defined in the parsimony and uncalibrated Bayesian analyses and is incompatible with the tip-dating analysis among the analyses (Fig. 18; Carballido et al., 2022), generally includes taxa or closely related to taxa of Lognkosauria (e.g., *Futalognkosaurus*, *Mendozasaurus*) and the titanosaurian clade with a biconvex first caudal vertebra (e.g., *Alamosaurus*, *Dreadnoughtus*), typically united by the lateral expansion of the spinodiapophyseal lamina in the posterior cervical vertebrae. These results differ in other analyses where Colossosauria includes Aeolosaurini/Rinconsauria and Lognkosauria as sister groups rather than with the titanosaurian clade with a biconvex first caudal, saltasaurids, and/or the Afro-Eurasian clade (González Riga et al., 2019; Carballido et al., 2022).

DISCUSSION AND CONCLUSIONS

Decades after its discovery, specimen Vb-621–640—the holotype of *Igai semkhu*—now represents, alongside *Mansourasaurus shahinae* (Sallam et al., 2018), the second titanosaurian species to be described from the uppermost Cretaceous (Campanian) Quseir Formation of the Western Desert oases of Egypt. Importantly, *Igai* reinforces the hypothesis of an Afro-Eurasian clade of latest Cretaceous titanosaurians, with the African representatives of this group being presently known only from the northeastern region of the continent, specifically, Egypt (Gorscak and O'Connor, 2016; Sallam et al., 2018; this paper). This stands in contrast to the hypothesized affinities of potentially penecontemporaneous titanosaurians from sub-Saharan Africa, namely *Rukwatitan* and *Shingopana* from the now recognized Upper Cretaceous Namba Member of the Galula Formation of southwestern Tanzania (Widlansky et al., 2018; Orr et al., 2021). At present, the known taxa and hypothesized phylogenetic relationships of Late Cretaceous African titanosaurians suggest there was a coarse northern/southern sauropod faunal division that may have existed on the continent during this time, with the northern African taxa having had closer relationships to Eurasian taxa whereas the southern forms maintained more typical Gondwanan affinities. All African and Malagasy titanosaurians from the latest Cretaceous (i.e., Campanian–Maastrichtian) were recovered

distantly related to one another and belong to/are closely related with one of the major titanosaurian clades: *Shingopana* with Rinconsauria/Aeolosaurini affinities; *Mansourasaurus* and *Igai* within the Afro-Eurasian clade of Saltasauridae; and *Rukwatitan* within Colossosauria. Concerning the latter, *Rukwatitan* and the Spanish *Abditosaurus* were recovered mid-grade with lognkosaurians and the titanosaurian clade with a biconvex first caudal vertebra within the larger Colossosauria—unlike the monophyletic Afro-Eurasian clade—in the uncalibrated Bayesian and tip-dating analyses, which suggests that the predominantly South American Colossosauria included representatives in Africa and Europe, albeit currently with fewer known taxa presently. The placement of *Abditosaurus* differs from that recovered by Vila et al. (2022); however, the current dataset has been revised and expanded compared with the older version they employed (see Supplementary Files). Interestingly, *Rapetosaurus* was recovered in all three analyses outside of these major clades, contra previous analyses placing the taxon closer to rinconsaurians and/or aeolosaurins (e.g., Gorscak and O'Connor, 2016, 2019). Older Eurasian titanosaurians such as *Normanniasaurus* from the Albian of France and *Tengrisaurus* from the Barremian–Aptian of Russia have also been recovered close to or within Colossosauria or Aeolosaurini and may indicate local/regional extirpations prior to the signal seen in the Late Cretaceous (Mannion et al., 2019; Averianov et al., 2021). How titanosaurian faunal diversity may have related to differences along potential latitudinal gradients and/or the specifics of African latest Cretaceous paleogeography remain unresolved questions given that our understanding of the biota and paleogeography of this continent during this interval is still developing. Overall, our phylogenetic analyses suggest that Late Cretaceous African faunas were as, or nearly as, diverse as those from elsewhere, such as South America. This perspective could not have been appreciated without the geologic, paleontologic, and collaborative efforts from recent years across the continent.

Apart from paleobiogeographic perspectives based on titanosaurians, recent insights regarding other latest Cretaceous dinosaurs of Africa have been derived from more fragmentary fossils, such as the type specimens (in both cases, isolated craniodental materials) of the abelisaurid theropod *Chenanisaurus* and the hadrosaurid ornithopod *Ajnabia* from upper Maastrichtian phosphate deposits exposed in the Ouled Abdoun Basin of Morocco (Longrich et al., 2017, 2021). These recently described Moroccan dinosaurs provide an expanded perspective on latest Cretaceous African terrestrial tetrapod paleobiogeography in adding data from the northwestern region of the continent and in introducing the possibility of potential longitudinal distinctions between faunal assemblages currently known in the northern part of Africa. From a paleobiogeographic standpoint, it may be useful to consider—at least preliminarily, as a tentative framework and as additional informative fossils are collected and described—the African mainland as having been divided into three general dinosaurian faunal regions during the latest Cretaceous: northwestern, mainly represented by the Moroccan abelisaurid, hadrosaurid, and sauropod remains (e.g., Pereda Suberbiola et al., 2004; Longrich et al., 2017, 2021); northeastern, represented primarily by the Egyptian titanosaurians (*Igai*, *Mansourasaurus*); and southern, represented by the Tanzanian titanosaurs of the Galula Formation (*Rukwatitan*, *Shingopana*). Furthermore, the inclusion of Madagascar expands this notion with a fourth faunal region during the latest Cretaceous—one with a rather unique faunal and paleobiogeographic history (Krause et al., 2019). In the northwest, the Moroccan hadrosaurid *Ajnabia* has been regarded as deeply nested within the otherwise European lambeosaurine subclade Arenysaurini (Longrich et al., 2021), a result that suggests a close faunistic association with southern Europe and mirrors paleobiogeographic conclusions drawn from the titanosaurians *Igai* and *Mansourasaurus* in northeastern Africa which, again, are also considered close relatives of European taxa (Sallam et al., 2018; current study). Thus far, no other hadrosaurid fossils have been found in Africa despite the clade having attained a near-global distribution during the Late Cretaceous. Yet, the then-contiguous Arabian Peninsula has yielded a handful of fragmentary fossils referred to Hadrosauroidea (Buffetaut et al., 2015), so the potential remains for the recovery of these ornithopods from northeastern Africa too. The Moroccan abelisaurid *Chenanisaurus* suggests a different paleobiogeographic scenario from that inferred from the latest Cretaceous African hadrosaurid and titanosaurians: a lineage that extends into the mid-Cretaceous and forms an unresolved polytomy with more ancient African members of this clade, *Kryptops palaios* and *Rugops primus* from Niger (Sereno et al., 2004; Sereno and Brusatte, 2008), and most other abelisaurid taxa (Longrich et al., 2017). However, it should be noted that these Moroccan taxa are based on very limited fossil remains which only capture a brief glimpse into the respective species and faunas of northwestern Africa. At present, latest Cretaceous dinosaur discoveries from mainland Africa appear to suggest that the evolutionary and paleobiogeographic history of these animals on this landmass may vary depending on the complex interplay between the tectonic history of the continents throughout the Cretaceous and the unique evolutionary paths and life histories of a given clade. Continued field discoveries and rigorous studies of latest Cretaceous dinosaur fossils of Africa promise to cast light on decades-old paleobiogeographic questions and enhance an already exciting and emerging perspective on these intriguing biotas that have, to this point, remained hidden in the sands of time.

LIST OF SUPPLEMENTARY FILES

GorscakEtAl_BEASTEqualRatesTipDatingModel.xml
GorscakEtAl_BEASTEqualRatesTree.tre
GorscakEtAl_BEASTVariableRatesTipDatingModel.xml
GorscakEtAl_BEASTVariableRatesTree.tre
GorscakEtAl_MrBayesEqualRatesNexus.nex
GorscakEtAl_MrBayesEqualRatesTree.tre
GorscakEtAl_MrBayesVariableRatesNexus.nex
GorscakEtAl_MrBayesVariableRatesTree.tre
GorscakEtAl_Nexus.nex
GorscakEtAl_Parsimony_MPTs_MajorityRule.nex
GorscakEtAl_TNT.tnt
Vb621_DorsalCentrum.ply.zip
Vb622_DorsalVert.ply.zip
Vb623_DorsalVert.ply.zip
Vb624_DorsalVert.ply.zip
Vb625_DorsalCentrum.ply.zip
Vb627_Coracoid.ply.zip
Vb628_Pubis.ply.zip
Vb630_Tibia.ply.zip
Vb631_Ulna.ply.zip
Vb633_MTCV.ply.zip
Vb635_Fibula.ply.zip
Vb636_MTTI.ply.zip
Vb637_MTTII.ply.zip
Vb638_MTCIV.ply.zip
Vb639_MTTII.ply.zip
Vb640_MTCI.ply.zip

ACKNOWLEDGMENTS

We thank L. Saladino Haney (Carnegie Museum of Natural History) for etymological consultation and advice. M.C.L. is grateful to M.F.W. and O. Rauhut (the latter of the Bayerische Staatssammlung für Paläontologie und Geologie) for access to Vb-621–640 and for technical discussions concerning the

specimen. J. Smith (Phenomenon Science) participated in these and other discussions and took photographs of most skeletal elements. W. Harbert (University of Pittsburgh) provided additional photos. M.C.L. also thanks E. Buffetaut (Centre National de la Recherche Scientifique), J. Wilson Mantilla (University of Michigan), and I. El-Dawoudi for further discussions on the specimen. Selected figures were skillfully prepared by A. McAfee and T. Mastalski (both Carnegie Museum of Natural History). D.S. cordially thanks paleontological preparators M. Kaiser and M. Schoele (both MfN) for their conservation and remedial treatment of the specimen, as well as R. Bussert (TUB) for research on historical field data associated with the type locality. E.G. thanks D. Ehrlich and J. Nassif for help with computer models and P. Mannion for discussions on the specimen. M.C.L.'s participation in the research was funded in part by Carnegie Museum of Natural History. The manuscript benefited from reviews by P. Gallina and P. Mannion and from editorial comments by S. Salisbury and P. Godoy. All authors are indebted to K. Werner Barthel and R. Böttcher (TUB) for discovering and collecting Vb-621–640 in 1977.

ORCID

Eric Gorscak http://orcid.org/0000-0002-4019-8301
Matthew C. Lamanna http://orcid.org/0000-0001-9845-0728

LITERATURE CITED

Abu El-Kheir, G., Abdel Gawad, M., Mohsen, S., & Ismael, H. (2019). A new record of sauropod dinosaur of southwestern desert of Egypt. *Geophysical Research Abstracts 21*:EGU2019-1680-1.

Ali, J. R., & Krause, D. W. (2011). Late Cretaceous bioconnections between Indo-Madagascar and Antarctica: refutation of the Gunnerus Ridge causeway hypothesis. *Journal of Biogeography 38*:1855–1872.

Apesteguía, S., Soto Luzuriaga, J. E., Gallina, P. A., Tamay Granda, J., & Guamán Jaramillo, G. A. (2020). The first dinosaur remains from the Cretaceous of Ecuador. *Cretaceous Research 108*:104345.

Aureliano, T., Ghilardi, A. M., Silva-Junior, J. C. G., Martinelli, A. G., Borges Ribeiro, L. C., Marinho, T., Fernandes, M. A., Ricardi-Branco, F., & Sander, P. M. (2020). Influence of taphonomy on histological evidence for vertebral pneumaticity in an Upper Cretaceous titanosaur from South America. *Cretaceous Research 108*:104337.

Aureliano, T., Ghilardi, A. M., Navarro, B. A., Fernandes, M. A., Ricardi-Branco, F., & Wedel, M. J. (2021). Exquisite air sac histological traces in a hyperpneumatized nanoid sauropod dinosaur from South America. *Scientific Reports 11*:24207.

Averianov, A. O., Sizov, A. V., & Skutschas, P. P. (2021). Gondwanan affinities of *Tengrisaurus*, Early Cretaceous titanosaur from Transbaikalia, Russia (Dinosauria, Sauropoda). *Cretaceous Research 122*:104731.

Barthel, K. W., & Böttcher, R. (1978). Abu Ballas Formation (Tithonian/Berriasian; Southwestern Desert, Egypt), a significant lithostratigraphic unit of the former "Nubian Series." *Mitteilungen der Bayerischen Staatssammlung für Paläontologie und historische Geologie 18*:153–166.

Barthel, K. W., & Herrmann-Degen, W. (1981). Late Cretaceous and early Tertiary stratigraphy in the Great Sand Sea and its SE margins (Farafra and Dakhla oases), SW Desert, Egypt. *Mitteilungen der Bayerischen Staatssammlung für Paläontologie und historische Geologie 21*:141–182.

Bonaparte, J. F. (1986). History of the terrestrial Cretaceous vertebrates of Gondwana. IV Congreso Argentino de Paleontología y Biostratigrafía:63–95.

Bonaparte, J. F. (1996). Cretaceous tetrapods of Argentina. *Münchner Geowissenschaftliche Abhandlungen A 30*:73–130.

Bonaparte, J. F., & Coria, R. A. (1993). Un nuevo y gigantesco saurópodo titanosaurio de la Formación Río Limay (Albiano–Cenomaniano) de la Provincia del Neuquén, Argentina. *Ameghiniana 30*:271–282.

Bonaparte, J. F., & Powell, J. E. (1980). A continental assemblage of tetrapods from the Upper Cretaceous beds of El Brete, northwestern Argentina (Sauropoda-Coelurosauria-Carnosauria-Aves). *Mémoires de la Société Géologique de France, Nouvelle Série 139*:19–28.

Bonaparte, J. F., Heinrich, W.-D., & Wild, R. (2000). Review of *Janenschia* Wild, with the description of a new sauropod from the Tendaguru beds of Tanzania and a discussion on the systematic value of procoelous caudal vertebrae in the Sauropoda. *Palaeontographica Abteilung A 256*:25–76.

Borsuk-Bialynicka, M. (1977). A new camarasaurid sauropod *Opisthocoelicaudia skarzynskii* gen. n., sp. n. from the Upper Cretaceous of Mongolia. *Palaeontologica Polonica 37*:5–63.

Bouckaert, R., Heled, J., Kühnert, D., Vaughan, T., Wu, C.-H., Xie, D., Suchard, M. A., Rambaut, A., & Drummond, A. J. (2014). BEAST 2: a software platform for Bayesian evolutionary analysis. *PLoS Computational Biology 10*:e1003537.

Brinkmann, W., & Buffetaut, E. (1990). Ein Dinosaurier-Teilskelett (Sauropoda) aus der Ober-Kreide von Ägypten. *Nachrichten-Deutsche Geologische Gesellschaft 43*:119–120.

Buffetaut, E., Escuillié, F., & Pohl, B. (2005). First theropod dinosaur from the Maastrichtian phosphates of Morocco. *Kaupia 14*:3–8.

Buffetaut, E., Hartman, A.-F., Al-Kindi, M., & Schulp, A. S. (2015). Hadrosauroid dinosaurs from the Late Cretaceous of the Sultanate of Oman. *PLoS ONE 10*:e0142692.

Calvo, J. O., Porfiri, J. D., González-Riga, B. J., & Kellner, A. W. A. (2007). Anatomy of *Futalognkosaurus dukei* Calvo, Porfiri, González-Riga & Kellner, 2007 (Dinosauria, Titanosauridae) from the Neuquén Group (Late Cretaceous), Patagonia, Argentina. *Arquivos do Museu Nacional, Rio de Janeiro 65*:511–526.

Campos, D. A., Kellner, A. W. A., Bertini, R. J., & Santucci, R. M. (2005). On a titanosaurid (Dinosauria, Sauropoda) vertebral column from the Bauru Group, Late Cretaceous of Brazil. *Arquivos do Museu Nacional, Rio de Janeiro 63*:565–593.

Carballido, J. L., & Sander, P. M. (2014). Postcranial axial skeleton of *Europasaurus holgeri* (Dinosauria, Sauropoda) from the Upper Jurassic of Germany: implications for sauropod ontogeny and phylogenetic relationships of basal Macronaria. *Journal of Systematic Palaeontology 12*:335–387.

Carballido, J. L., Otero, A., Mannion, P. D., Salgado L., & Moreno, A. P. (2022). Titanosauria: a critical reappraisal of its systematics and the relevance of the South American record; pp. 269–298 in A. Otero, J. L. Carballido, & D. Pol (eds.), *South American Sauropodomorph Dinosaurs*. Springer, Cham, Switzerland.

Castro, D. F., Bertini, R. J., Santucci, R. M., & Medeiros, M. A. (2007). Sauropods of the Itapecuru Group (lower/middle Albian), Sao Luís-Grajaú Basin, Maranhão state, Brazil4*Revista Brasileira de Paleontologia 10*:195–200.

Cerda, I. A., Salgado, L., & Powell, J. E. (2012). Extreme postcranial pneumaticity in sauropod dinosaurs from South America. *Paläontologische Zeitschrift 86*:441–449.

Cerda, I. A., Zurriaguz, V. L., Carballido, J. L., González, R., & Salgado, L. (2021). Osteology, paleohistology and phylogenetic relationships of *Pellegrinisaurus powelli* (Dinosauria: Sauropoda) from the Upper Cretaceous of Argentinean Patagonia. *Cretaceous Research 128*:104957.

Churcher, C. S. (1995). Giant Cretaceous lungfish *Neoceratodus tuberculatus* from a deltaic environment in the Quseir (= Baris) Formation of Kharga Oasis, Western Desert of Egypt. *Journal of Vertebrate Paleontology 15*:845–849.

Csiki, Z., Codrea, V., Jipa-Murzea, C., & Godefroit, P. (2010). A partial titanosaur (Sauropoda, Dinosauria) skeleton from the Maastrichtian of Nâlat¸Vad, Hat¸eg Basin, Romania. *Neues Jahrbuch für Geologie und Paläontologie Abhandlungen 258*:297–324.

Curry Rogers, K. (2009). The postcranial osteology of *Rapetosaurus krausei* (Sauropoda: Titanosauria) from the Late Cretaceous of Madagascar. *Journal of Vertebrate Paleontology 29*:1046–1086.

Curry Rogers, K., & Wilson, J. A. (2014). *Vahiny depereti*, gen. et sp. nov., a new titanosaur (Dinosauria, Sauropoda) from the Upper Cretaceous Maevarano Formation, Madagascar. *Journal of Vertebrate Paleontology 34*:606–617.

Davies, T. G., Rahman, I. A., Lautenschlager, S., Cunningham, J. A., Asher, R. J., Barrett, P. M., Bates, K. T., Bengtson, S., Benson, R. B. J., Boyer, D. M., Braga, J., Bright, J. A., Claessens, L. P. A. M., Cox, P. G., Dong, X., Evans, A. R., Falkingham, P. L., Friedman,

M., Garwood, R. J. … Donoghue, P. C. J. (2017). Open data and digital morphology. *Proceedings of the Royal Society B: Biological Sciences 284*:20170194.

de Jesus Faria, C. C., González Riga, B., dos Anjos Candeiro, C. R., da Silva Marinho, T., Ortiz David, L., Simbras, F. M., Castanho, R. B., Muniz, F. P., & da Costa Pereira, P. V. L. G. (2015). Cretaceous sauropod diversity and taxonomic succession in South America. *Journal of South American Earth Sciences 61*:154–163.

D'Emic, M. D. (2012). The early evolution of titanosauriform sauropod dinosaurs. *Zoological Journal of the Linnean Society 166*: 624–671.

D'Emic, M. D., & Wilson, J. A. (2012). Bone histology of a dwarf sauropod dinosaur from the latest Cretaceous of Jordan and a possible biomechanical explanation for "titanosaur-type" bone histology. *Journal of Vertebrate Paleontology*, *Program and Abstracts 2012*:83.

Díez Díaz, V., Pereda Suberbiola, X., & Sanz, J. L. (2013a). The axial skeleton of the titanosaur *Lirainosaurus astibiae* (Dinosauria: Sauropoda) from the latest Cretaceous of Spain. *Cretaceous Research 43*:145–160.

Díez Díaz, V., Pereda Suberbiola, X., & Sanz, J. L. (2013b). Appendicular skeleton and dermal armour of the Late Cretaceous titanosaur *Lirainosaurus astibiae* (Dinosauria: Sauropoda) from Spain. *Palaeontologia Electronica 16*:19A.

Díez Díaz, V., Mocho, P., Páramo, A., Escaso, F., Marcos-Fernández, F., Sanz, J. L., & Ortega, F. (2016). A new titanosaur (Dinosauria, Sauropoda) from the Upper Cretaceous of Lo Hueco (Cuenca, Spain). *Cretaceous Research 68*:49–60.

Díez Díaz, V., Gorscak, E., Lamanna, M. C., Schwarz, D., & El-Dawoudi, I. (2017). The metatarsus of a Late Cretaceous titanosaur (Dinosauria: Sauropoda) from the Kharga Oasis of Egypt. *Zitteliana 91*:31–32.

Díez Díaz, V., Garcia, G., Pereda Suberbiola, X., Jentgen, B., Stein, K., Godefroit, P., & Valentin, X. (2018). The titanosaurian dinosaur *Atsinganosaurus velauciensis* (Sauropoda) from the Upper Cretaceous of southern France: new material, phylogenetic affinities, and palaeobiogeographical implications. *Cretaceous Research 91*:429–456.

Díez Díaz, V., Garcia, G., Pereda Suberbiola, X., Jentgen-Ceschino, B., Stein, K., Godefroit, P., & Valentin, X. (2021). A new titanosaur (Dinosauria: Sauropoda) from the Upper Cretaceous of Velaux-La-Bastide Neuve (southern France). *Historical Biology 33*:2998–3017.

El Atfy, H., Sallam, H., Jasper, A., & Uhl, D. (2016). The first evidence of paleo-wildfire from the Campanian (Late Cretaceous) of North Africa. *Cretaceous Research 57*:306–310.

El-Dawoudi, I., Abuelkheir, G. A., Mahmoud, H., Darwish, M. H., & Sallam, H. M. (2017). A new dinosaur (Sauropoda: Titanosauria) partial skeleton from the Late Cretaceous of the Kharga Oasis, New Valley, Western Desert of Egypt. *Scientific Program of the 55th Annual Scientific Meeting, Geological Society of Egypt*:24.

Ezcurra, M. D., & Novas, F. E. (2016). Theropod dinosaurs from Argentina. *Contribuciones del Museo Argentino de Ciencias Naturales 6*:139–156.

Fathy, D., Wagreich, M., Ntaflos, T., & Sami, M. (2021). Paleoclimatic variability in the southern Tethys, Egypt: insights from the mineralogy and geochemistry of Upper Cretaceous lacustrine organic-rich deposits. *Cretaceous Research 126*:104880.

Filippi, L. S., & Garrido, A. C. (2008). *Pitekunsaurus macayai* gen. et sp. nov., nuevo titanosaurio (Saurischia, Sauropoda) del Cretácico Superior de la Cuenca Neuquina, Argentina. *Ameghiniana 45*:575–590.

Gallina, P. A., & Apesteguía, S. (2011). Cranial anatomy and phylogenetic position of the titanosaurian sauropod *Bonitasaura salgadoi*. *Acta Palaeontologica Polonica 56*:45–60.

Gallina, P. A., & Apesteguía, S. (2015). Postcranial anatomy of *Bonitasaura salgadoi* (Sauropoda, Titanosauria) from the Late Cretaceous of Patagonia. *Journal of Vertebrate Paleontology 35*: e924957.

Gallina, P. A., & Otero, A. (2015). Reassessment of *Laplatasaurus araukanicus* (Sauropoda: Titanosauria) from the Upper Cretaceous of Patagonia, Argentina. *Ameghiniana 52*:487–501.

Gallina, P. A., Canale, J. I., & Carballido, J. L. (2021). The earliest known titanosaur sauropod dinosaur. *Ameghiniana 58*:35–51.

Garcia, G., Amico, S., Fournier, F., Thouand, E., & Valentin, X. (2010). A new titanosaur genus (Dinosauria, Sauropoda) from the Late Cretaceous of southern France and its paleobiogeographic implications. *Bulletin de la Société Géologique de France 181*:269–277.

Gemmellaro, M. (1921). Rettili maëstrichtiani d'Egitto. *Giornale di Scienze Naturali ed Economiche 32*:339–351.

Goloboff, P. A., & Catalano, S. A. (2016). TNT version 1.5, including a full implementation of phylogenetic morphometrics. *Cladistics 32*:221–238.

Goloboff, P. A., Farris, J. S., & Nixon, K. C. (2008). TNT, a free program for phylogenetic analysis. *Cladistics 24*:774–786.

Gomani, E. M. (2005). Sauropod dinosaurs from the Early Cretaceous of Malawi, Africa. *Palaeontologia Electronica 8*:1–37.

González Riga, B. J., Lamanna, M. C., Ortiz David, L. D., Calvo, J. O., & Coria, J. P. (2016). A gigantic new dinosaur from Argentina and the evolution of the sauropod hind foot. *Scientific Reports 6*:19165.

González Riga, B. J., Mannion, P. D., Poropat, S. F., Ortiz David, L. D., & Coria, J. P. (2018). Osteology of the Late Cretaceous Argentinean sauropod dinosaur *Mendozasaurus neguyelap*: implications for basal titanosaur relationships. *Zoological Journal of the Linnean Society 184*:136–181.

González Riga, B. J., Lamanna, M. C., Otero, A., Ortiz David, L. D., Kellner, A. W. A., & Ibiricu, L. M. (2019). An overview of the appendicular skeletal anatomy of South American titanosaurian sauropods, with definition of a newly recognized clade. *Anais da Academia Brasileira de Ciências 91*:e20180374.

Gorscak, E. (2016). Characterizing African Cretaceous continental faunas: paleobiogeographical patterns and new insights from sub-Saharan African titanosaurian sauropod dinosaurs. *Journal of Vertebrate Paleontology, Program and Abstracts 2016*:146.

Gorscak, E., & O'Connor, P. M. (2016). Time-calibrated models support congruency between Cretaceous continental rifting and titanosaurian evolutionary history. *Biology Letters 12*:20151047.

Gorscak, E., & O'Connor, P. M. (2019). A new African titanosaurian sauropod dinosaur from the middle Cretaceous Galula Formation (Mtuka Member), Rukwa Rift Basin, southwestern Tanzania. *PLoS ONE 14*:e0211412.

Gorscak, E., Sertich, J., & Kyalo Manthi, F. (2019). Titanosaurian sauropod dinosaur fossils from the Upper Cretaceous Lapur Sandstone (Turkana Grits), Turkana Basin, northwestern Kenya. *Journal of Vertebrate Paleontology, Program and Abstracts 2019*:108.

Gorscak, E., O'Connor, P. M., Stevens, N. J., & Roberts, E. M. (2014). The basal titanosaurian *Rukwatitan bisepultus* (Dinosauria, Sauropoda) from the middle Cretaceous Galula Formation, Rukwa Rift Basin, southwestern Tanzania. *Journal of Vertebrate Paleontology 34*: 1133–1154.

Gorscak, E., O'Connor, P. M., Roberts, E. M., & Stevens, N. J. (2017). The second titanosaurian (Dinosauria: Sauropoda) from the middle Cretaceous Galula Formation, southwestern Tanzania, with remarks on African titanosaurian diversity. *Journal of Vertebrate Paleontology 37*:e1343250.

Gorscak, E., Lamanna, M. C., Díez Díaz, V., Schwarz, D., Salem, B., Abu El-Kheir, G., & Sallam, H. (2020). A titanosaurian sauropod from the Campanian Quseir Formation of the Kharga Oasis, Egypt, supports Afro-Eurasian dinosaur faunal connectivity during the Late Cretaceous. *Journal of Vertebrate Paleontology*, *Program and Abstracts 2020*.

Griffin, C. T., Stocker, M. R., Colleary, C., Stefanic, C. M., Lessner, E. J., Riegler, M., Formoso, K., Koeller, K., & Nesbitt, S. J. (2021). Assessing ontogenetic maturity in extinct saurian reptiles. *Biological Reviews 96*:470–525.

Hocknull, S. A., Wilkinson, M., Lawrence, R. A., Konstantinov, V., Mackenzie, S., & Mackenzie, R. (2021). A new giant sauropod, *Australotitan cooperensis* gen. et sp. nov., from the mid-Cretaceous of Australia. *PeerJ 9*:e11317.

Huene, F. von. (1929). Los saurisquios y ornitisquios del Cretáceo Argentino. *Anales del Museo de La Plata 3*:1–196.

Jain, S. L., & Bandyopadhyay, S. (1997). New titanosaurid (Dinosauria: Sauropoda) from the Late Cretaceous of central India. *Journal of Vertebrate Paleontology 17*:114–136.

Jianu, C. M., & Weishampel, D. B. (1999). The smallest of the largest: a new look at possible dwarfing in sauropod dinosaurs. *Geologie en Mijnbouw 78*:335–343.

Kass, R. E., & Raftery, A. E. (1995). Bayes factors. *Journal of the American Statistical Association 90*:773–795.

Kear, B. P., Rich, T. H., Vickers-Rich, P., Ali, M. A., Al-Mufarreh, Y. A., Matari, A. H., Al-Massari, A. M., Nasser, A. H., Attia, Y., & Halawani, M. A. (2013). First dinosaurs from Saudi Arabia. *PLoS ONE 8*:e84041.

Khosla, A., & Bajpai, S. (2021). Dinosaur fossil records from India and their palaeobiogeographic implications: an overview. *Journal of Palaeosciences 70*:193–212.

Krause, D. W., Rogers, R. R., Forster, C. A., Hartman, J. H., Buckley, G. A., & Sampson, S. D. (1999). The Late Cretaceous vertebrate fauna of Madagascar: implications for Gondwanan paleobiogeography. *GSA Today 9*:1–7.

Krause, D. W., O'Connor, P. M., Curry Rogers, K., Sampson, S. D., Buckley, G. A., & Rogers, R. R. (2006). Late Cretaceous terrestrial vertebrates from Madagascar: implications for Latin American biogeography. *Annals of the Missouri Botanical Garden 93*:178–208.

Krause, D. W., Sertich, J. J. W., O'Connor, P. M., Curry Rogers, K., & Rogers, R. R. (2019). The Mesozoic biogeographic history of Gondwanan terrestrial vertebrates: insights from Madagascar's fossil record. *Annual Review of Earth and Planetary Sciences 47*:519–553.

Lacovara, K. J., Lamanna, M. C., Ibiricu, L. M., Poole, J. C., Schroeter, E. R., Ullmann, P. V., Voegele, K. K., Boles, Z. M., Carter, A. M., Fowler, E. K., Egerton, V. M., Moyer, A. E., Coughenour, C. L., Schein, J. P., Harris, J. D., Martínez, R. D., & Novas, F. E. (2014). A gigantic, exceptionally complete titanosaurian sauropod dinosaur from southern Patagonia, Argentina. *Scientific Reports 4*:6196.

Lamanna, M. C. (2013). Last of the Gondwanan giants: Late Cretaceous dinosaurs from the Southern Hemisphere; p. 13 in C. R. A. Candeiro, E. B. Machado, & Y. M. Alves (eds.), *Abstract Book*, *1st Brazilian Dinosaur Symposium. Paleontologia em Destaque*, *Boletim Informativo da Sociedade Brasileira de Paleontologia*, *Special Edition*. Universidade Federal de Uberlândia, Campus Pontal-Ituiutaba, Ituiutaba, Brazil.

Lamanna, M. C., & Hasegawa, Y. (2014). New titanosauriform sauropod dinosaur material from the Cenomanian of Morocco: implications for paleoecology and sauropod diversity in the Late Cretaceous of North Africa. *Bulletin of Gunma Museum of Natural History 18*:1–19.

Lamanna, M. C., Gorscak, E., Díez Díaz, V., Schwarz, D., & El-Dawoudi, I. (2017). Reassessment of a partial titanosaurian sauropod dinosaur skeleton from the Upper Cretaceous (Campanian) Quseir Formation of the Kharga Oasis, Egypt. *Zitteliana 91*:50–51.

Lamanna, M. C., Case, J. A., Roberts, E. M., Arbour, V. M., Ely, R. C., Salisbury, S. W., Clarke, J. A., Malinzak, D. E., West, A. R., & O'Connor, P. M. (2019). Late Cretaceous non-avian dinosaurs from the James Ross Basin, Antarctica: description of new material, updated synthesis, biostratigraphy, and paleobiogeography. *Advances in Polar Science 30*:228–250.

Le Loeuff, J. (2005). Osteology of *Ampelosaurus atacis* (Titanosauria) from southern France; pp. 115–137 in V. Tidwell & K. Carpenter (eds.), *Thunder-Lizards: The Sauropodomorph Dinosaurs*. Indiana University Press, Bloomington.

Leanza, H. A., Apesteguía, S., Novas, F. E., & de la Fuente, M. S. (2004). Cretaceous terrestrial beds from the Neuquén Basin (Argentina) and their tetrapod assemblages. *Cretaceous Research 25*:61–87.

Lehman, T. M., & Coulson, A. B. (2002). A juvenile specimen of the sauropod dinosaur *Alamosaurus sanjuanensis* from the Upper Cretaceous of Big Bend National Park, Texas. *Journal of Paleontology 76*:156–172.

Lewis, P. O. (2001). A likelihood approach to estimating phylogeny from discrete morphological character data. *Systematic Biology 50*:913–925.

Li, L.-G., Li, D.-Q., You, H.-L., & Dodson, P. (2014). A new titanosaurian sauropod from the Hekou Group (Lower Cretaceous) of the Lanzhou-Minhe Basin, Gansu Province, China. *PLoS ONE 9*: e85979.

Longman, H. A. (1933). A new dinosaur from the Queensland Cretaceous. *Memoirs of the Queensland Museum 10*:131–144.

Longrich, N. R., Pereda-Suberbiola, X., Jalil, N.-E., Khaldoune, F., & Jourani, E. (2017). An abelisaurid from the latest Cretaceous (late Maastrichtian) of Morocco, North Africa. *Cretaceous Research 76*:40–52.

Longrich, N. R., Pereda Suberbiola, X., Pyron, R. A., & Jalil, N.-E. (2021). The first duckbill dinosaur (Hadrosauridae: Lambeosaurinae) from Africa and the role of oceanic dispersal in dinosaur biogeography. *Cretaceous Research 120*:104678.

Mahmoud, M. S. (1998). Palynological dating of the Quseir Formation, Kharga Oasis (Egypt). *Arab Gulf Journal of Scientific Research 16*:267–281.

Mahmoud, M. S. (2003). Palynology and palaeoenvironment of the Quseir Formation (Campanian) from central Egypt. *Journal of African Earth Sciences 36*:135–148.

Mallison, H., & Wings, O. (2014). Photogrammetry in paleontology—a practical guide. *Journal of Paleontological Techniques 12*:1–31.

Mannion, P. D., & Calvo, J. O. (2011). Anatomy of the basal titanosaur (Dinosauria, Sauropoda) *Andesaurus delgadoi* from the mid-Cretaceous (Albian–early Cenomanian) Río Limay Formation, Neuquén Province, Argentina: implications for titanosaur systematics. *Zoological Journal of the Linnean Society 163*:155–181.

Mannion, P. D., & Otero, A. (2012). A reappraisal of the Late Cretaceous Argentinean sauropod dinosaur *Argyrosaurus superbus*, with a description of a new titanosaur genus. *Journal of Vertebrate Paleontology 32*:614–638.

Mannion, P. D., Upchurch, P., Barnes, R. N., & Mateus, O. (2013). Osteology of the Late Jurassic Portuguese sauropod dinosaur *Lusotitan atalaiensis* (Macronaria) and the evolutionary history of basal titanosauriforms. *Zoological Journal of the Linnean Society 168*:98–206.

Mannion, P. D., Upchurch, P., Schwarz, D., & Wings, O. (2019). Taxonomic affinities of the putative titanosaurs from the Late Jurassic Tendaguru Formation of Tanzania: phylogenetic and biogeographic implications for eusauropod dinosaur evolution. *Zoological Journal of the Linnean Society 185*:784–909.

Marsh, O. C. (1878). Principal characters of American Jurassic dinosaurs. Part I. *American Journal of Science, Series 3 16*:411–416.

Martill, D. M., Frey, E., & Sadaqah, R. M. (1996). The first dinosaur from the Hashemite Kingdom of Jordan. *Neues Jahrbuch für Geologie und Paläontologie Monatshefte 1996*:147–154.

Martin, V. (1994). Baby sauropods from the Sao Khua Formation (Lower Cretaceous) in northeastern Thailand. *Gaia 10*:147–153.

Martínez, R. D., Giménez, O., Rodríguez, J., Luna, M., & Lamanna, M. C. (2004). An articulated specimen of the basal titanosaurian (Dinosauria: Sauropoda) *Epachthosaurus sciuttoi* from the early Late Cretaceous Bajo Barreal Formation of Chubut Province, Argentina. *Journal of Vertebrate Paleontology 24*:107–120.

Martínez, R. D. F., Lamanna, M. C., Novas, F. E., Ridgely, R. C., Casal, G. A., Martínez, J. E., Vita, J. R., & Witmer, L. M. (2016). A basal lithostrotian titanosaur (Dinosauria: Sauropoda) with a complete skull: implications for the evolution and paleobiology of Titanosauria. *PLoS ONE 11*:e0151661.

Mateus, O., Polcyn, M. J., Jacobs, L. L., Araújo, R., Schulp, A. S., Marinheiro, J., Pereira, B., & Vineyard, D. (2012). Cretaceous amniotes from Angola: dinosaurs, pterosaurs, mosasaurs, plesiosaurs, and turtles; pp. 71–105 in *Actas de V Jornadas Internacionales sobre Paleontología de Dinosaurios y su Entorno*, Salas de los Infantes, Burgos.

Matzke, N. J. (2015). BEASTmasteR: automated conversion of NEXUS data to BEAST2 XML format, for fossil tip-dating and other uses. PhyloWiki. Available at http://phylo.wikidot.com/beastmaster.

Matzke, N. J., & Irmis, R. B. (2018). Including autapomorphies is important for paleontological tip dating with clocklike data, but not with non-clock data. *PeerJ 6*:e4553.

McIntosh J. S. (1990). Sauropoda; pp. 345–401 in D. B. Weishampel, P. Dodson, & H. Osmólska (eds.), *The Dinosauria*. University of California Press, Berkeley.

Novas, F. E. (2009). *The Age of Dinosaurs in South America*. Indiana University Press, Bloomington & Indianapolis, 452 pp.

Novas, F. E., Chatterjee, S., Rudra, D. K., & Datta, P. M. (2010). *Rahiolisaurus gujaratensis*, n. gen. n. sp., a new abelisaurid theropod from the Late Cretaceous of India; pp. 45–62 in S. Bandyopadhyay (ed.), *New Aspects of Mesozoic Biodiversity*. Lecture Notes in Earth Sciences 132. Springer-Verlag, Berlin and Heidelberg.

Novas, F. E., Agnolín, F. L., Ezcurra, M. D., Porfiri, J., & Canale, J. I. (2013). Evolution of the carnivorous dinosaurs during the Cretaceous: the evidence from Patagonia. *Cretaceous Research 45*:174–215.

O'Connell, T. L., Wilson, J. A., & Zalmout, I. S. (2012). Air space proportion in a dorsal vertebra of a new titanosaur (Dinosauria: Sauropoda) from Jordan. *Journal of Vertebrate Paleontology, Program and Abstracts 2012*:151.

O'Connor, P. M., Gottfried, M. D., Stevens, N. J., Roberts, E. M., Ngasala, S., Kapilima, S., & Chami, R. (2006). A new vertebrate fauna from

the Cretaceous Red Sandstone Group, Rukwa Rift Basin, southwestern Tanzania. *Journal of African Earth Sciences 44*:277–288.

Orr, T. J., Roberts, E. M., Wurster, C. M., Mtelela, C., Stevens, N. J., & O'Connor, P. M. (2021). Paleoclimate and paleoenvironment reconstruction of paleosols spanning the Lower to Upper Cretaceous from the Rukwa Rift Basin, Tanzania. *Palaeogeography, Palaeoclimatology, Palaeoecology 577*:110539.

Otero, A. (2010). The appendicular skeleton of *Neuquensaurus*, a Late Cretaceous saltasaurine sauropod from Patagonia, Argentina. *Acta Palaeontologica Polonica 55*:399–426.

Owen, R. (1842). Report on British fossil reptiles, Part II. *Reports of the British Association for the Advancement of Science 11*:60–204.

Owusu Agyemang, P. C., Roberts, E. M., Bussert, R., Evans, D., & Müller, J. (2019). U-Pb detrital zircon constraints on the depositional age and provenance of the dinosaur-bearing Upper Cretaceous Wadi Milk Formation of Sudan. *Cretaceous Research 97*:52–72.

Pereda Suberbiola, X., Bardet, N., Iarochène, M., Bouya, B., & Amaghzaz, M. (2004). The first record of a sauropod dinosaur from the Late Cretaceous phosphates of Morocco. *Journal of African Earth Sciences 40*:81–88.

Poropat, S. F., Upchurch, P., Mannion, P. D., Hocknull, S. A., Kear, B. P., Sloan, T., Sinapius, G. H. K., & Elliott, D. A. (2015). Revision of the sauropod dinosaur *Diamantinasaurus matildae* Hocknull et al. 2009 from the mid-Cretaceous of Australia: implications for Gondwanan titanosauriform dispersal. *Gondwana Research 27*:995–1033.

Poropat, S. F., Nair, J. P., Syme, C. E., Mannion, P. D., Upchurch, P., Hocknull, S. A., Cook, A. G., Tischler, T. R., & Holland, T. (2017). Reappraisal of *Austrosaurus mckillopi* Longman, 1933 from the Allaru Mudstone of Queensland, Australia's first named Cretaceous sauropod dinosaur. *Alcheringa* 41:543–580.

Poropat, S. F., Mannion, P. D., Upchurch, P., Tischler, T. R., Sloan, T., Sinapius, G. H. K., Elliott, J. A., & Elliott, D. A. (2020). Osteology of the wide-hipped titanosaurian sauropod dinosaur *Savannasaurus elliottorum* from the Upper Cretaceous Winton Formation of Queensland, Australia. *Journal of Vertebrate Paleontology 40*:e1786836.

Poropat, S. F., Kundrát, M., Mannion, P. D., Upchurch, P., Tischler, T. R., & Elliott, D. A. (2021). Second specimen of the Late Cretaceous Australian sauropod dinosaur *Diamantinasaurus matildae* provides new anatomical information on the skull and neck of early titanosaurs. *Zoological Journal of the Linnean Society 192*:610–674.

Powell, J. E. (1986). *Revisión de los Titanosauridos de America del Sur*. Ph.D. dissertation, Universidad Nacional de Tucumán, Argentina, 493 pp.

Powell, J. E. (1992). Osteologia de *Saltasaurus loricatus* (Sauropoda - Titanosauridae) del Cretácico Superior del noroeste Argentino; pp. 165–230 in J. L. Sanz & A. D. Buscalioni (eds.), *Los Dinosaurios y Su Entorno Biotico*. Instituto 'Juan de Valdés,' Cuenca.

Powell, J. E. (2003). Revision of South American titanosaurid dinosaurs: palaeobiological, palaeobiogeographical and phylogenetic aspects. *Records of the Queen Victoria Museum 111*:1–173.

Rauhut, O. W. M. (1999). A dinosaur fauna from the Late Cretaceous (Cenomanian) of northern Sudan. *Palaeontologia Africana 35*: 61–84.

Rauhut, O. W. M., & Werner, C. (1995). First record of the family Dromaeosauridae (Dinosauria: Theropoda) in the Cretaceous of Gondwana (Wadi Milk Formation, northern Sudan). *Paläontologische Zeitschrift 69*:475–489.

Rauhut, O. W. M., & Werner, C. (1997). First record of a Maastrichtian sauropod dinosaur from Egypt. *Palaeontologia Africana 34*:63–67.

Reguero, M. A., Tambussi, C. P., Coria, R. A., & Marenssi, S. A. (2013). Late Cretaceous dinosaurs from the James Ross Basin, West Antarctica. *Geological Society, London, Special Publications 381*:99–116.

Reguero, M. A., Gasparini, Z., Olivero, E. B., Coria, R. A., Fernández, M. S., O'Gorman, J. P., Gouiric-Cavalli, S., Acosta Hospitaleche, C., Bona, P., Iglesias, A., Gelfo, J. N., Raffi, M. E., Moly, J. J., Santillana, S. N., & Cárdenas, M. (2022). Late Campanian-early Maastrichtian vertebrates from the James Ross Basin, West Antarctica: updated synthesis, biostratigraphy, and paleobiogeography. *Anais da Academia Brasileira de Ciências 94*:e20211142.

Roberts, E. M., O'Connor, P. M., Stevens, N. J., Gottfried, M. D., Jinnah, Z. A., Ngasala, S., Choh, A. M., & Armstrong, R. A. (2010). Sedimentology and depositional environments of the Red Sandstone Group, Rukwa Rift Basin, southwestern Tanzania: new insight into Cretaceous and Paleogene terrestrial ecosystems and tectonics in sub-equatorial Africa. *Journal of African Earth Sciences 57*:179–212.

Ronquist, F., Teslenko, M., van der Mark, P., Ayres, D. L., Darling, A., Höhna, S., Larget, B., Liu, L., Suchard, M. A., & Huelsenbeck, J. P. (2012). MrBayes 3.2: efficient Bayesian phylogenetic inference and model choice across a large model space. *Systematic Biology 61*:539–542.

Rozadilla, S., Agnolín, F., Manabe, M., Tsuihiji, T., & Novas, F. E. (2021). Ornithischian remains from the Chorrillo Formation (Upper Cretaceous), southern Patagonia, Argentina, and their implications on ornithischian paleobiogeography in the Southern Hemisphere. *Cretaceous Research 125*:104881.

Salem, B. S., Abu El-Kheir, G., Lamanna, M. C., El-Sayed, S., & Sallam, H. M. (2020). A new titanosaurian sauropod dinosaur partial skeleton from the Late Cretaceous (Campanian) of the Kharga Oasis, Western Desert of Egypt. *Journal of Vertebrate Paleontology, Program and Abstracts 2020*.

Salem, B. S., O'Connor, P. M., Gorscak, E., El-Sayed, S., Sertich, J. J. W., Seiffert, E., & Sallam, H. M. (2021). Dinosaur remains from the Upper Cretaceous (Campanian) of the Western Desert, Egypt. *Cretaceous Research 123*:104783.

Salgado, L. (1996). *Pellegrinisaurus powelli* nov. gen. et sp. (Sauropoda, Titanosauridae) from the Upper Cretaceous of Lago Pellegrini, northwestern Patagonia, Argentina. *Ameghiniana 33*:355–365.

Salgado, L., Apesteguía, S., & Heredia, S. E. (2005). A new specimen of *Neuquensaurus australis*, a Late Cretaceous saltasaurine titanosaur from north Patagonia. *Journal of Vertebrate Paleontology 25*: 623–634.

Salgado, L., & de Souza Carvalho, I. (2008). *Uberabatitan ribeiroi*, a new titanosaur from the Marília Formation (Bauru Group, Upper Cretaceous), Minas Gerais, Brazil. *Palaeontology 51*:881–901.

Salgado, L., Gallina, P. A., & Paulina Carabajal, A. (2015). Redescription of *Bonatitan reigi* (Sauropoda: Titanosauria), from the Campanian–Maastrichtian of the Río Negro Province (Argentina). *Historical Biology 27*:525–548.

Sallam, H. M., O'Connor, P. M., Kora, M., Sertich, J. J. W., Seiffert, E. R., Faris, M., Ouda, K., El-Dawoudi, I., Saber, S., & El-Sayed, S. (2016). Vertebrate paleontological exploration of the Upper Cretaceous succession in the Dakhla and Kharga oases, Western Desert, Egypt. *Journal of African Earth Sciences 117*:223–234.

Sallam, H. M., Gorscak, E., O'Connor, P. M., El-Dawoudi, I., El-Sayed, S., Saber, S., Kora, M., Sertich, J. J. W., Seiffert, E. R., & Lamanna, M. C. (2018). New Egyptian sauropod reveals Late Cretaceous dinosaur dispersal between Europe and Africa. *Nature Ecology and Evolution 2*:445–451.

Sanz, J. L., Powell, J. E., Le Loeuff, J., Martínez, R., & Pereda Suberbiola, X. (1999). Sauropod remains from the Upper Cretaceous of Laño (northcentral Spain). Titanosaur phylogenetic relationships. *Estudios del Museo de Ciencias Naturales de Alava 14*:235–255.

Schulp, A. S., Hanna, S. S., Hartman, A. F., & Jagt, J. W. M. (2000). A Late Cretaceous theropod caudal vertebra from the Sultanate of Oman. *Cretaceous Research 21*:851–856.

Schulp, A. S., O'Connor, P. M., Weishampel, D. B., Al-Sayigh, A. R., Al-Harthy, A., & Jagt, J. W. M. (2008). Ornithopod and sauropod dinosaur remains from the Maastrichtian Al-Khod Conglomerate, Sultanate of Oman. *Sultan Qaboos University Journal of Science 13*:27–32.

Sereno, P. C., & Brusatte, S. L. (2008). Basal abelisaurid and carcharodontosaurid theropods from the Lower Cretaceous Elrhaz Formation of Niger. *Acta Palaeontologica Polonica 53*:15–46.

Sereno, P. C., Wilson, J. A., & Conrad, J. L. (2004). New dinosaurs link southern landmasses in the mid-Cretaceous. *Proceedings of the Royal Society B: Biological Sciences 271*:1325–1330.

Sertich, J., Sampson, S., Loewen, M., Gathogo, P., Brown, F., & Kyalo Manthi, F. (2005). Dinosaurs of Kenya's rift: fossil preservation in the Lubur Sandstone of northern Kenya. *Journal of Vertebrate Paleontology 25*:114A.

Sertich, J., Kyalo Manthi, F., Sampson, S., Loewen, M., & Getty, M. (2006). Rift Valley dinosaurs: a new Late Cretaceous vertebrate fauna from Kenya. *Journal of Vertebrate Paleontology 26*:124A.

Sertich, J., O'Connor, P., Seiffert, E., & Kyalo Manthi, F. (2013). A giant abelisaurid theropod from the latest Cretaceous of northern

Turkana, Kenya. *Journal of Vertebrate Paleontology*, *Program and Abstracts 2013*:211.
Silva Junior, C. G. J., Marinho, T. S., Martinelli, A. G., & Langer, M. C. (2019). Osteology and systematics of *Uberabatitan ribeiroi* (Dinosauria; Sauropoda): a Late Cretaceous titanosaur from Minas Gerais, Brazil. *Zootaxa 4577*:401–438.
Smith, J. B., & Lamanna, M. C. (2006). An abelisaurid from the Late Cretaceous of Egypt: implications for theropod biogeography. *Naturwissenschaften 93*:242–245.
Smith, J. B., Lamanna, M. C., Lacovara, K. J., Dodson, P., Smith, J. R., Poole, J. C., Giegengack, R., & Attia, Y. (2001). A giant sauropod dinosaur from an Upper Cretaceous mangrove deposit in Egypt. *Science 292*:1704–1706.
Stromer, E. (1932). Ergebnisse der Forschungreisen Prof. E. Stromers in den Wüsten Ägyptens. II. Wirbeltierreste der Baharîje-Stufe (unterstes Cenoman). 11. Sauropoda. *Abhandlungen der Bayerischen Akademie der Wissenschaften, Mathematisch-naturwissenschaftliche Abteilung, Neue Folge 10*:3–21.
Stromer, E., & Weiler, W. (1930). Ergebnisse der Forschungsreisen Prof. E. Stromers in den Wüsten Ägyptens. VI. Beschreibung von Wirbeltier-Resten aus dem nubischen Sandstein Oberägyptens und aus ägyptischen Phosphaten nebst Bemerkungen über die Geologie der Umgegend von Mahamîd in Oberägypten. *Abhandlungen der Bayerischen Akademie der Wissenschaften, Mathematisch-naturwissenschaftliche Abteilung, Neue Folge 7*:1–42.
Stadler, T., Kühnert, D., Bonhoeffer, S., & Drummond, A. J. (2013). Birth–death skyline plot reveals temporal changes of epidemic spread in HIV and hepatitis C virus (HCV). *Proceedings of the National Academy of Sciences 110*:228–233.
Ullmann, P. V., & Lacovara, K. J. (2016). Appendicular osteology of *Dreadnoughtus schrani*, a giant titanosaurian (Sauropoda, Titanosauria) from the Upper Cretaceous of Patagonia, Argentina. *Journal of Vertebrate Paleontology 36*:e1225303.
Upchurch, P., Barrett, P. M., & Dodson, P. (2004). Sauropoda; pp. 259–322 in D. B. Weishampel, P. Dodson, & H. Osmólska (eds.), *The Dinosauria*, second edition. University of California Press, Berkeley.
Vila, B., Sellés, A., Moreno-Azanza, M., Razzolini, N. L., Gil-Delgado, J. A., Canudo, J. I., & Galobart, À. (2022). A titanosaurian sauropod with Gondwanan affinities in the latest Cretaceous of Europe. *Nature Ecology and Evolution 6*:288–296.
Voegele, K. K., Lamanna, M. C., & Lacovara, K. J. (2017). Osteology of the dorsal vertebrae of the giant titanosaurian sauropod dinosaur *Dreadnoughtus schrani* from the Late Cretaceous of Argentina. *Acta Palaeontologica Polonica 62*:667–681.
Voegele, K. K., Ullmann, P. V., Lamanna, M. C., & Lacovara, K. J. (2021). Myological reconstruction of the pelvic girdle and hind limb of the giant titanosaurian sauropod dinosaur *Dreadnoughtus schrani*. *Journal of Anatomy 37*:1–22.
Wedel, M. J. (2003). The evolution of vertebral pneumaticity in sauropod dinosaurs. *Journal of Vertebrate Paleontology 23*:344–357.
Wedel, M. J., & Taylor, M. P. (2013). Caudal pneumaticity and pneumatic hiatuses in the sauropod dinosaurs *Giraffatitan* and *Apatosaurus*. *PLoS ONE 8*:e78213.
Wedel, M. J., Cifelli, R. L., & Sanders, R. K. (2000). Osteology, paleobiology, and relationships of the sauropod dinosaur *Sauroposeidon*. *Acta Palaeontologica Polonica 45*:343–388.
Widlansky, S. J., Clyde, W. C., O'Connor, P. M., Roberts, E. M., & Stevens, N. J. (2018). Paleomagnetism of the Cretaceous Galula Formation and implications for vertebrate evolution. *Journal of African Earth Sciences 139*:403–420.
Wiechmann, M. F. (1999a). Ein Titanosaurier-Teilskelett aus dem Campan von Ägypten/Western Desert. *Jahrestagung der Paläontologischen Gesellschaft*, *Zürich 69*:81–82.
Wiechmann, M. F. (1999b). *Ein Titanosaurier-Teilskelett aus dem Campan von Ägypten – Western Desert*. Unpublished Diploma thesis, Institut für Paläontologie, Freien Universität Berlin, 93 pp.
Wilson, J. A. (1999). A nomenclature for vertebral laminae in sauropods and other saurischian dinosaurs. *Journal of Vertebrate Paleontology 19*:639–653.
Wilson J. A. (2002). Sauropod dinosaur phylogeny: critique and cladistic analysis. *Zoological Journal of the Linnean Society 136*:217–276.
Wilson, J. A. (2012). New vertebral laminae and patterns of serial variation in vertebral laminae of sauropod dinosaurs. *Contributions from the Museum of Paleontology, the University of Michigan 30*:321–336.
Wilson, J. A., & Upchurch, P. (2003). A revision of *Titanosaurus* Lydekker (Dinosauria – Sauropoda), the first dinosaur genus with a 'Gondwanan' distribution. *Journal of Systematic Palaeontology 1*:125–160.
Wilson, J. A., Sadiq Malkani, M., & Gingerich, P. D. (2001). New crocodyliform (Reptilia, Mesoeucrocodylia) from the Upper Cretaceous Pab Formation of Vitakri, Balochistan (Pakistan). *Contributions from the Museum of Paleontology, the University of Michigan 30*:321–336.
Wilson, J. A., Sereno, P. C., Srivastava, S., Bhatt, D. K., Khosla, A., & Sahni, A. (2003). A new abelisaurid (Dinosauria, Theropoda) from the Lameta Formation (Cretaceous, Maastrichtian) of India. *Contributions from the Museum of Paleontology, the University of Michigan 31*:1–42.
Wilson, J. A., Malkani, M. S., & Gingerich, P. D. (2005). A sauropod braincase from the Pab Formation (Upper Cretaceous, Maastrichtian) of Balochistan, Pakistan. *Gondwana Geological Magazine*, *Special Volume 8*:101–109.
Wilson, J. A., Mustafa, H., & Zalmout, I. (2006). Latest Cretaceous reptiles from the Hashemite Kingdom of Jordan. *Journal of Vertebrate Paleontology 26*:140A.
Wilson, J. A., D'Emic, M. D., Ikejiri, T., Moacdieh, E. M., & Whitlock, J. A. (2011a). A nomenclature for vertebral fossae in sauropods and other saurischian dinosaurs. *PLoS ONE 6*:e17114.
Wilson, J. A., Barrett, P. M., & Carrano, M. T. (2011b). An associated partial skeleton of *Jainosaurus* cf. *septentrionalis* (Dinosauria: Sauropoda) from the Late Cretaceous of Chhota Simla, central India. *Palaeontology 54*:981–998.
Wilson, J. A., Pol, D., Carvalho, A. B., & Zaher, H. (2016). The skull of the titanosaur *Tapuiasaurus macedoi* (Dinosauria: Sauropoda), a basal titanosaur from the Lower Cretaceous of Brazil. *Zoological Journal of the Linnean Society 178*:611–662.
Zaghloul, E. A. (2021). Geology of Dakhla Oasis, Western Desert, Egypt; pp. 29–44 in E. Iwasaki, A. M. Negm, & S. F. Elbeih (eds.), *Sustainable Water Solutions in the Western Desert, Egypt: Dakhla Oasis*. Springer Nature Switzerland AG, Cham.
Zaher, H., Pol, D., Carvalho, A. B., Nascimento, P. M., Riccomini, C., Larson, P., Juarez-Valieri, R., Pires-Domingues, R., da Silva Jr., N. J., & de Almeida Campos, D. (2011). A complete skull of an Early Cretaceous sauropod and the evolution of advanced titanosaurians. *PLoS ONE 6*:e16663.
Zurriaguz, V., & Powell, J. (2015). New contributions to the presacral osteology of *Saltasaurus loricatus* (Sauropoda, Titanosauria) from the Upper Cretaceous of northern Argentina. *Cretaceous Research 54*:283–300.
Zurriaguz, V. L., & Cerda, I. A. (2017). Caudal pneumaticity in derived titanosaurs (Dinosauria: Sauropoda). *Cretaceous Research 73*: 14–24.

Handling Editor: Steven Salisbury.
Phylogenetics Editor: Pedro Godoy.